ULPGC
Universidad de
Las Palmas de
Gran Canaria

Doctorado en Ingenierías Química, Mecánica y de Fabricación

Las Palmas de Gran Canaria, abril de 2021

ESTUDIO EXPERIMENTAL DE DIFERENTES COMBINACIONES DE BIOMATERIALES CON MATRIZ DE ÁCIDO POLILÁCTICO EN FABRICACIÓN ADITIVA CON FINES BIOMÉDICOS

Autor:

Ricardo Donate González

Director:

Mario Domingo Monzón Verona

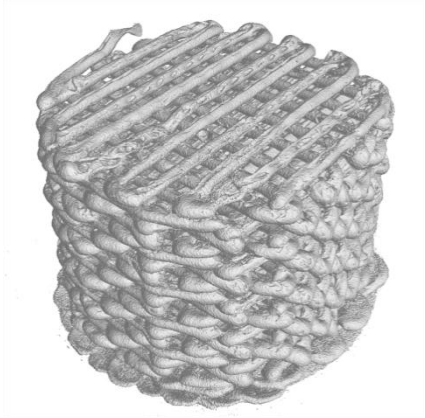

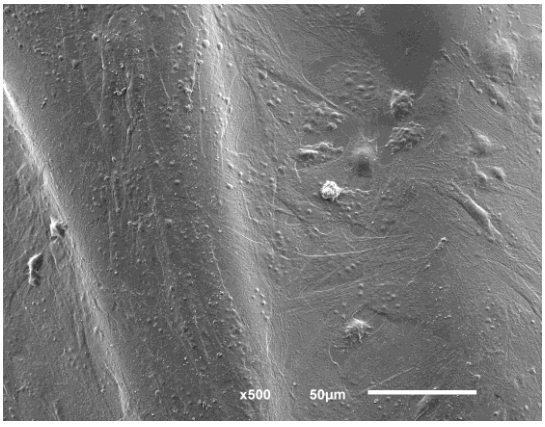

UNIVERSIDAD DE LAS PALMAS
DE GRAN CANARIA

D Mario Domingo Monzón Verona, COORDINADOR DEL PROGRAMA DE DOCTORADO en Ingenierías Química, Mecánica y de Fabricación DE LA UNIVERSIDAD DE LAS PALMAS DE GRAN CANARIA,

INFORMA,

Que la Comisión Académica del Programa de Doctorado, en su sesión de fecha _____ tomó el acuerdo de dar el consentimiento para su tramitación, a la tesis doctoral titulada "Estudio experimental de diferentes combinaciones de biomateriales con matriz de ácido poliláctico en fabricación aditiva con fines biomédicos" presentada por el doctorando D. Ricardo Donate González y dirigida por el Doctor Mario Domingo Monzón Verona, solicitando la Mención Internacional por disponer de los requisitos para ello de acuerdo con el Artº 18 del Reglamento de Estudios de Doctorado.

Y para que así conste, y a efectos de lo previsto en el Artº 11 del Reglamento de Estudios de Doctorado (BOULPGC 7/10/2016) de la Universidad de Las Palmas de Gran Canaria, firmo la presente en Las Palmas de Gran Canaria, a ___ de _____ de dos mil veintiuno.

UNIVERSIDAD DE LAS PALMAS DE GRAN CANARIA

UNIVERSIDAD DE LAS PALMAS DE GRAN CANARIA
ESCUELA DE DOCTORADO

Programa de doctorado en Ingenierías Química, Mecánica y de Fabricación

Título de la Tesis

Estudio experimental de diferentes combinaciones de biomateriales con matriz de ácido poliláctico en fabricación aditiva con fines biomédicos.

Tesis Doctoral presentada por D. Ricardo Donate González

Dirigida por el Dr. D. Mario Domingo Monzón Verona

El Director, **El Doctorando,**

Las Palmas de Gran Canaria, a 28 de abril de 2021

AGRADECIMIENTOS

Esta tesis doctoral ha sido cofinanciada por la Agencia Canaria de Investigación, Innovación y Sociedad de la Información de la Consejería de Economía, Industria, Comercio y Conocimiento y por el Fondo Social Europeo (FSE) Programa Operativo Integrado de Canarias 2014-2020, Eje 3 Tema Prioritario 74 (85%).

A mi director, Dr. Mario Monzón, por todo el apoyo brindado en el desarrollo de este trabajo.

A mi tutor, Dr. Nizardo Benítez, por ofrecerme su consejo siempre que lo he necesitado.

A todos mis compañeros del grupo de investigación en Fabricación Integrada y Avanzada, quienes además de haberme prestado su ayuda han hecho más ameno y entretenido el camino.

Gracias también al Dr. Francisco Rodríguez Esparragón y los compañeros de la Unidad de Investigación del Hospital Universitario de Gran Canaria Dr. Negrín, por su apoyo y consejo en el desarrollo de los ensayos biológicos.

I would like to thank Professor Chaozong Liu and Professor Ling Wang for giving me the opportunity to work in their research groups at the University College London and Xi'an Jiaotong University, respectively. Thanks also to them and to all the members of their groups for their kind help.

A nivel personal, gracias a mis amigos por estar siempre ahí, a Minerva y Mari por su ayuda, a mi hermano y mis padres por su apoyo incondicional durante todo este tiempo. Gracias a María Elena, por todo.

RESUMEN

El **objetivo principal** de esta tesis es proponer y evaluar diferentes estrategias que permitan obtener estructuras soporte mediante técnicas de fabricación aditiva, basadas en el empleo de una matriz de ácido poliláctico (PLA) y con el objetivo de su aplicación biomédica.

Este objetivo general se aborda a través de los siguientes **objetivos específicos**:

1. Optimizar las condiciones operativas de trabajo para la fabricación de estructuras soporte (conocidas como scaffolds en el campo biomédico) de base PLA mediante un proceso de extrusión de material (ISO/ASTM 52900: 2015), comúnmente conocido como modelado por deposición fundida (FDM). El diseño de los scaffolds se desarrolló de manera específica para la aplicación concreta de las estructuras 3D.

2. Formular mezclas de biomateriales capaces de proporcionar propiedades mejoradas en estructuras soporte de Ingeniería de Tejidos. Se introdujeron aditivos cerámicos en la matriz de PLA para mejorar la osteoconductividad del material polimérico y ajustar el perfil de degradación, las propiedades biológicas y mecánicas de las piezas 3D.

3. Estudiar el efecto de los tratamientos superficiales aplicados a las estructuras 3D. Con la modificación de la topografía y la química de la superficie de los scaffolds se busca afectar positivamente la interacción entre la célula y el material. Se evaluaron diferentes métodos de tratamiento con plasma de oxígeno y otros haciendo uso de disoluciones alcalinas aplicadas a las estructuras de PLA.

4. Introducir sustancias de origen biológico como recubrimientos bioactivos de los scaffolds después de su tratamiento superficial. Se desarrolló un procedimiento de recubrimiento con extractos de Aloe Vera para superficies de PLA, con el objetivo de aumentar la biofuncionalidad de la estructura 3D.

5. Caracterizar los scaffolds obtenidos como resultado de la aplicación de las estrategias anteriormente mencionadas. La evaluación de las propiedades de las piezas 3D funcionalizadas incluyó su caracterización morfológica, fisicoquímica, calorimétrica y mecánica. Además, teniendo en cuenta la aplicación biomédica prevista de los scaffolds de PLA desarrollados, se evaluaron sus propiedades biológicas en términos de adhesión y proliferación celular.

El tema de tesis propuesto se encuentra relacionado con las siguientes **líneas de investigación** del programa de doctorado en Ingenierías Química, Mecánica y de Fabricación:

- Caracterización y desarrollo de procesos de fabricación aditiva: FDM y sinterizado.
- Microfabricación aditiva de plásticos.
- Biomateriales para aplicaciones de ingeniería médica.

En las últimas décadas, las estrategias de **Ingeniería de Tejidos y Medicina Regenerativa** se han asentado como herramientas prometedoras para la regeneración del tejido óseo, con el objetivo de superar las limitaciones impuestas por las técnicas tradicionales de injerto. Algunos inconvenientes relacionados con la aplicación de estas últimas incluyen: morbilidad y dolor en el lugar de implantación, reabsorción variable, alta tasa de fallo en sitios específicos, falta de propiedades osteoinductivas, transmisión de patógenos, rechazo inmunológico y la necesidad de una segunda cirugía. La aplicación de técnicas de Ingeniería de Tejidos busca eludir las limitaciones anteriormente mencionadas al combinar células, estructuras soporte biocompatibles y moléculas bioactivas para inducir la regeneración de tejidos óseos afectados por procesos degenerativos, quirúrgicos o traumáticos.

Uno de los enfoques más prometedores en este campo es la implantación de estructuras porosas (scaffolds) biodegradables que imiten la composición de la matriz extracelular del tejido óseo, se asemejan a su estructura y posean propiedades mecánicas adecuadas para soportar el tejido durante su crecimiento. Otras características importantes que deben poseer los **scaffolds destinados a la regeneración ósea** incluyen: osteoconductividad, osteoinductividad, osteointegridad, respuesta no inmunogénica o tóxica, estructura de poros altamente interconectada, porosidad adecuada para permitir la transferencia de masa, potencial para encapsular biomoléculas y facilidad de fabricación con un coste relativamente bajo.

Teniendo en cuenta los requisitos de los scaffolds óseos, las técnicas de **fabricación aditiva** constituyen una potente herramienta para este tipo de aplicaciones, ya que permiten obtener estructuras 3D con un diseño específico en función de las características del paciente y las necesidades de los cirujanos para su implantación. Estas técnicas ofrecen además un control preciso sobre el tamaño y forma de los poros, así como de la porosidad de las piezas, de manera que estas características pueden ajustarse para imitar la función del tejido nativo óseo.

El **PLA** se ha utilizado ampliamente como material base para la fabricación de scaffolds en el campo de la Ingeniería de Tejidos aplicada a la regeneración de hueso, principalmente debido a su biocompatibilidad, biodegradabilidad, propiedades mecánicas adecuadas y perfil de degradación ajustable. El PLA también presenta buena procesabilidad mediante técnicas de fabricación aditiva, especialmente mediante procesos de extrusión. La aplicación biomédica de los scaffolds de PLA, sin embargo, se ve obstaculizada por la baja hidrofilicidad de su superficie, la falta de grupos reactivos en su estructura química de cadena y la liberación de subproductos ácidos durante su degradación, lo que podría conducir a una fuerte respuesta inflamatoria y afectar la regeneración del tejido. Los métodos propuestos para contrarrestar estos inconvenientes y **mejorar la biofuncionalidad** de los scaffolds de PLA incluyen:

1) La incorporación de aditivos a la matriz de PLA.

2) La aplicación de tratamientos superficiales a la estructura 3D.

3) La aplicación de recubrimientos bioactivos.

Las publicaciones científicas derivadas de esta tesis doctoral cubren las estrategias mencionadas, proponiendo métodos experimentales para mejorar las propiedades de los estructuras de base PLA obtenidas por AM y destinadas a la regeneración de tejido óseo. En total, se presentan cuatro trabajos publicados y otro actualmente en fase de revisión. Estos trabajos suponen el núcleo central del trabajo desarrollado, justifican la unidad temática y permiten la presentación de la presente tesis bajo la modalidad de **tesis por compendio de publicaciones**.

En el artículo "Additive manufacturing of PLA-based scaffolds intended for bone regeneration and strategies to improve their biological properties" se aborda el **estado del arte** de los scaffolds de base PLA obtenidos mediante técnicas de fabricación aditiva y destinados a la regeneración ósea. En un primer apartado de introducción se presentan los principales problemas y enfoques en el campo de la Ingeniería de Tejidos aplicada a la regeneración de hueso, el uso de materiales biodegradables para la fabricación de scaffolds y las características, ventajas y desventajas del uso de PLA como material base. A continuación, se presentan las características de los tejidos óseos, así como las estrategias y criterios de diseño de los scaffolds destinados a su regeneración. La parte principal de este trabajo es la sección relacionada con la aplicación de técnicas de fabricación aditiva para la obtención de scaffolds óseos con matriz de PLA. En la última sección, se presentan las estrategias disponibles para funcionalizar las piezas 3D de base PLA, incluyendo el empleo de aditivos, la aplicación de tratamientos superficiales y el uso de recubrimientos superficiales con compuestos bioactivos. Este trabajo fue publicado en la revista científica e-Polymers (ISSN: 1618-7229) en octubre de 2020.

La primera estrategia para mejorar las propiedades de la matriz de PLA, que comprende el **uso de aditivos** en combinación con el material base, se evaluó en la publicación de título "Comparison between calcium carbonate and β-tricalcium phosphate as additives of 3D printed scaffolds with polylactic acid matrix". Concretamente, el material base se combinó con partículas de carbonato de calcio ($CaCO_3$) y beta-fosfato tricálcico (β-TCP) para producir filamentos continuos que luego se utilizaron para la fabricación de scaffolds mediante FDM. Las estructuras 3D, obtenidas mediante el uso de diferentes combinaciones de estos materiales, se evaluaron para aplicaciones de regeneración de tejidos óseos en cuanto a sus características morfológicas, mecánicas y biológicas. Ambos aditivos cerámicos generaron un aumento en la porosidad, hidrofilicidad y rugosidad superficial de los scaffolds, favoreciendo así la adhesión y proliferación celular, tal y como se confirmó mediante microscopía electrónica de barrido (SEM). La introducción simultánea de ambos aditivos cerámicos en la matriz de PLA condujo a los mejores resultados en términos de actividad metabólica de células humanas de hueso cultivadas in vitro durante 7 días. Este trabajo fue publicado en la revista científica Journal of Tissue Engineering and Regenerative Medicine (ISSN: 1932-6254) en febrero de 2020.

De acuerdo con los resultados obtenidos en el trabajo anterior, los scaffolds composite que mostraron más potencial para la regeneración del tejido óseo (PLA:$CaCO_3$:β-TCP 95:2.5:2.5) se ensayaron en condiciones de **degradación** enzimática. Para acelerar la degradación del material base se utilizaron enzimas *Proteinasa K* y las muestras se caracterizaron mediante

microscopía óptica, SEM, pruebas de compresión y análisis termogravimétrico y calorimétrico. La velocidad de degradación de las estructuras 3D se incrementó con el uso de aditivos. Estos resultados se atribuyeron a la liberación de las partículas de aditivo y al tamaño de poro y la porosidad estadísticamente mayores de los scaffolds composite en comparación con los de PLA sin aditivos. Mejorar la tasa de degradación de los scaffolds de PLA impresos en 3D podría ser una ventaja para su aplicación en el campo de la Ingeniería de Tejidos, considerando el largo tiempo requerido para la degradación completa de las estructuras de PLA in vivo. Este trabajo, de título "Enzymatic degradation study of PLA-based composite scaffolds", fue publicado en la revista científica Reviews on Advanced Materials Science (ISSN: 1605-8127) en mayo de 2020.

En el trabajo de título "On the effectiveness of oxygen plasma and alkali surface treatments to modify the properties of polylactic acid scaffolds" se evaluó una segunda estrategia para mejorar las propiedades de los scaffolds de PLA: el **tratamiento superficial** de las estructuras 3D. Se aplicaron diferentes métodos de tratamiento superficial a las estructuras de PLA, incluyendo tratamientos con plasma y disoluciones alcalinas. Por un lado se propusieron tratamientos con plasma de oxígeno a baja presión con diferentes tiempos de exposición. En el caso de los tratamientos con álcalis se trabajó con disoluciones de hidróxido de sodio variando su concentración. Además, se estudió el efecto de una etapa final de lavado con ácidos orgánicos o inorgánicos en las características de las estructuras tratadas con disoluciones alcalinas. Las muestras se analizaron inmediatamente después de la aplicación de los tratamientos y dos semanas después, con el fin de evaluar la pérdida de las modificaciones introducidas con el paso del tiempo. La incorporación de grupos carboxilo a la superficie del PLA fue predominante en el caso de los tratamientos alcalinos. Por el contrario, los tratamientos con plasma de oxígeno generaron principalmente grupos hidroxilo en la superficie tratada, lo que condujo a una mayor hidrofilicidad sin afectar la morfología de la estructura. Este trabajo se envió a la revista científica Polymers (ISSN: 2073-4360) en abril de 2021 y actualmente se encuentra en revisión.

Una tercera estrategia para mejorar la biofuncionalidad de los scaffolds de PLA destinados a la regeneración de hueso consistió en la **aplicación de recubrimientos** de Aloe vera. Los resultados de esta evaluación se presentaron en la publicación de título "Evaluation of Aloe Vera Coated Polylactic Acid Scaffolds for Bone Tissue Engineering". Después de tratar la superficie de las estructuras 3D con plasma de oxígeno, utilizando un método descrito en el trabajo anterior, se utilizaron extractos de Aloe vera a diferentes valores de pH para recubrir las piezas. La modificación de la superficie del material base debido a la incorporación de compuestos bioactivos de Aloe vera se evaluó mediante análisis de espectroscopia de fotoelectrones emitidos por rayos X (XPS) y mediciones del ángulo de contacto. De los resultados del ensayo de degradación enzimática se dedujo una relación entre el pH del extracto de Aloe vera utilizado como recubrimiento y la velocidad de degradación de las muestras. Así, por ejemplo, el recubrimiento de Aloe vera aplicado a pH 3 retrasó la degradación de las estructuras en comparación al resto de grupos ensayados. Los scaffolds de PLA tratados con plasma de oxígeno y luego recubiertos con Aloe vera a pH 3 mostraron también los mejores resultados en términos de actividad metabólica de osteoblastos humanos cultivados durante 10 días in vitro. Se obtuvieron diferencias

estadísticamente muy significativas ($p < .001$) entre este grupo y las muestras tratadas con plasma, lo que confirma la mayor biofuncionalidad de los scaffolds recubiertos con Aloe vera y su potencial de aplicación para la regeneración de tejido óseo. Este trabajo fue publicado en la revista científica Applied Sciences (ISSN: 2076-3417) en abril de 2020.

Cabe señalar que la **combinación de estas estrategias** permite obtener una estructura 3D funcionalizada tanto en su superficie como en el interior. Aunque este enfoque combinado no fue explorado en los trabajos publicados, se obtuvieron resultados experimentales relacionados con esta estrategia durante el desarrollo del proyecto de tesis. Los scaffolds composite recubiertos con extractos de Aloe vera mostraron una mejora significativa de su biofuncionalidad en términos de actividad metabólica celular. La adhesión y la proliferación de osteoblastos humanas cultivados en los scaffolds durante 13 días resultaron cuantitativamente superiores con la aplicación de los recubrimientos a pH 3 y 4.

A pesar de los prometedores resultados obtenidos en este trabajo con los scaffolds composite, se encontraron limitaciones impuestas por la técnica de fabricación en la producción de los mismos. La formación de aglomerados de partículas cerámicas restringió el uso de aditivos a un porcentaje de concentración máxima en la mezcla del 5%. La mejora de los procesos de mezcla y extrusión de los filamentos composite necesarios para alimentar la impresora 3D permitiría mejorar la dispersión de las partículas cerámicas en la matriz de PLA. De esa manera, se podría utilizar una mayor concentración de los aditivos para generando una mejora aún mayor de las propiedades del material base.

Otra de las **líneas de investigación futuras** comprende una caracterización química más amplia de los scaffolds para evaluar el tipo de enlaces formados y los compuestos bioactivos incorporados a la superficie después de la aplicación de los diferentes recubrimientos de Aloe Vera propuestos. Estos resultados proporcionarían información sobre cuál de los componentes del extracto de Aloe vera tiene un efecto de mejora de la actividad metabólica de las células óseas.

Además, a parte de los estudios de degradación enzimática in vitro presentados en este trabajo, se propone la realización de una prueba de degradación hidrolítica de las estructuras 3D. Dado que las condiciones hidrolíticas son más representativas de las condiciones de implantación in vivo, los resultados de esta prueba proporcionarían información relevante sobre el perfil de degradación de los scaffolds de base PLA y en qué medida la liberación de los aditivos cerámicos puede contrarrestar la disminución del pH del medio circundante debido a la degradación de la matriz polimérica.

Los scaffolds de base PLA desarrollados en la presente tesis muestran potencial para su aplicación en la regeneración de tejidos óseos. Además, estas estructuras biofuncionalizadas pueden servir como base para la fabricación de scaffolds bifásicos destinados a regiones articulares. El ensamblaje de los scaffolds de PLA para la regeneración de hueso con estructuras porosas destinadas a la regeneración del cartílago permitiría obtener la unidad osteocondral.

INDEX

1. INTRODUCTION

In this first section, the main objectives of the thesis entitled "**Experimental study of different combinations of biomaterials with polylactic acid matrix in Additive Manufacturing with biomedical purposes**" are presented. The scientific publications derived from this work are also specified.

As this doctoral thesis is presented under the modality of **compendium of publications**, the justification of the thematic unit is carried out, emphasizing the relationship between the different articles and how they constitute a good summary of the work developed.

1.1. OBJETIVES

The **main objective** of this thesis is to propose and evaluate different strategies that allow obtaining functionalised support structures by Additive Manufacturing techniques (AM), based on polylactic acid (PLA) and for Tissue Engineering applications.

This general objective has been addressed through the following **specific objectives**:

1. To optimize the operating work conditions to manufacture polylactic acid-based support structures (known as scaffolds in the biomedical field) by a material extrusion process (ISO/ASTM 52900:2015), commonly known as fused deposition modelling (FDM). A specific scaffold design was also developed for the targeted application of the 3D constructs.

2. To formulate mixtures of biomaterials capable of providing improved properties in tissue-engineered support structures applicable to joint regions. Ceramic additives were introduced into the polylactic acid matrix to enhance the osteoconductivity of the base material and tailor the degradation profile, biological properties and mechanical characteristics of the 3D construct.

3. To study the effect of surface treatments applied to the 3D structures. The modification of the scaffold's topography and surface chemistry aims to positively affect cell-material interaction. Different oxygen plasma and alkali treatments methods applied to PLA scaffolds were evaluated.

4. To introduce substances of biological origin as bioactive coatings of the surface-treated scaffolds. A coating procedure using Aloe Vera extracts was developed for PLA surfaces, aiming to increase the biofunctionality of the 3D structure.

5. To characterize the scaffolds obtained as a result of the application of the aforementioned strategies. The assessment of the properties of the functionalized 3D constructs included their morphological, physicochemical, calorimetric and mechanical characterization. In addition, and taking into account the intended biomedical application of the PLA-based scaffolds developed, their biological properties were evaluated in terms of cell attachment and proliferation.

A graphical summary of the work carried out is presented in Figure 1.

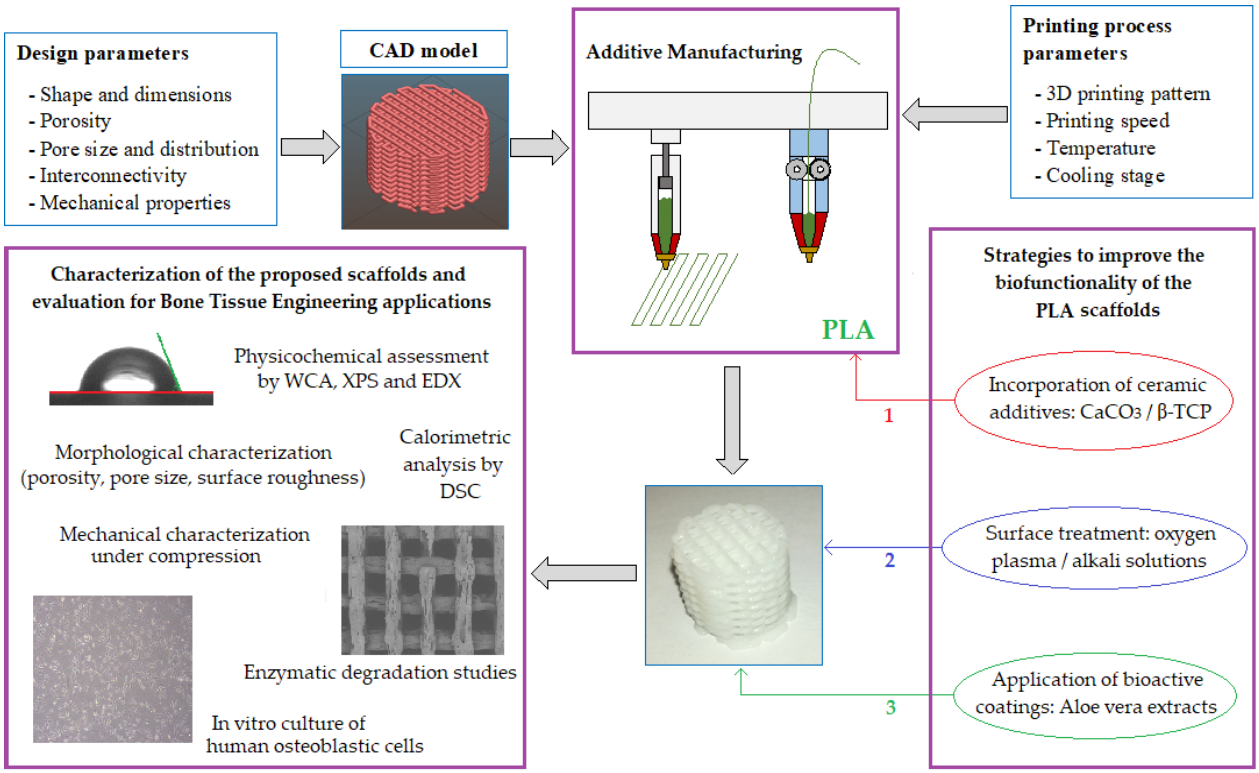

Figure 1. Schematic summary of the work developed in the present doctoral thesis.

1.2. PUBLICATIONS

The scientific publications derived from this doctoral thesis comprise four published works and another one currently in the revision phase. A summary of each publication is presented below.

Donate, R.; Monzón, M.; Alemán-Domínguez, M.E. Additive manufacturing of PLA-based scaffolds intended for bone regeneration and strategies to improve their biological properties. *e-Polymers* **2020**, *20*, 571–599.

This extensive review addresses the **State of the Art** of PLA-based scaffolds obtained by AM techniques and intended for bone regeneration. The main issues and approaches in the Bone Tissue Engineering field are presented, including the use of biodegradable materials for scaffold manufacturing. More specifically, the characteristics, advantages and disadvantages on the use of PLA as base material are summarized. In addition, in order to better understand the requirements for bone regeneration, the characteristics of this type of tissue are presented, as well as the design strategies and criteria for bone scaffolds. The main part of this work is the section related to the application of AM techniques for PLA-based bone scaffolds manufacturing. In particular, the focus was put on vat photopolymerization, powder bed fusion and material extrusion methods, since these are AM technologies extensively employed for polymeric-based scaffold manufacturing. In the last section, the

available strategies to functionalize PLA-based 3D construct are presented, including the combination of the matrix with additives, the application of surface treatments and the use of surface coatings with biological substances. This work was published on October 2020 in e-Polymers scientific journal (ISSN: 1618-7229, JCR-2019 impact factor: 1.675**,** Q3 in the area Polymer Science).

Donate, R.; Monzón, M.; Ortega, Z.; Wang, L.; Ribeiro, V.; Pestana, D.; Oliveira, J.M.; Reis, R.L. Comparison between calcium carbonate and β-tricalcium phosphate as additives of 3D printed scaffolds with polylactic acid matrix. *J Tissue Eng Regen Med* **2020**, 14, 272–283.

The **use of additives** as a first strategy to improve the properties of the PLA matrix was evaluated in this work. The base material was combined with calcium carbonate ($CaCO_3$) and beta-tricalcium phosphate (β-TCP) particles to produce continuous filaments that were later used to manufacture composite scaffolds by FDM. The 3D structures obtained by using different combinations of these materials were evaluated for Bone Tissue Engineering applications and their morphological, mechanical, and biological were assessed. Both ceramic additives induced an increase in the porosity, hydrophilicity and surface roughness of the scaffolds, thus favouring cell attachment and proliferation, as confirmed by scanning electron microscopy (SEM) observations. Quantitatively, the samples containing both additives (PLA:$CaCO_3$:β-TCP 95:2.5:2.5) showed the best results in terms of metabolic activity of human osteoblastic osteosarcoma cells, according to the CCK-8 test method. This work was published on February 2020 in the Journal of Tissue Engineering and Regenerative Medicine (ISSN: 1932-6254, JCR-2019 impact factor: 3.078, Q2 in the areas Engineering and Biomedical).

Donate, R.; Monzón, M.; Alemán-Domínguez, M.E.; O.; Ortega, Z. Enzymatic degradation study of PLA-based composite scaffolds. *Rev Adv Mater Sci* **2020**, 59, 170–175.

Using to the results obtained in the previous work, the composite scaffolds that showed more potential for bone tissue regeneration (PLA:$CaCO_3$:β-TCP 95:2.5:2.5) were tested under enzymatic **degradation** conditions. *Proteinase K* enzymes were used to accelerate the degradation of the base material and the samples were characterized by optical microscopy, scanning electron microscopy, compression testing and thermogravimetric and calorimetric analysis. The degradation rate of the 3D printed scaffolds was increased with the incorporation of the additives. This result was related to release of the ceramic particles and the enhanced microporosity of composite structures. This work was published on May 2020 in Reviews on Advanced Materials Science scientific journal (ISSN: 1605-8127, JCR-2019 impact factor: 1.197, Q4 in the area Materials Science).

Donate, R.; Alemán-Domínguez, M.E.; Monzón, M. On the effectiveness of oxygen plasma and alkali surface treatments to modify the properties of polylactic acid scaffolds. (Under review).

A second strategy to improve the PLA-based scaffolds properties was evaluated in this work: the **surface treatment** of the polymeric 3D structures. Low-pressure oxygen plasma treatments at different exposure times were proposed, while the concentration of sodium

hydroxide solutions was varied in the case of alkali treatments. Also, the effect of a washing step using organic or inorganic acids on the surface-treated structures was studied. The samples were tested right after applying the treatments and two weeks later, in order to evaluate the loss of modifications introduced over time. The incorporation of carboxyl groups to the PLA surface prevailed in the case of alkali treatments. In contrast, oxygen plasma treatments mainly generated hydroxyl groups in the treated surface, which led to an increased hydrophilicity without affecting the morphology of the structure. This work was submitted on April 2021 to Polymers scientific journal (ISSN: 2073-4360, JCR-2019 impact factor: 3.426, Q1 in the area Polymer Science) and is currently under review.

Donate, R.; Alemán-Domínguez, M.E.; Monzón, M.; Yu, J.; Rodríguez-Esparragón, F.; Liu, C. Evaluation of Aloe Vera Coated Polylactic Acid Scaffolds for Bone Tissue Engineering. *Appl Sci* **2020**, 10, 2576.

In this study, Aloe vera coatings were proposed as a third strategy to improve the biofunctionality of PLA scaffolds intended for bone regeneration. After surface-treating the 3D constructs with oxygen plasma, using a method described in our previous work, Aloe vera extracts at different pH values were used to coat the structures. The surface modification of the base material due to the **incorporation of bioactive compounds** was assessed by X-ray photoelectron spectroscopy (XPS) analysis and water contact angle measurements. The results of the enzymatic degradation test suggested a relation between the pH of the Aloe vera extract and the degradation rate of the samples. Finally, the in vitro culture of human osteoblast-like cells on the scaffolds showed that coated samples promoted cell metabolic activity. This work was published on April 2020 in Applied Sciences scientific journal (ISSN: 2076-3417, JCR-2019 impact factor: 2.217, Q2 in the area Engineering).

1.3. JUSTIFICATION

In the last decades, **Tissue Engineering and Regenerative Medicine** strategies have emerged as promising tools for bone tissue regeneration, aiming to overcome the limitations imposed by the traditional bone grafts techniques. Some drawbacks related to the application of auto-, allo- and xeno-grafts for bone healing are: donor-site morbidity and pain, variable resorption, high rate of failure in specific sites, supply limitation, lack of osteoinductive properties, pathogen transmission, immune rejection and the need of a second surgery [1]. Bone Tissue Engineering (BTE) could circumvent the aforementioned limitations by combining cells, biocompatible constructs and bioactive molecules to induce the regeneration of bone tissues affected by degenerative, surgical or traumatic processes.

One of the most promising approaches of BTE is the implantation of **porous biodegradable scaffolds** that mimic the composition of the extracellular matrix (ECM) of bone tissue, resemble its structure, and possess sufficient mechanical properties to support the tissue during its growth. Other important features of scaffolds intended for bone regeneration include: osteoconductivity, osteoinductivity, osteointegrity, non-immunogenic

and nontoxic response, highly interconnected pore structure, adequate porosity to allow mass transfer, potential to encapsulate biomolecules and ease of manufacturing at relatively low cost [1,2].

Taking into account the requirements for bone scaffolds, **Additive Manufacturing** (AM) techniques constitute a powerful tool for BTE applications, since they allow obtaining tissue-engineered constructs with a specific design based on the patient and the surgeons' needs for their implantation. AM techniques offer precise control over pore size, pore shape and porosity of the scaffolds, which could be adjusted to mimic the function of native bone tissue [3].

PLA has been extensively used as base material for scaffold manufacturing in the BTE field, mainly due to its biocompatibility, biodegradability, suitable mechanical properties and tunable degradation rate. PLA has also a good processability by AM techniques, especially by material extrusion processes [4]. The biomedical application of PLA scaffolds, however, is hindered by the low hydrophilicity of their surface, the lack of reactive side chain groups and the release of acidic degradation byproducts, which could lead to a strong inflammatory response and affect tissue regeneration [5]. Proposed methods to counteract these drawbacks and **enhance the biofunctionallity of PLA scaffolds** include:

1) The incorporation of additives to the PLA matrix: allows tailoring the degradation profile, biological and mechanical properties of the construct [6,7].

2) The application of surface treatments to the 3D structure: aims to modify its topography and surface chemistry, thus enhancing cell attachment [8,9].

3) The application of bioactive coatings: generally takes place after the surface treatment of the scaffolds, as the adhesion of bioactive compounds to the structure is enhanced [10,11].

The scientific publications derived from this doctoral thesis cover the aforementioned strategies, proposing experimental methods to improve the properties of PLA-based scaffolds obtained by AM and intended for bone regeneration. In this way, the following relations can be noted:

- The works entitled “Comparison between calcium carbonate and β-tricalcium phosphate as additives of 3D printed scaffolds with polylactic acid matrix” and “Enzymatic degradation study of PLA-based composite scaffolds” comprised the manufacturing, characterization and evaluation of **composite** PLA-based scaffolds for their application in the BTE field.

- On the other hand, the effect of different **surface treatments** applied to the PLA scaffolds were assessed in the work entitled “On the effectiveness of oxygen plasma and alkali surface treatments to modify the properties of polylactic acid scaffolds”.

- Finally, the publication "Evaluation of Aloe Vera Coated Polylactic Acid Scaffolds for Bone Tissue Engineering" was focused on the evaluation of an innovative **coating** based on the incorporation of bioactive compounds from Aloe vera extracts.

- The **theoretical framework** of all the publications mentioned above was presented in the review paper entitled "Additive manufacturing of PLA-based scaffolds intended for bone regeneration and strategies to improve their biological properties".

It is worth noting that the combination of the latter strategies allows obtaining a 3D structure that is functionalized both on its surface and at the bulk. Although this combined approach was not explored in the published works, experimental results related to this strategy were obtained during the development of the thesis project. The more relevant findings in this regard are included in section 4.2.

The thesis topic is related to the following **research lines** of the doctoral program in Chemical, Mechanical and Manufacturing Engineering:

- Characterization and development of Additive Manufacturing processes: FDM and sintering.
- Additive microfabrication of plastics.
- Biomaterials for medical engineering applications.

1.4. REFERENCES

1. Roseti, L.; Parisi, V.; Petretta, M.; Cavallo, C.; Desando, G.; Bartolotti, I.; Grigolo, B. Scaffolds for Bone Tissue Engineering: State of the art and new perspectives. *Mater Sci Eng C* 2017, *78*, 1246–1262.
2. Wubneh, A.; Tsekoura, E.K.; Ayranci, C.; Uludağ, H. Current state of fabrication technologies and materials for bone tissue engineering. *Acta Biomater* **2018**, *80*, 1–30.
3. Henkel, J.; Woodruff, M.A.; Epari, D.R.; Steck, R.; Glatt, V.; Dickinson, I.C.; Choong, P.F.M.; Schuetz, M.A.; Hutmacher, D.W. Bone Regeneration Based on Tissue Engineering Conceptions — A 21st Century Perspective. *Bone Res* **2013**, *3*, 216–248.
4. Chiulan, I.; Frone, A.; Brandabur, C.; Panaitescu, D. Recent Advances in 3D Printing of Aliphatic Polyesters. *Bioengineering* **2017**, *5*, 2.
5. Araque-Monrós, M.C.; Vidaurre, A.; Gil-Santos, L.; Gironés Bernabé, S.; Monleón-Pradas, M.; Más-Estellés, J. Study of the degradation of a new PLA braided biomaterial in buffer phosphate saline, basic and acid media, intended for the regeneration of tendons and ligaments. *Polym Degrad Stab* **2013**, *98*, 1563–1570.
6. Puppi, D.; Chiellini, F.; Piras, A.M.; Chiellini, E. Polymeric materials for bone and cartilage repair. *Prog Polym Sci* **2010**, *35*, 403–440.

7. Esposito Corcione, C.; Gervaso, F.; Scalera, F.; Padmanabhan, S.K.; Madaghiele, M.; Montagna, F.; Sannino, A.; Licciulli, A.; Maffezzoli, A. Highly loaded hydroxyapatite microsphere/ PLA porous scaffolds obtained by fused deposition modelling. *Ceram Int* **2019**, *45*, 2803–2810.

8. Wang, M.; Favi, P.; Cheng, X.; Golshan, N.H.; Ziemer, K.S.; Keidar, M.; Webster, T.J. Cold atmospheric plasma (CAP) surface nanomodified 3D printed polylactic acid (PLA) scaffolds for bone regeneration. *Acta Biomater* **2016**, *46*, 256–265.

9. Yamaguchi, M.; Shinbo, T.; Kanamori, T.; Wang, P.C.; Niwa, M.; Kawakami, H.; Nagaoka, S.; Hirakawa, K.; Kamiya, M. Surface modification of poly(L-lactic acid) affects initial cell attachment, cell morphology, and cell growth. *J Artif Organs* **2004**, *7*, 187–193.

10. Teixeira, B.N.; Aprile, P.; Mendonça, R.H.; Kelly, D.J.; Thiré, R.M. da S.M. Evaluation of bone marrow stem cell response to PLA scaffolds manufactured by 3D printing and coated with polydopamine and type I collagen. *J Biomed Mater Res - Part B Appl Biomater* **2019**, *107*, 37–49.

11. Martin, V.; Ribeiro, I.A.; Alves, M.M.; Gonçalves, L.; Claudio, R.A.; Grenho, L.; Fernandes, M.H.; Gomes, P.; Santos, C.F.; Bettencourt, A.F. Engineering a multifunctional 3D-printed PLA-collagen-minocycline-nanoHydroxyapatite scaffold with combined antimicrobial and osteogenic effects for bone regeneration. *Mater Sci Eng C* **2019**, *101*, 15–26.

2. PUBLISHED WORKS

Additive manufacturing of PLA-based scaffolds intended for bone regeneration and strategies to improve their biological properties

Review Article

Ricardo Donate*, Mario Monzón, and María Elena Alemán-Domínguez

Additive manufacturing of PLA-based scaffolds intended for bone regeneration and strategies to improve their biological properties

https://doi.org/10.1515/epoly-2020-0046
received October 30, 2019; accepted July 06, 2020

Abstract: Polylactic acid (PLA) is one of the most commonly used materials in the biomedical sector because of its processability, mechanical properties and biocompatibility. Among the different techniques that are feasible to process this biomaterial, additive manufacturing (AM) has gained attention recently, as it provides the possibility of tuning the design of the structures. This flexibility in the design stage allows the customization of the parts in order to optimize their use in the tissue engineering field. In the recent years, the application of PLA for the manufacture of bone scaffolds has been especially relevant, since numerous studies have proven the potential of this biomaterial for bone regeneration. This review contains a description of the specific requirements in the regeneration of bone and how the state of the art have tried to address them with different strategies to develop PLA-based scaffolds by AM techniques and with improved biofunctionality.

Keywords: polylactic acid, bone tissue engineering, composite materials

1 Introduction

1.1 Tissue engineering (TE): issues and strategies

TE aims to replace or restore damaged tissue by using artificial constructs that direct new tissue formation. This field integrates knowledge from biology, materials science, mechanical engineering and clinical sciences, offering new opportunities to treat patients that suffer from diseases and injuries affecting tissues like bone, cartilage, skin, nerves or even blood vessels (1–5). TE strategies commonly involve the combination and manipulation of cells, biodegradable constructs and bioactive molecules to induce the formation of new specific tissue. The final construct should resemble the structure and mechanical characteristics of the tissue to be regenerated in order to maintain the tissue functionality (6,7). One of the most promising approaches to reach the objectives of TE is the use of a scaffolding structure which would support the tissue during its growth (8,9). Scaffolds for TE applications must possess specific characteristics including biocompatibility, suitable mechanical properties, ease of sterilization, high porosity, high surface area and controllable interconnected porosity to enhance cell growth and support vascularization (6,10). Porosity and pore size play a major role on the functionality of 3D scaffolds, as the formation of new tissues depends on the characteristics of the interconnected network of the structure (11–14). Besides, it is imperative to consider the relationship between the mechanical and mass transport properties during its design stage (15). The scaffolding structure may be combined with living cells (16), growth factors (16), bioactive substances (17) or drugs (18) to increase the biological functionality of the implant. Efforts are even been made to design scaffolds that could mimic the functions of the extracellular matrix (ECM) by incorporating bioactive signals on the construct's surface with precise spatial distribution, thus opening the possibility of controlling cell response (19,20). In Figure 1, different research strategies for the use of PLA-based scaffolds for bone regeneration discussed in this work are summarized.

1.2 Biomaterials: interest of biodegradable materials

Scaffolds used in TE are usually made of titanium (21), bioceramic materials (22), natural or synthetic polymers (23)

* **Corresponding author: Ricardo Donate,** Departamento de Ingeniería Mecánica, Universidad de Las Palmas de Gran Canaria, Campus Universitario de Tafira s/n, 35017, Las Palmas, Spain, e-mail: ricardo.donate@ulpgc.es; tel: +34-928-45-8603
Mario Monzón, María Elena Alemán-Domínguez: Departamento de Ingeniería Mecánica, Universidad de Las Palmas de Gran Canaria, Campus Universitario de Tafira s/n, 35017, Las Palmas, Spain

and composites (24). All of these are biomaterials, that is, materials that can be integrated in the surrounding tissue without eliciting any undesirable host reaction. While biocompatibility is a mandatory requirement for TE scaffolds, biodegradability of the engineered structure is a characteristic of utmost interest associated with the group of polymeric biomaterials. Complete integration of a degradable polymeric scaffold with new tissue can be achieved as the byproducts of the degradation process are excreted or reabsorbed into the patient's body, without the need of an explant surgical procedure or surgical revision (25,26). Biodegradable scaffolds are a really interesting option in TE applications, as they degrade at a rate that (ideally) matches the growth rate of the tissue to be regenerated. The degradation profile of these scaffolds should ensure sufficient mechanical support while the new tissue is being formed, as well as no immune or inflammatory response of the surrounding tissues due to the release of the scaffold's degradation byproducts (27).

Different materials have been explored to manufacture biodegradable scaffolds, including both synthetic and natural polymers. Among the latter, it is possible to highlight the work related to the use of collagen (28), chitosan (29) or alginate (30). Regarding synthetic polymers, the most promising ones are polycaprolactone (PCL) (31), polylactic acid (PLA) (32,33) and poly(lactide-*co*-glycolide) (PLGA) (34). Synthetic polymers have steady and standard properties than can be modified in a relatively easy way during their industrial production. In contrast, the properties of natural polymers are highly dependent on the source of the material (35). As natural polymers can be found in the ECM, polymers of natural origin have, in general, better biofunctionality than the synthetic ones, which lack in bioactivity, have lower hydrophilicity and, therefore, are not able to promote cell adhesion (36). However, synthetic polymers have higher processability, more controllable degradation rates and better mechanical properties, as they are stiffer than natural polymers. The combination of natural and synthetic polymers is a promising approach to overcome the above-mentioned limitations.

1.3 PLA as base material for scaffold manufacturing: advantages and disadvantages

PLA is a biodegradable thermoplastic aliphatic polyester that has been extensively used in TE applications as base material for scaffolds intended for bone, cartilage,

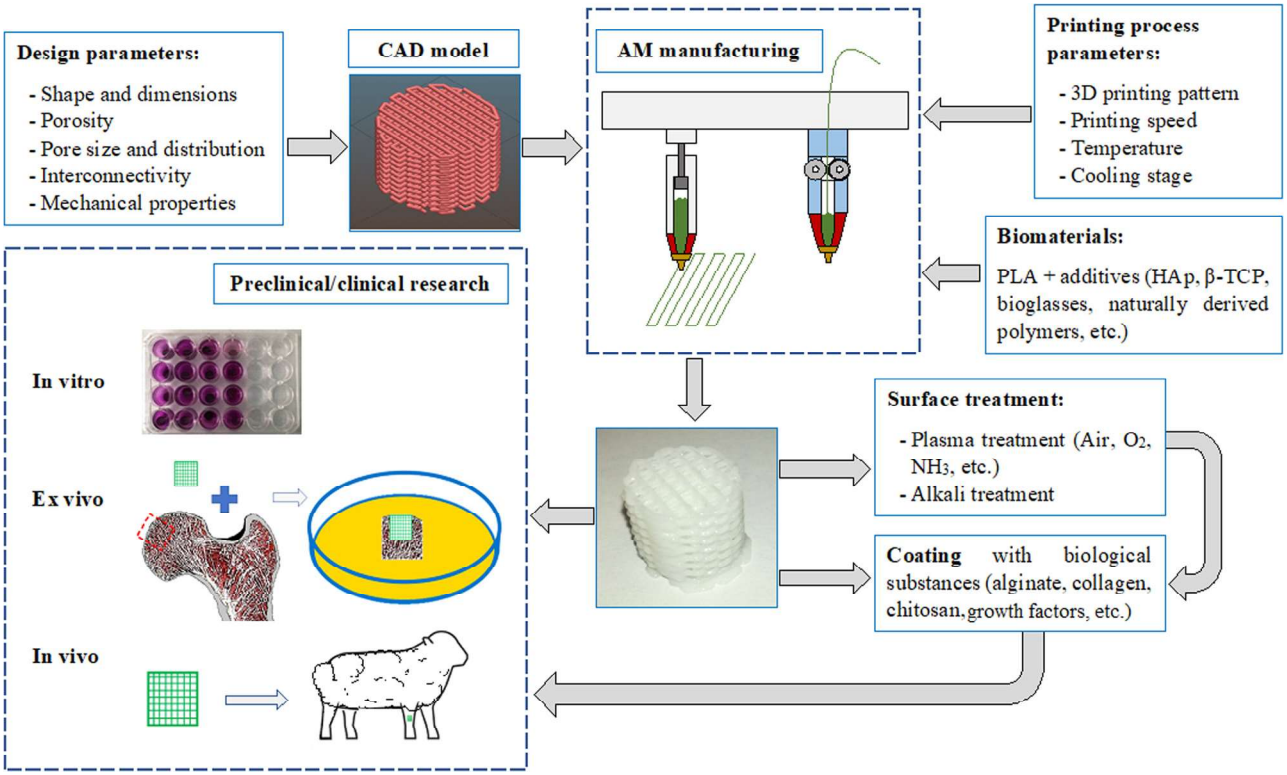

Figure 1: Research strategies for the application of PLA-based scaffolds in the bone tissue engineering field.

tendon, neural or vascular regeneration (26). This is a biomaterial that has been approved by the Food and Drug Administration for direct contact with biological fluids (37) and that can be obtained from renewable resources at relatively low costs. The most generally used methods to produce PLA are direct polycondensation of lactic acid and ring opening polymerization (ROP) of lactide, which is the cyclic dimer of lactic acid (38,39). Lactic acid (2-hydroxycarboxylic acid) is a chiral molecule with two stereoisomers: L-lactic acid and D-lactic acid (39). The direct polycondensation method is especially effective to obtain copolymers resulting from the combination of L-lactic acid with other monomers. Even though this method is a cheaper option than ROP, the process has a major limitation related to the simultaneous production of water and organic solvents, which can lead to the reduction of the molecular weight of the final product. Unlike the previous method, ROP allows to obtain PLA with high molecular weight, using lactides as precursors of the reaction. As lactides are chiral molecules, PLA can come in different stereochemical forms: poly(L-lactic acid) (PLLA), poly(D-lactic acid) (PDLA) and poly(D,L-lactic acid) (PDLLA) (40) (Figure 2). By modifying the initial composition, the properties of the polymer can be adjusted to the specific application (39). Properties of PLA also depend on its processing temperature and molecular weight.

An important property of PLA is the crystallinity ratio, which is influenced by the stereochemistry and thermal history of the polymer. Crystallinity influences many polymers' final characteristics, including mechanical properties, degradation rate, glass transition temperature and melting temperature (41,42). PLA with high crystallinity rate is obtained with a low content of D-enantiomer, while the polymer can be fully amorphous with D-content higher than a 20%. The glass transition temperature (T_g) of PLA is usually in the range from 50°C to 65°C, being the melting temperature (T_m) around 170–180°C. A decrease in the crystallinity rate of the polymer causes a decrease in both temperatures (43). On the other hand, the molecular weight of the polymer has an impact on the mechanical properties of the polymer and its degradation profile. The long time needed for the complete degradation *in vivo* of high molecular weight PLA samples has been pointed out as one of the causes in the appearance of inflammatory reactions in the surrounding tissues (44). For that reason, PLA with low molecular weight is preferred for TE applications because of its higher degradation rate, which in any case should match the rate of tissue growth and provide sufficient mechanical support.

Due to its biocompatibility, biodegradability and suitable mechanical properties, PLA has been extensively used in the biomedical field, including applications like suture, bone fixation material, drug delivery systems and TE (45). PLA has also a good processability by different techniques and, as we have mentioned before, its degradation rate, physical and mechanical properties can be adjusted over a wide range by modifying the molecular weight or the copolymer ratio (6). For example, PDLA is mainly used in drug delivery systems due to its faster degradation rate, while PLLA is the most chosen option for load-bearing applications because of its superior mechanical properties (46). PLLA has a T_g in the range of 60–65°C, a melting temperature of around 175°C and a mechanical strength of 4.8 GPa (26). PLLA also has a higher biological activity, showing more potential for its use in the TE field. On the other hand, because of its high mechanical stability and biocompatibility *in vivo*, PDLLA have recently gained attention as a base material for drug-delivery systems and scaffold manufacturing (46).

Biodegradability is another important characteristic of PLA for its application as base material for scaffold manufacturing, as it can be completely degraded by random hydrolytic chain scission, generating monomers of lactic acid that are eliminated from the patient's body through the tricarboxylic acid cycle (42,47). Two mechanisms have been reported for PLA degradation: surface erosion, in which degradation is located at the polymer–water interface, and bulk erosion, in which a homogeneous degradation is observed over the polymer's surface (48). PLA degradation occurs by uptake of water followed by the hydrolysis of ester bonds (46). This hydrolytic degradation is initiated in the amorphous regions of the material, which ester links are more easily broken by its reaction with water. This first step is followed by the reorganization of the polymeric chains as a consequence of its increased mobility. Then, the degradation process advances towards crystalline regions of the material, initially less exposed to it due to their ordered structure (49). There seems to be also a contribution to the degradation of PLA caused by enzymes from the local environment, but it is yet clear if they act enhancing the degradation rate or simply favoring the removal of degradation byproducts (39).

The influence of the initial degree of crystallinity on the degradation rate of PLA is a controversial matter in the literature, as some authors have concluded that the hydrolysis of amorphous polymers is faster due to the lack of crystalline regions (46), while others defend the hypothesis that a higher crystallinity of PLA increases the degradation rate due to an increase in

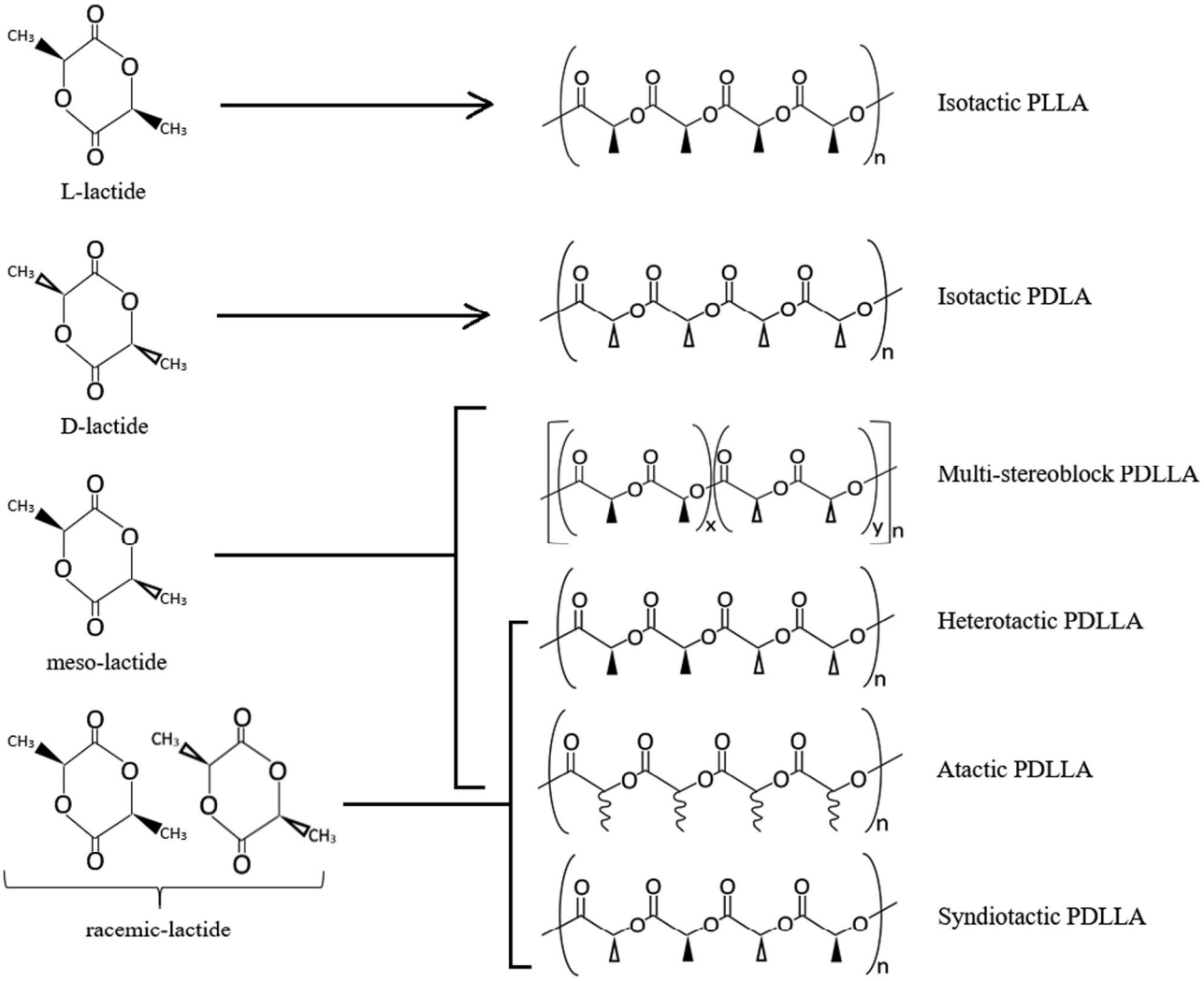

Figure 2: Lactide isomers and stereochemical forms of PLA.

hydrophilicity (50). In the end, the material properties should be adjusted so the PLA-based scaffold can be completely degraded while providing mechanical support and without causing any adverse tissue reaction until being eliminated from the human body through metabolic pathways. The generally slow degradation rate of PLA (sometimes up to several years) (44), the abrupt release of the acidic degradation byproducts or its accumulation because of an inefficient removal from the surroundings of the scaffold's location, could generate a strong inflammatory response, affecting cell growth and tissue regeneration (49). This is actually the major limitation for the application of PLA as base material for TE applications. Several strategies have been proposed in order to counteract the acidic byproducts and stabilize the pH of the surrounding tissues, including the use of low molecular weight PLA (51) and the combination of the polymeric matrix with basic compounds such as bioactive glasses (BG) and calcium phosphates (CaP) (52,53).

Some other important drawbacks of PLA are: (i) its poor toughness, as it is a brittle material with less than a 10% elongation at break (54); (ii) the lack of reactive side-chain groups, which make it difficult to induce surface or bulk modifications to improve its properties (37); and especially (iii) its low hydrophilicity (55), having a water contact angle of around 80°. The latter disadvantage generates poor wetting properties and a lack of cell attachment and interaction between the polymer and the surrounding tissues (56). Taking all these characteristics into account, PLA bioactivity has to be enhanced for its use in the target TE application. In this review, we discuss the published work describing the advances on the development of PLA-based scaffolds for bone tissue

engineering (BTE) obtained through additive manufacturing (AM) techniques. Strategies to improve the functionality of the scaffolds are also discussed.

2 PLA-based scaffolds for bone regeneration

2.1 Characteristics of bone tissue

The increasing ageing and life expectancy of global population is a challenge for the therapeutic alternatives currently available for the treatment of hard tissue affections, like those related to bone tissue loss due to degenerative (57), surgical or traumatic processes. During the last decades, important advances in surgical techniques for skeletal reconstruction have been presented, aiming to relieve patient's pain, improve their quality of life and also reduce social healthcare costs. BTE is the most promising technique to be used for bone regeneration, being an alternative to the conventional bone grafts. The latter strategy for bone healing includes auto-, allo- and xenografts, which application is hindered by some important drawbacks, e.g., donor-site morbidity and pain, difficult graft resorption, lack of osteoinductive properties, immune rejection and risk of pathogen transfer (6,58). BTE could eliminate the aforementioned issues by the implantation of porous scaffolds that mimic the natural bone ECM, being generally combined with osteogenic cells and morphogenic signals to promote cell growth, proliferation and differentiation (58). Hence, a broad knowledge of the characteristics of bone tissue is essential when designing the support structures for its regeneration.

Bone is a composite material with an organic phase representing around a 30% of the weight and an inorganic phase as the remaining 70%. The organic phase is mainly type-I collagen and water, but also contains small amounts of bone-resident cells (around a 2%) (59), glycoproteins, glycosaminoglycans and proteoglycans (60). The inorganic phase is composed of CaP, the majority of those being hydroxyapatite crystals (HAp, $Ca_{10}(PO_4)_6(OH)_2$). The Ca:P ratio in the mineral phase varies between 1.37 and 1.87, due to the heterogeneous presence of additional ions, such as bicarbonates, citrates, magnesium, potassium, strontium, zinc and sodium (2,60). The tensile strength and fracture toughness of the bone are related to the organic phase, while the compressive strength is provided by the inorganic one (60).

Regarding its structure, bone is a highly vascularized complex heterogeneous tissue with hierarchical organization levels. In a macro-scale level, bone has two main structural patterns: cancellous bone and cortical bone (58) (Figure 3). Cancellous or trabecular bone comprises the inner part of the tissue, which has a structure with high porosity (30–90%) (61) and host the majority of bone metabolic activities (59). Given its highly vascularized structure, cancellous bone represents only around a 20% of the bone mass. The remaining 80% corresponds to cortical bone, which in contrast roughly represents a 10% of its volume (2). Cortical bone comprises the dense boundary (less than 10% of porosity) (62) that surrounds and protects the inner more fragile trabecular part. The cortical bone possesses higher elastic modulus and stiffness, mainly due to its higher mineralization content, providing sufficient mechanical support for weight bearing. While the compressive strength of cortical bone is in the range of 130–220 MPa, with Young's modulus ranging from 17 to 20 GPa, these properties are in the range of 5–10 MPa and 50–100 MPa respectively, for cancellous bone (59,60). Cancellous bone is characterized by a higher level of toughness and, because of its porous structure, its great capacity for sudden stress damping (2), but also by a very low tensile strength (59). Micro- and nanostructure levels of bone hierarchical architecture comprise the ECM and its composite structure, in which collagen fibers reinforced by HAp crystals provide the compressive strength and high fracture toughness of bone (58).

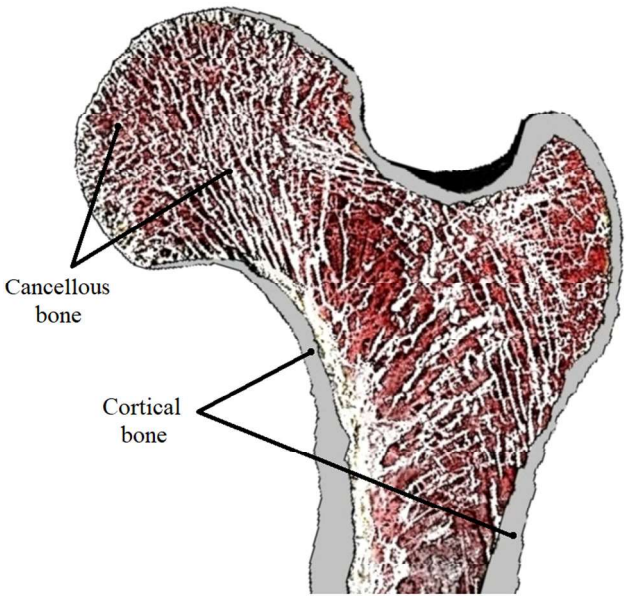

Figure 3: Cortical and trabecular bone structure.

Bone undergoes a continuous process of remodeling controlled by the action of osteocyte, osteoblast and osteoclast cells, which interact with growth factors, hormones and signaling molecules to maintain the bone health (60). Osteoclasts are responsible for bone resorption, while osteoblasts simultaneously carry out the formation of the new tissue (62). A balance between osteoclastic bone resorption and osteoblastic bone formation should exist to get a good remodeling process. The formation of new tissue, also called osteogenesis, can occur by two different pathways: endochondral ossification or intramembranous ossification. Intramembranous bone formation involves the direct differentiation of mesenchymal cells into osteoblasts, while in the endochondral process the mesenchymal cells first differentiate into chondrocytes, which then deposits a cartilaginous layer that is finally mineralized and replaced by new bone tissue (60). Upon micro- or nanofractures, the bone is self-repaired by bone remodeling, following the intramembranous and endochondral processes, without the formation of scar tissue (58,63).

2.2 Bone scaffolds design strategies and criteria

Scaffolds intended to be used for bone regeneration should possess a similar composition, mechanical properties and hierarchical structure of that of natural bone, and more importantly, they must mimic the physiological functions of the ECM. Ideal scaffolds for bone regeneration have the following characteristics (6,59,60):

- Biocompatibility and biofunctionality
- Non-immunogenic and nontoxic
- Biodegradability, with a degradation rate that matches the tissue regeneration growth rate
- Osteoconductivity, having favorable surface characteristics for cells to adhere and proliferate
- Osteoinductivity, which implies the recruitment and stimulation of immature cells to differentiate them into preosteoblast cells to later induce new bone ingrowth
- Osteointegrity, ensuring a strong adhesion between the scaffolds, the new bone tissue and its surroundings
- Be easily manufactured at relatively low cost
- Biomaterials composition similar to that of native bone tissue
- Highly interconnected pore structure, with engineered porosity and pore size to enhance cells proliferation and allow mass transfer (nutrients and metabolic waste)
- Potential to encapsulate biomolecules (growth factors, stem cells, anti-inflammatory agents, etc.)
- Adequate mechanical integrity until complete degradation of the structure.

One of the most important parameters for scaffold design is the pore size of the final structure. For bone regeneration, pore sizes reported in the literature range from 20 to 1,500 μm, with no general consensus about the optimal value to maximize the osteogenic process while ensuring the necessary mechanical support (47,64). Generally, pore sizes in the range of 75–100 μm promote the formation of unmineralized bone tissue, while smaller pores are prone to occlusion and can only be penetrated by fibrous tissue (6,59). Mineralized bone tissue can be formed by using scaffolds with pore sizes larger than 200 μm, but values higher than 300 μm are required in order to ensure vascularization (47,62). Pore sizes in the range of 300–500 μm should be suitable to enhance bone formation and avoid osteochondral ossification (6). Pore interconnectivity is another important geometrical parameter to take into account the design of bone scaffolds, as it directly influences the diffusion of nutrients and the removal of metabolic waste, being at the same time a critical parameter to ensure continuous bone tissue ingrowth (65–67).

Porosity levels higher than 50% are generally needed to allow vascularization, with values even exceeding 90% for some bone scaffolds found in the literature (68). Porosity also affects cell attachment and biodegradation rate, as they depend on the available surface area for the interaction with cells. Therefore, higher values of porosity would positively affect the biofunctionality of the scaffold, but it would affect at the same time its mechanical properties. The mechanical strength of the structure decreases by increasing the porosity, which hinders the use of highly porous scaffolds for its application in the regeneration of load-bearing applications. On the other hand, cell–material interactions for bone tissue ingrowth are not only influenced by the mechanical properties of the scaffold (69) but also by its surface properties, including topography, surface chemistry, hydrophilicity and surface energy and charge (59,70–72). The selection or design of biomaterials for bone scaffold manufacturing should take into account all these properties to ensure a good performance from the mechanical and biofunctional point of view.

2.3 Scaffolds with functional properties intended for bone tissue regeneration

A wide range of biomaterials has been used in the replacement of bone tissue. The most traditional group of materials are metals, especially those based on titanium and its alloys (73). Titanium scaffolds and prostheses provide excellent biocompatibility and mechanical performance, being widely used for bone defects treatment (13,74). However, its non-biodegradability limits the prospects of use of this biomaterial in the field of BTE. Besides, titanium-based implants have a mismatch on the mechanical properties with the surrounding tissue due to their high elastic modulus. This difference causes the appearance of the stress shielding effect (25), which aims to be reduced by using porous structures manufactured by AM techniques such as electron beam melting (75) or selective laser melting (76). In addition, titanium is a bioinert material, being unable to interact with the bone. Different strategies have been proposed to overcome this drawback, as the one presented by Song et al. (74), who applied a surface activation and HAp coating method to improve the bone-material integration of 3D printing titanium scaffolds.

In this sense, bioceramic is the type of material with a higher potential to interact effectively with the host tissue, since HAp represents around 65% of bone mass (77). Although HAp is a widely used biomaterial for bone regeneration because of its great osteoinductive capacity (13), its poor biodegradability is a major limitation that restricts its clinical use. Apart from HAp, calcium carbonate (78), bioglasses (79) and CaP (80) are also promising substances in the TE field. In the latter group, we can find one of the biomaterials that have recently attracted more interest for bone regeneration, which is the β-tricalcium phosphate (β-TCP, $Ca_3(PO_4)_2$). Unlike HAp, β-TCP presents complete bioresorbability, apart from a good processability by 3D printing techniques (81). Regarding bioglasses, they possess excellent bioactivity and bone binding ability, promoting the formation of a HAp-like layer after the scaffold is implanted (82). However, ceramic-based scaffolds exhibit poor mechanical properties (high brittleness), which hinder its application in the field of BTE as requirements for load-bearing bone regeneration cannot be fulfilled.

In contrast to metals and bioceramics, polymers have great design flexibility, being possible to adjust their composition, degradation rate and structure to the specific requirements (13). Besides, in order to mimic the natural bone structure and composition, there is a trend to combine ceramic materials and polymeric materials, using natural or synthetic polymers as base materials for scaffold manufacturing. Some examples of natural polymers used as base materials of bone composite scaffolds include collagen (83), alginate (84), chitosan (85), hyaluronic acid (86) and silk (87). Among the synthetic polymers, PLA (68), PCL (88) and PLGA (89) are the most commonly used as base materials, mainly due to their biodegradability, biocompatibility and good processability. The work of Domingos et al. (90) represents a good example of this type of composite materials. These authors achieved an enhancement of the mechanical properties and *in vitro* biological performance of PCL-based scaffolds by the incorporation of micro- and nano-hydroxyapatite particles. Definitely, synthetic biopolymer-based composites are of special interest as they possess the required strength to match the properties of bone (2). In the next sections, we will focus on the use of PLA as base material of scaffolds intended to regenerate bone tissue.

2.4 Different techniques for manufacturing of PLA-based porous scaffolds

PLA has been extensively investigated in BTE applications due to its biocompatibility, good processability, adequate mechanical properties and tunable degradation rate, among other favorable properties already commented in Section 1.3. A great number of fabrication processes have been successfully used to manufacture 3D scaffolds using PLA as base material. In Table 1, a summary of PLA-based scaffolds reported in the literature for bone tissue regeneration and their manufacturing process is shown. Particle/salt leaching (91–93), solvent casting (94,95), phase separation (96,97), gas foaming (98), freeze-drying (99) and electrospinning (100,101) are some of the most extensively used methods for bone scaffold manufacturing. However, these conventional methods have some limitations that hinder their application for BTE (102,103):

* Poor reproducibility
* It is difficult to control pore shape, size and geometry
* Uncontrolled and sometimes limited interconnectivity
* Cannot allow full control of scaffolds shape and dimensions
* Use of toxic solvents.

AM techniques have gained great attention in the last decade for bone scaffold manufacturing as a strategy

to overcome these limitations. The possibility of customizing porous constructs with a precise architecture to adapt them to the patients' needs made these processes a powerful tool for TE applications. In Table 1, no AM techniques are included, as the application of these manufacturing processes to obtain PLA scaffolds for BTE will be discussed in depth in the next section.

3 Additive manufacturing of PLA-based scaffolds for bone tissue regeneration

AM techniques are based on building geometrically complex structures by a sequential layer-by-layer deposition of material controlled from computer-designed models (124). 3D models can be created by using image data acquired from biomedical imaging techniques or by a computer-aided design (CAD) software, allowing the design of fully customized3D structures (125). The file obtained is then converted to STL (that stands for "STereoLithography" or "Standard Tessellation Language") or another format that can be suitable for the AM machine. Once transferred to the equipment, the mesh data is digitized and divided into 2D layers to obtain the sequence of material deposition. The setup of the manufacturing process could include parameters like temperature, layer thickness, nozzle diameter or power source or material flow. After the layer-by-layer deposition, some AM methods need a postprocessing step for supporting material removal (126).

According to ISO/ASTM 52900:2015 Standard, AM technologies can be classified into the following categories: (1) vat photopolymerization, (2) powder bed fusion, (3) material extrusion, (4) material jetting, (5) binder jetting, (6) sheet lamination and (7) directed energy deposition. With this set of techniques, it is possible to obtain TE constructs with patient-specific

Table 1: Examples of different techniques for PLA-based bone scaffolds manufacturing

Manufacturing process	Composition	Ref.
Salt leaching	PLA/β-TCP nanoparticles	91
Particle leaching	PLLA/β-TCP	92
	PLLA (chitosan-coated)	93
Porogen leaching	PLLA (HAp/collagen coated)	104
Solvent casting/salt leaching	PDLLA/nHAp	94
	PLA/CaP glass	95
	PDLLA (CaP-coated)	105
Solvent casting/particulate leaching	PLA/pennisetum purpureum	106 and 107
Solvent casting/particulate leaching/sol-gel	PLA/HAp/lignocellulose/BG	108
Thermally induced phase separation (TIPS)	PLLA/HAp	96
	PLLA/HAp	97
	PLLA/nHAp	109
	PLLA/β-TCP nanoparticles	110
	PLLA/chitosan/P24 peptide	111
	PDLLA (plasma-treated)	112
TIPS/salt leaching	PLLA/β-TCP nanoparticles	113
TIPS/gelatin leaching/supercritical CO_2 drying	PDLLA	114
Rapid volume expansion phase separation	PLA/β-TCP	115
Gas foaming	PLA/phosphate glass	116
	PLLA/HA and PLLA/β-TCP	98
Freeze-drying	PLA/collagen/nano-HAp	99
	PLA/chitosan/gelatin/nHAp	117
In situ precipitation and freeze-drying	PLA/chitosan/HAp	118
Freeze-drying/porogen leaching	PLLA/collagen/dexamethasone	119
Freeze extraction/porogen leaching	PLLA/PCL/nHAp	120
	PLLA(HAp-coated)	121
Electrospinning	PLA/mesoporous bioglass	100
	PLLA (mineralized)/strontium	101
	PLLA/siloxane-doped vaterite	122
	PLLA (plasma-treated)	123

design that could also be adapted to the surgeons needs for its implantation (103). The great control that they offer over the pore size, pore shape and porosity of the structure allows to tailor the structural, physical and biological properties of the scaffold to mimic native tissue function (127). As mentioned in Section 2.2, porosity plays a key role in cell–cell communication and cell–ECM interaction, nutrients and metabolic waste diffusion and in the mechanical properties of the structures. The possibility of controlling these parameters offers a great advantage compared to other manufacturing techniques commonly used to obtain bone scaffolds, such as the ones listed previously in Table 1.

In this section, PLA-based scaffolds for bone regeneration obtained by AM techniques are highlighted. In particular, we will focus on vat photopolymerization, powder bed fusion and material extrusion methods, as these are the AM technologies that have been extensively employed for polymeric-based scaffold manufacturing (127–129).

3.1 Vat photopolymerization

Vat photopolymerization is an AM process where the build of each layer of material is produced by the photocrosslinking of the monomers in the resin, which react to create a solid structure. The radiation needed to cure each layer of material can be applied through two different methods: by a laser-based approach (Figure 4), commonly known as stereolithography (SLA) (130), or by a digital light projection approach, commonly referred to as DLP (Figure 5). The resolution of this technique at commercial level is around 50 µm (130,131), which is below the one obtained, for example, by extrusion-based processes (132), allowing the manufacture of more complex 3D designs. Because of its high resolution and the precision of the geometries that can be obtained, SLA has been one of the earliest 3D printing methods used in BTE (13). However, the main limitation for a wide implementation of this technique for TE applications is the need of biocompatible photocurable materials, which may exhibit inadequate biodegradation rates and biocompatible behavior.

PLA oligomers can be functionalized with methacrylate end groups in order to obtain a photocurable resin (133–135). The methacrylate groups are introduced in the structure normally by previously creating hydroxyl-terminating oligomers, which are able to react

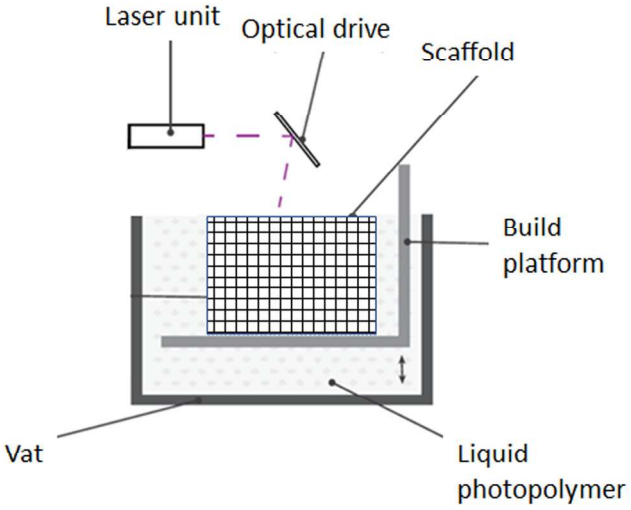

Figure 4: Vat photopolymerization by laser light source (SLA technique).

with methacrylic anhydride (134,136,137). As the reactive species must be in the liquid state, PLA resins need to be diluted in solvents. When the viscosity of the medium is high enough to allow a suitable solidification of the material, the solvents used are usually reactive, such as methyl methacrylate, butane-dimethacrylate and *N*-vinyl-2-pyrrolidone (134). These substances are not easily biodegradable, so their introduction in the formulation limits the biomedical application of the final parts. For this reason, nonreactive diluents are desirable, especially those with a suitable polarity to be washed with biocompatible liquids to remove any trace during the postprocessing stage. Nevertheless, when nonreactive solvents are used, problems related to shrinkage may appear. Melchels et al. (134) used ethyl lactate as solvent and they analyzed the importance of the chemical structure's design of the oligomers on the properties of the final additive-manufactured structures, demonstrating the relationship between the degree of swelling of the parts and the arm length of the star-shaped oligomers. Another issue regarding the creation of innovative chemical structures in order to obtain a photocurable polymer that can be processed through SLA, is the ability of the body to remove their degradation products, as kidneys are not able to remove water-soluble polymer above 200 kg/mol (136). Melchels et al. (138) have analyzed this matter through spectroscopy and they concluded that the products have a suitable molecular weight to ensure renal clearance.

An alternative approach in the design of PLA-based scaffolds through SLA is the use of copolymers of this material. For example, Seck et al. (137) used a copolymer

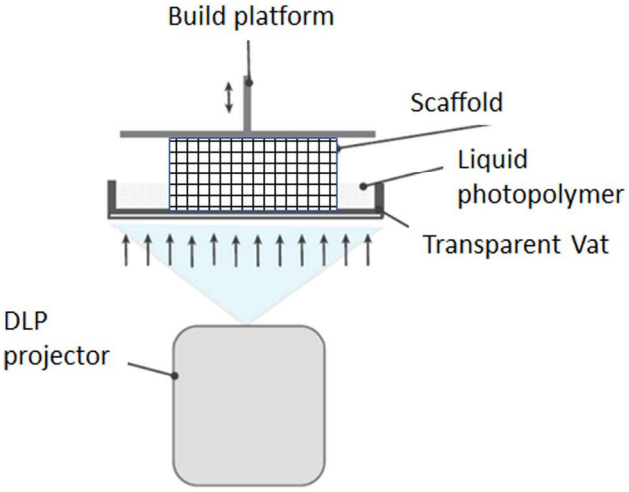

Figure 5: Vat photopolymerization by controlled area light source (DLP technique).

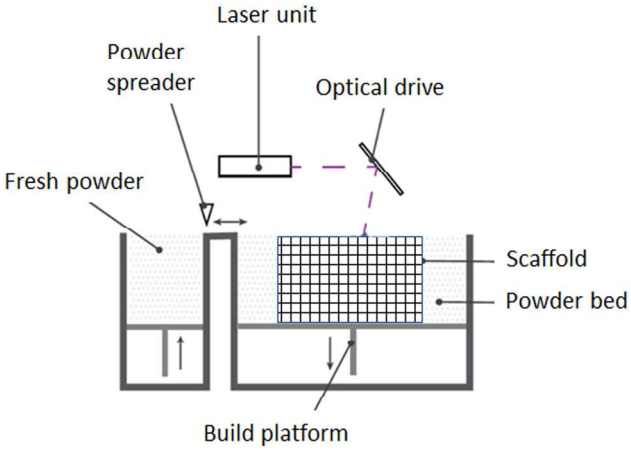

Figure 6: Laser powder bed fusion (SLS technique).

of poly(D,L-lactide) and poly(ethylene glycol) (PEG) to obtain structures manufactured through SLA techniques with relatively good results. Regarding the possibility of using composite materials, Ronca et al. (133) reported the manufacturing of structures containing up to 20% of nanosized hydroxyapatite. As expected, the energy of the curing light must be increased with the concentration of the additive (139). Although it is possible to find in the literature complex scaffolds for BTE obtained by SLA, some limitations of the technique have hindered its use for this application, like restrictions on the layer thickness and laser irradiation to avoid overcuring or potentially cytotoxic effects when working with encapsulated cells (13). This method is also generally more expensive and time-consuming than other AM techniques, requiring complementary instrumentation in order to produce biomedical devices.

3.2 Powder bed fusion

Powder bed fusion, also known as selective laser sintering (SLS), is an AM technique based on the melting of powder particles by the action of a focused laser beam, which sinters the material to create 3D structures according to a computer-designed layer-by-layer pattern (15,140). After printing a layer, new powder is added to the vat of the equipment and then sintered (Figure 6). Thin layers with heights in the range of 20–150 µm can be deposited. Once the process has finished, the manufactured part is removed and cleaned to eliminate any trace of powder. SLS parts may need further postprocessing (such as polishing or drying) depending on the specific application (127). This approach is ruled by the energy parameters of the laser beam and the material characteristics, such as the particles size and the viscosity of the molten material. Some of the advantages of SLS include its high resolution, the lack of need of a support material or structure that must be removed later and the possibility of avoiding the use of organic solvents. This technique is also relatively fast and cost-effective. These characteristics enable the manufacturing of complex 3D constructs using a variety of materials, including polymeric, metal and ceramic powders. Metallic powders are generally used to obtain 3D structures that could be applied in BTE for the regeneration of load-bearing bones, while the polymeric materials are preferred for non-load-bearing applications (13).

In the biomedical field, several disadvantages of SLS are related to the high temperature needed in this process, as it limits the selection of biomaterials for scaffold manufacturing, prevents the combination of these materials with cells and could lead to the degradation of the material by chain scission, cross-linking or oxidation processes (13,15). Different authors have also reported the presence of two levels of porosity in SLS parts: the macroporosity obtained through the CAD design (which will determine the mechanical properties of the parts and their vascularization) and the microporosity that is a consequence of the incomplete melting of the material during the sintering process due to high melt viscosity (141,142). This hierarchical architecture and the high microporosity of the final structure will affect the biological performance of the scaffold and its mechanical properties. On the other hand, the final pore size depends on the spreading characteristics of the powder, which in turn depends on the size of the particles used (13). The need of a small

and homogeneous particle size of the raw material could be considered the main limitation of this technique, as the optimal range for SLS processing is between 10 and 100 μm (143). Furthermore, the particles must be rounded to ensure material fluidity and prevent their agglomeration (144).

The use of PLA for the manufacturing of 3D scaffolds by SLS remains limited compared to other biodegradable polymers, such as PCL (143). Commercial PLA is typically delivered in the form of millimeter-sized pellets, so a method for preparing particles with smaller size before the SLS process is essential to ensure a high resolution of the 3D constructs. PLA particles in the micro- and nanoranges can be obtained through different techniques, such as emulsion/extraction, salting out, spray-drying, microfluidic techniques or mechanical milling (145). Solvent-related methods allow a good control of the size and shape of the PLA particles, but the use of toxic organic solvents for dissolving the polymeric chains (dichloromethane, chloroform, etc.) hinders medical approval and industrial-scale application. In contrast, organic solvents are not used in mechanical milling methods, which can also be upscaled more easily. However, particle size reduction of PLA by milling can only be achieved till a certain extent and the shape of the particles is generally highly irregular (144).

Despite the aforementioned limitations, some examples of PLA particle size reduction can be found in the state of the art. In this regard, Zhou et al. (141) used an emulsion/solvent evaporation technique to create PLA/carbonated HAp nanospheres. They used poly(vinyl alcohol) as the emulsifier and dichloromethane as the organic solvent, obtaining with this procedure PLA particles with sizes between 5 and 30 μm. To avoid the use of toxic solvents, Gayer et al. (144) have proposed to substitute this procedure by a mechanical one, developing PLA/calcium carbonate powders with suitable properties for SLS. The composites were prepared by dry impact milling and later sieving. Approximately, 25% of additive content was used in combination with four different inherent viscosity grade PLA (PLLA or PDLLA). The powder that includes the PLA with the lowest value of this property (1.0 dl/g) was the one that showed the best results in terms of processability, having also the smallest average particle size diameter (50 μm). Samples manufactured by SLS using this composite powder promoted cell viability of osteoblast-like cells, confirming the potential application of this scaffold for BTE applications.

In addition to the limitations related to the particle size, some authors reported the low mechanical properties of PLA sintered scaffolds, proposing the introduction of different additives to overcome this limitation. This is the approach followed by Shuai et al. (146), who added phospholipid-coated nanodiamond particles to improve the mechanical properties of PLLA-based SLS scaffolds. The compressive strength, compressive modulus and Vickers hardness of the sintered composite structures greatly increased compared with unmodified PLLA scaffolds (by 162.8%, 163.2% and 88.2%, respectively), due to the higher dispersion of the nanodiamond particles promoted by the phospholipid coating. A better dispersion is achieved since the hydrophobic tails of the phospholipids repel each other, after being the hydrophilic heads bonded to the nanodiamond particles surface. A decrease in the water contact angle of the scaffold is also reported when the percentage of additive particles is increased, favoring as a result of cell adhesion, proliferation and differentiation. The use of composite powders to improve the mechanical strength of the scaffolds has also been evaluated by Gayer et al. (147), who analyzed the properties of SLS-manufactured PDLLA/β-TCP 50/50 scaffolds. The effect of particle size, filler particle size and polymer molecular weight on the processability was also assessed in this study using the same composition of biomaterials. Again, the best results in terms of processability were obtained for the composite powder with lower particle size (around 35 μm) and melt viscosity, leading to scaffolds with lower porosity and, therefore, higher mechanical strength.

3.3 Material extrusion processes

Extrusion-based processes consist of the layer-by-layer deposition of materials through a nozzle tip, following a designed pattern, to obtain complex 3D structures. This technology is commonly known as fused deposition modeling (FDM) when low-melting-point thermoplastic materials are used. The material is fed to the AM equipment in the form of a continuous solid filament (generally with a diameter of 1.50 or 1.75 mm), being melted in a heated printhead and extruded over a build plate using a pinch roller system (148) (Figure 7). Each printed layer adheres to the previous one, hardens as it is cooled by a fan and then binds with the layer that is added on the top to form a solid construct. The printhead moves in the x–y plane to deposit the polymer in a semimolten state and then advances to an upper layer by its movement in the z-axis. Typically, stepper motors are

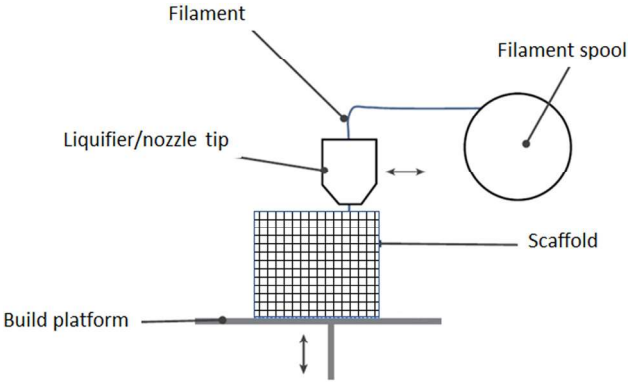

Figure 7: Material extrusion of thermoplastic material (FDM technique).

used to move the extrusion head and adjust the flow rate (149).

FDM is one of the most widely used AM techniques for scaffold fabrication, as it allows the manufacturing of 3D custom-made constructs. It is at the same time a flexible, low-cost and easy to implement technology, with immediate availability of printing materials. These advantages, coupled with the possibility of obtaining scaffolds with controlled porosity and pore size, are some of the reasons why FDM is nowadays a technique with great potential in the biomedical field. Regarding its drawbacks, the use of relatively high processing temperatures prevents the combination of cells or temperature-sensitive biological compounds with the polymer matrix during the scaffold's production process (bottom-up approach) (13). Therefore, a top-down approach is required, consisting in the seeding of cells onto the surface of the scaffold after its manufacturing by the FDM method. Another important limitation is its low resolution when compared to other AM techniques (127), despite FDM-manufactured scaffolds have been obtained with high resolution (150). Furthermore, support materials are needed when the structures to be printed have sharp or long overhangs. A two-nozzle printer is required in these cases (148).

For biomedical applications, PLA, PCL, PLGA and their blends with other biomaterials, are among the preferred options to obtain FDM-produced scaffolds (13). PLA is indeed one of the most spread materials for the fabrication of parts by this technique not only for the biomedical sector, but also for general applications (151). PLA scaffolds intended to be used in the biomedical field can be even obtained with low-cost FDM-based printers (152). Apart from the aforementioned advantages of PLA as a base material for scaffold manufacturing, this biomaterial has suitable thermal characteristic for FDM processability, being generally extruded at temperatures between 200°C and 230°C (148). The process conditions should be adjusted so the material do not suffer from excessively high shear stress during extrusion, as this could promote the degradation of the polymer or affect its biocompatibility (13). PLA-based composite materials can also be processed by FDM with the objective of improving the matrix characteristics (153,154). The final properties of the 3D printed structure will depend on the biomaterials used and the manufacturing process parameters.

The type of printing pattern used to manufacture the FDM scaffold for BTE has great influence on its vascularization, mechanical properties and cell ingrowth. Most of the proposed scaffold structures do not attempt to mimic the damaged tissue. Instead, they follow a uniform rectangular pattern with regular porosity and pore size. One example of scaffolds manufacturing using this configuration is found in the study of Grémare et al. (42), who developed and characterized rectangular-pattern PLA scaffolds obtained by FDM. Regardless of the pore size of the structure (150, 200 and 250 µm), both reasonable mechanical properties and human bone marrow stromal cells (hBMSCs) growth were obtained.

More complex printing patterns have been used in order to better resemble the architecture of natural bone, such the honeycomb-like structure with controlled porosity and pore size designed by Hutmacher et al. (155). The authors concluded that the honeycomb design conferred suitable mechanical properties to the structure for its use in BTE applications. The material used in this study was PCL, being the first work where the FDM technology was applied for the manufacturing of TE scaffolds. A more recent example of the use of this designed pattern is the work of Zhao et al. (156), in which the influence of the honeycomb structure characteristics on the mechanical properties of PLA scaffolds was discussed. Scaffolds with 90% porosity and compression modulus of 70.4 ± 11.4 MPa were obtained. An alternative complex designed configuration is the gyroid printing pattern, which gives as a result a mesh with curved-shape branches and nodes with four junction points. Germain et al. (157) used this configuration to produce PLA scaffolds by FDM and compare them to commonly used strut-based structures. The porosity of the scaffolds manufactured was in the range of 70%–75% with pore projections of around 800 µm, thus ensuring a good tissue vascularization. The spring shape of these structures showed great potential for bone regeneration, due to its isotropic behavior

regarding compression, robustness and mechanical energy absorption capacity. Unlike rectangular-patterned scaffolds, whose mechanical properties are strongly influenced by the printing orientation of the struts (158), the gyroid scaffolds could bear compressive efforts coming from any direction with the same effectiveness. According to the analysis of the stress–strain curves obtained from the compression test, the scaffolds with gyroid pattern had an apparent compression modulus of 50 MPa and a more deformable behavior compared to strut-based scaffolds.

Apart from the modification of the printing pattern, there are other strategies to modify the internal and external configuration of the scaffolds when trying to mimic the hierarchical architecture of bone. One example is the combination of FDM and gas foaming techniques proposed by Song et al. (159), which allow them to obtain a final structure with two different pore size levels with interconnected porosity. Briefly, PLA was combined with poly(vinyl alcohol) (PVA) to obtain continuous filaments suitable for FDM. After manufacturing the composite scaffolds, they were subjected to a gas foaming process to generate micropores in the structure. Finally, the temporary PVA phase was water-etched to extract it and create open pores. The final PLA scaffolds had macropores ranging from 100 to 800 μm and micropores in the range of 2–10 μm. Despite this promising configuration for BTE, the mechanical properties of the scaffolds manufactured using this procedure are too poor to ensure the support of the growth of the new bone tissue.

Numerous studies can be found in the literature regarding the influence of other printing parameters on the mechanical strength of the PLA scaffolds obtained by FDM. For example, Ouhsti et al. (149) concluded that there is a strong dependence between the deposition angle, the extruder temperature and the printing speed with the final mechanical properties of the scaffolds. Specifically, they analyzed the tensile strength and Young's modulus of PLA 3D printed scaffolds. On the other hand, Dave et al. (160) assessed the influence of layer height, infill density and printing speed on the mechanical properties under compression load. Their results suggest a high dependence of the compressive strength on the infill density, while no significant effects were obtained by modifying the layer height or the printing speed. On the other hand, Murugan et al. (161) pointed out that the extrusion temperature used to manufacture the constructs also affects their tensile strength and Young's modulus. Too high processing temperatures could also lead to an important reduction of the polymer's molecular weight (42).

Aside from the need of ensuring sufficient mechanical support, PLA-based scaffolds obtained by FDM should possess the appropriate biological properties to promote cell ingrowth. In this regard, the biocompatibility of PLA can be maintained after the FDM process, showing the constructs no cytotoxicity toward osteoblast-like cells. For example, Grémare et al. (42) cultured hBMSCs onto 3D printed PLA scaffolds, obtaining good results in terms of metabolic activity and cell distribution over the porous structure. Regarding cell differentiation, the micro- and nanotopography of the scaffold surface is one of the most important factors affecting osteogenic processes, supporting the differentiation of mesenchymal stems cells (MSCs) toward specific lineages (162). In contrast, macropatterns generated by the FDM equipment have not seem to induce this effect, as concluded by Alksne et al. (163). In order to stimulate cell differentiation, one possible approach is the combination of the PLA matrix with bioactive coatings. In a recent work, Teixeira et al. (164) manufactured PLA scaffolds by FDM and then coated them by immersion in polydopamine (PDA) and type I collagen (COL) solutions. The PDA/COL-coated PLA scaffolds showed improved cell adhesion and enhanced metabolic activity of MSCs during the first week of culture. Also, ECM components, specifically collagen and calcium, were deposited in a higher extend (after 14 days) when the coating was applied to the structures. At day 21, despite obtaining no significant difference in terms of cell proliferation and ECM compound deposition, coated scaffolds showed an alkaline phosphatase (ALP) activity 500 times higher compared to the unmodified samples. These results are a good indicator of the ability of the proposed scaffolds to stimulate osteogenic differentiation.

An alternative modification of PLA scaffolds manufactured by FDM in order to improve its biological properties is the combination of the base material with natural or ceramic additives. In a study of Zhang et al. (165), a comparison between PLA/HAp scaffolds, β-TCP ceramics 3D structures and partially demineralized bone matrices (DBM) was conducted regarding cell proliferation and differentiation *in vitro*, as well as bone repair capacity *in vivo*. The PLA/HAp printed scaffolds were designed with a pore size of 500 μm and porosity around 60%. These constructs possessed good biocompatibility and cell viability according to the results, promoting cell adhesion and proliferation of the bone marrow stromal cells (BMSCs) seeded onto the structures. Furthermore, cell differentiation was also enhanced by the PLA/HAp according to the ALP test and the gene expression analysis of osteopontin and type I collagen osteogenic markers. On the other hand, for the *in vivo* evaluation of

the scaffolds a critical-size rat calvarial defect model was used. PLA/HAp scaffolds showed again a favorable biocompatibility, higher degradation rate and improved osteoinductivity.

Another extrusion-based AM process is the one known as 3D bioprinting, which consists in the continuous extrusion of biomaterials by an air-pressure, piston-assisted or screw-assisted system to build 3D constructs according to a CAD-designed model (166). The most common method involves the application of pressure from a compressed gas to an ink-containing syringe in order to extrude the material through a micronozzle (167). The base material used in 3D bioprinting is generally a soft hydrogel, such as gelatin, collagen, laminin, fibronectin, alginate, chitosan, silk fibroin or gelatin methacryloyl (GelMA) (166,168). A good integrity of the 3D printed structure is ensured by using cross-linking methods after or even during the manufacturing process. Chemical- and photo-crosslinking (using UV light) after deposition are among the preferred options. This technology is implemented in most commercial units of bioprinters and bioplotters (Figure 8), in which viscous natural hydrogels can be printed in combination with synthetic polymers (hybrid scaffolds), ceramic materials (composite scaffolds) or even cells (cell-loaded scaffolds).

The possibility of incorporating cells during the manufacture of the scaffold is the major advantage of 3D bioprinting, avoiding their seeding onto the structure afterward (157). Cell-laden hydrogels are commonly referred to as "bioinks." The incorporation of cells and other bioactive compounds is feasible since this technique do not involve a heating process. Biomaterials with high cell densities can be deposited without negatively affecting the material processability or cell viability. In this regard, a recent study by Diamantides et al. (169) showed that the density of the cells incorporated affects the rheological properties of collagen bioinks, obtaining an improved printability as this parameter is increased. The proposed constructs for cartilage regeneration were seeded with chondrocytes up to a concentration of 100×10^6 cells/mL, maintaining high cell viability through a 14 days test. Some other aspects of 3D bioprinting include the ability to print high viscosity materials and struts with increased thickness by tuning the process parameters (flow rate, pressure, etc.).

Regarding its limitations, 3D bioprinting has a poorer resolution compared to FDM-related techniques. In order to overcome this drawback, narrower nozzles and higher driving pressures could be used, but a potential decrease in cell viability is generated as a consequence of these modifications due to shear stress effects on cells (170). Therefore, the optimization of the resolution-printing speed balance is required when the objective is to obtain highly porous structures which can provide a suitable environment for cell growth. Biomaterials with shear-thinning characteristics are an interesting option to fulfil this objective, as they possess high flowability under high shear rates, but become a viscous gel when they exit the nozzle and the shear stress is removed (166). On the other hand, although some studies have demonstrated that the appropriate selection of the process conditions can lead to the manufacturing of highly vascularized structures (171), this is still a matter of concern for 3D bioprinting application. One approach to address this issue is the use of sacrificial material, which are removed after the printing process to generate the vascularization channels (168). Sacrificial materials, such as gelatin or carbohydrate glass (168), are incorporated simultaneously during the printing material deposition, providing mechanical support for the upper layers of the structure. This methodology increases the complexity of the process since two different printheads are needed. Also, the number of methods for sacrificial material removal is limited because of the requirement that they should not elicit any cytotoxicity effect on the final structure.

Figure 8: PLA scaffolds obtained by 3D bioprinting using a BioX 3D bioprinter (Cellink, Sweden).

3D bioprinting has been applied for the manufacture of scaffolds intended to regenerate vessels (171), neuronal tissues (172), cartilage (168) and bone (173). For the latter tissue and in order to meet the mechanical requirements, which generally cannot be satisfied using a sole material, the use of multicomponent bioinks and hybrids scaffolds has been widely proposed (168).

Despite the literature regarding the application of PLA for scaffolds manufacturing using 3D bioprinting is quite reduced, some examples of the use of PLA for bone regeneration as base material can be found. In that sense, Serra et al. (150) developed high-resolution 3D printed PLA-based scaffolds with added PEG and CaP glass particles. PEG was used as a plasticizer to improve the material processing. The CaP glass particles were mixed in a 1:1 relation with a 95/5 w/w% blend of PLA and PEG particles. The scaffolds obtained by 3D bioprinting at low temperature (40°C ± 5°C) showed high interconnectivity and uniform distribution of the additive glass particles, which increased the roughness and hydrophilicity of the surface. Both improvements promoted MSCs adhesion. Scaffolds containing both additives showed a very well-spread morphology of the cells. In a later work of Serra et al. (174), the authors extended the study to combinations of this biomaterial comprising a 5%, 10% and 20% of PEG in its blend with the PLA matrix. No CaP glass particles were added this time, as the objective was to analyze the influence of PEG on the scaffold final properties. It was concluded that the mechanical properties of the structure decreased with the increasing amount of PEG particles, while the degradation of the scaffolds is enhanced. Hence, the properties of the constructs can be tailored by modifying the percentage of plasticizer incorporated to the formulation of the blend. Taking into account the results of both studies, the best combination proposed by the authors is the combination of PLA, PEG and CaP glass particles, both from the biological and mechanical points of view.

In a totally different approach, the use of PLA as cell-laden microcarrier (MC) in 3D bioprinting constructs has been explored by Levato et al. (175) MCs are particles designed to promote attachment and proliferation of cells thanks to its high specific surface area. In this work, MSCs-laden PLA MCs were encapsulated in gelatin methacrylamide-gellan gum (GelMA-GG) bioinks. The results obtained from the characterization of the 3D printing structures showed that the PLA-MCs improved the compressive modulus and at the same time stimulated cell adhesion, bone matrix deposition and osteogenic differentiation. Mechanical reinforcement and enhanced cell viability were achieved without lowering the processability of the base bioink. A proof of application of the methodology proposed was presented in the form of a biphasic osteochondral scaffold, which consisted of a bone part with MC-laden bioink and a cartilage part made by using the GelMA-GG bioink without the MCs.

4 Strategies to improve PLA biological properties for bone tissue regeneration

As explained along the previous sections, PLA has favorable properties for its application in the biomedical field, including its biocompatibility, biodegradability, good processability and mechanical properties. However, its use in regenerative medicine is limited due to its hydrophobicity, which hinders cell adhesion and proliferation, and the release of acidic byproducts during the degradation process. In order to counteract these drawbacks and increase the bioactivity and osteoconductivity of PLA bone scaffolds, a variety of methods have been presented in the literature. In this section, the incorporation of additives, the application of surface treatments and the use of surface coatings with bioactive compounds are reviewed. We will focus on the use of these methods to improve PLA-based scaffolds properties obtained by AM techniques and intended to be used for bone regeneration.

4.1 Use of additives

The design of composite materials allows to tailor and optimize the biological and mechanical properties of PLA-based scaffolds, also offering the possibility of adjusting the biodegradation profile and rate of the manufactured structure (6). The biomaterials that have shown more potential for this purpose are bioceramics, specifically HAp, β-TCP, ceramic bioglasses and other CaP compounds. The incorporation of ceramic additives to the PLA matrix has been demonstrated to improve the hydrophilicity, osteoconductivity, mineralization upon implantation and mechanical properties of the 3D structures. Furthermore, given the basic nature of bioceramics compounds, they act as buffer agents during the degradation process, counteracting the pH decrease in the surroundings of the scaffolds and reducing the risk of formation of localized areas with an acidic environment (148) that could lead to an inflammatory response. Among the biomaterials mentioned, HAp is the one that has attracted more attention as an additive of PLA-based scaffolds. In the study of Niaza et al. (176) HAp was incorporated in the form of micro- and nanoparticles to the PLA matrix. Firstly, a mixture of both biomaterials was extruded to produce a continuous filament containing a 15% w/w of HAp. Then, this

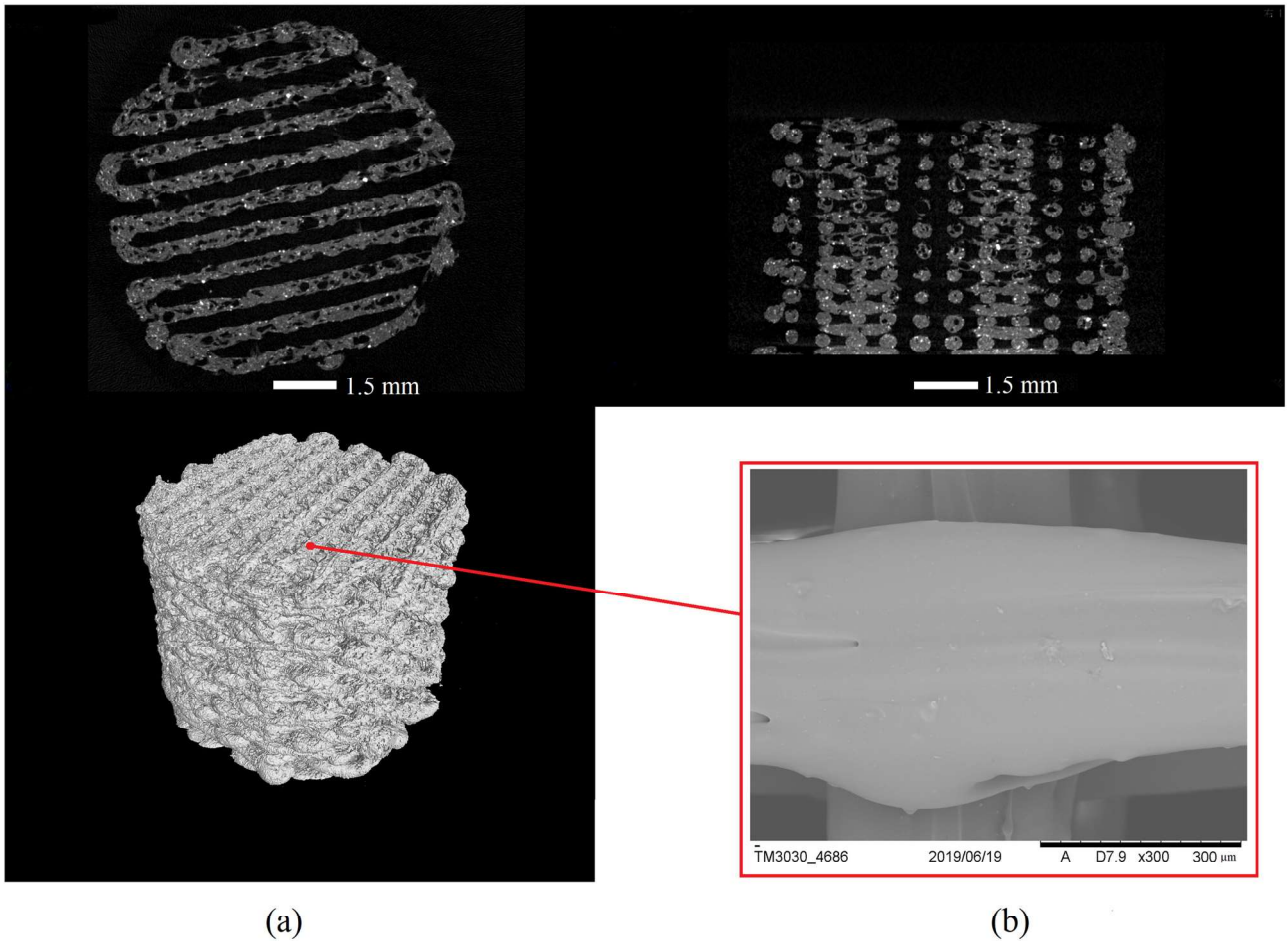

Figure 9: Images of 3D printed PLA-based composite scaffold, using β-TCP particles as additive, obtained by (a) scanning electron microscopy (SEM; Hitachi TM 3030 at an acceleration voltage of 15 kV) and (b) micro-computed tomography (micro-CT; Y. Cheetah, YXLON Ltd).

filament was used to manufacture rectangular-shape porous scaffolds by FDM. The final porosity of the structure was barely of a 30%. Despite having a porosity lower than the range recommended in the literature for cancellous bone regeneration (61,68), these scaffolds showed promising results in terms of mechanical properties, which were improved by the HAp nanorods introduced in the formulation. As an example of the incorporation of ceramic additives to the PLA matrix, Figure 9 shows images related to the morphological analysis of PLA-based composite scaffolds, containing β-TCP as additive, that have been recently developed by our group.

With the objective of improving not only the mechanical characteristics of the PLA matrix, but also its bioactivity, Esposito Corcione et al. (177) studied the feasibility of producing high HAp-loaded filaments to be 3D-printed using low-cost FDM equipment. Continuous composite filaments were successfully obtained using a twin-screw extruder after feeding it with particle mixtures comprising 5%, 15%, 30% and 50% of HAp. By using this solvent-free method, a good dispersion of the ceramic particles was achieved even at the highest concentration level studied. Samples manufactured by FDM technique showed no significant modification of the properties measured for the filaments (glass transition temperature, melting point, degradation temperature and crystallinity rate). The same authors recently presented another work (153) where they delved into the manufacturing of scaffolds by FDM using filaments containing a 50% of HAp. In this case, the additive was incorporated in the form of microspheres synthesized by spray drying and then mixed with the PLA by an extrusion process to obtain the filaments. Thermogravimetric results confirmed the presence of the additive in a 50% concentration, while the glass transition temperature and the degree of crystallinity

of the PLA matrix were not affected by the incorporation of the additive. From the morphological point of view, a homogeneous dispersion of HAp microspheres was confirmed, as well as an increase in the surface roughness. Although the theoretical porosity of the structures according to the CAD model was equal to 50%, scaffolds containing only PLA showed a porosity value of approximately 39%, while the result for the composite scaffolds was about 55%. The higher porosity of the PLA/HAp constructs led to a decrease in the mechanical properties, assessed by measuring the Young's modulus of the structures under compression testing (238.98 ± 19.05 MPa and 124.04 ± 25.21 MPa for PLA and PLA/HA scaffolds, respectively). Taking all the results into account, the authors concluded that the incorporation of a high load of HAp induced the formation of porous and rough strands, increasing the available surface area for cell adhesion, while lowering the mechanical properties of the structure to a value still in the range reported for cancellous bone (178). Therefore, composite scaffolds with improved osteoconductivity for BTE applications can be obtained with this method.

A deeper mechanical characterization of PLA-based composite scaffolds was carried out by Senatov et al. (179), who studied both compression and shape memory properties of 3D printed PLA/HAp 15 wt% scaffolds. These scaffolds had an average pore size of 700 μm and a porosity of 30%. Samples were subjected to compression–heating–compression cycles repeated up to the fracture of the sample, alternating compression forces at a strain rate of 15% and temperatures up to 80°C. The use of HAp particles as additive of the PLA matrix led to a significant increase of yield strength, strength at 15% strain and Young's modulus. In addition, no significant cracking of the structure or delamination of the layers was observed after the first compression test. Then, the PLA/HAp scaffolds were able to withstand three compression–heating–compression cycles, showing shape recovery rates in the range of 96–98%. In contrast, PLA samples were destroyed after two cycles. Despite the good results in terms of shape recovery, the mechanical properties were decreased in a proportion of a 20% after each cycle. Despite the promising capacity of these structures to "heal" the cracks that could appear during their *in vivo* application, the temperature needed to activate this recovery process (53°C according to the results of this work) is far above the internal temperature of the body (37°C). Other strategies should be applied to reduce the shape memory onset temperature without reducing the favorable mechanical properties of the proposed scaffolds.

Apart from ceramics additives, an alternative approach is to combine the PLA matrix with natural polymers or their derivatives. A good example is the work of Wei et al. (180), who investigated the microstructure and mechanical properties of scaffolds comprising PLA and different amounts of *o*-carboxymethyl chitosan (CMC). The scaffolds were manufactured by FDM after extruding continuous filaments of 100/0, 90/10, 80/20, 70/30, 60/40 and 50/50 w/w% PLA/CMC blends. The experimental work was complemented with the findings obtained by applying a molecular dynamics simulation method, revealing the molecular interaction mechanism between different components in PLA/CMC composites. The addition of CMC improved the hydrophilicity of the scaffold's surface, as can be concluded from the water contact angle measurements. The value of this parameter was reduced from approximately 75° to about 30° when the composition was PLA/CMC 50/50 w/w%. The introduction of the additive also reduced the fractional free volume and chain motion capability, resulting in a better processability of the material. Regarding the mechanical characterization, the tensile modulus increased with the concentration of CMC used, confirming the capacity of the additive to act as a reinforcement agent of the PLA matrix. On the other hand, the maximum tensile strength was obtained for samples containing a 20% of CMC, which were attributed to have the strongest intermolecular interaction between PLA and CMC components, being the experimental results in agreement with the calculated ones. Higher concentrations of the additive led to a decrease of this property due to the phase separation of the materials and the subsequent aggregation behavior of CMC. These results confirm the possibility of tuning the morphological, mechanical and biological properties of PLA-based scaffolds for BTE applications by incorporating additives in a controlled proportion.

4.2 Surface treatment

In spite of the suitable properties of PLA in terms of biocompatibility, the hydrophobicity of this material limits it interaction with extracellular proteins and cells. In order to improve the biological properties of PLA constructs for bone tissue regeneration, one effective approach is to apply a surface treatment to the 3D structure, aiming to modify its topography or surface chemistry. These surface changes can induce a positive effect on the attachment of cells and biological

compounds to the structure (181,182). Surface treatments can be used as the final modification of the 3D construct or as a previous step before coating the structures with bioactive compounds, as they allow an effective immobilization of these substances with the polymeric matrix (183,184).

As the coating strategies for PLA-based scaffolds in BTE will be discussed in the next section, we will now focus on the surface treatments generally used, being alkali treatments one of the most common options. This method basically consists on the immersion of the structures into a sodium hydroxide (NaOH) solution with an optimized concentration and during a certain time to obtain the desired surface modifications. One example of its application can be found in the work of Martin et al. (185), who treated PLA scaffolds manufactured by FDM using a 1:1 NaOH 0.25 M and ethanol 96% (v/v) solution. The samples were immersed during 4 h at room temperature with continuous stirring, then washed with citric acid 0.5% (w/v) and deionized water. Different collagen mixtures containing antibiotics and citrate-HAp nanoparticles were used as bioactive coatings of the treated structures. Unlike in the traditional alkali treatment, where hydroxyl groups are chemically incorporated to the PLA surface by nucleophilic attack to the ester bonds, the use of citric acid after hydrolysis also induced the formation of carboxyl groups bonding. In this way, a significant increment of the hydrophilicity and surface roughness has been reported (186). There are also references in the literature about the use of alkali treatments without further modifications to the structure, as proposed in the work of Nam et al. (187) These authors assessed cell adhesion on PDLLA and PDLLA/PLGA films treated by immersion in a 1 N NaOH solution. A strong influence of treatment time on surface wettability and, consequently, on cell affinity was confirmed.

Despite its proved efficiency, alkali surface treatments could introduce undesirable morphology changes and, more importantly, affect the bulk mechanical properties (188). Plasma treatment, in contrast, is one of the most explored techniques used to modify the surface chemistry of PLA-based constructs without changing the bulk properties of the material (189). This treatment is able to create functional groups with a higher water affinity, such as carboxyl (–COOH) and hydroxyl (–OH) groups (190,191). Therefore, the hydrophilicity of the surface is increased, as experimentally confirmed by the reduction of the water contact angle of the treated material (Figure 10). In the study of Nakagawa et al. (190), the authors obtained a decrease of this parameter from 77.4° to 39.8° after applying an air plasma treatment over PLA samples manufactured by injection molding. This modification induces an improvement in the biological performance of the scaffolds by enhancing cell adhesion capacity. Similar results regarding the hydrophilicity increase of the surface were obtained by Jordá-Vilaplana et al. (192), who also studied injected molded PLA samples treated with plasma. In addition, the authors observed topography changes in the surface due to some material removal, enhancing the roughness of the structure in a nanometric scale. Apart from air, other gases can be used for the plasma treatment of the samples to functionalize the surface. In the work of Yang et al. (182), an anhydrous ammonia (NH_3) plasma treatment was applied to porous PLA-based scaffolds to improve their hydrophilicity and cell affinity. This objective was fulfilled after the incorporation of N-containing groups to the treated surface. Not only cell adhesion and proliferation can be improved by these methods, but also cell morphology, as concluded by Yamaguchi et al. (193), who observed a close-contact extensive spreading of epithelial cells on plasma-treated PLLA constructs compared to unmodified samples. For the latter, cells showed small and round morphology and proliferated separately from one another.

For BTE applications, Wang et al. (194) have investigated the use of cold atmospheric plasma (CAP) technique to treat the surface of PLA scaffolds obtained by 3D printing. The objective was to modify the roughness and chemical composition of the constructs in the nanolevel, aiming to mimic the ECM properties of bone tissue. Different exposure times (0, 1, 3, and 5 min) were studied and the scaffolds were treated both on their top and bottom sides. Results showed that the different CAP treatments applied to the structures increased the hydrophilicity, roughness and oxygen to carbon ratio of the surface. The modifications introduced on the surface chemistry and nanoscale morphology effectively promoted the attachment and proliferation of osteoblast and BMSCs. Interestingly, the most promising results were obtained for the PLA scaffolds treated with plasma for 1 min. These findings showed the great potential of surface treatments to enhance the biofunctionality of PLA-based to be applied in BTE applications.

On the other hand, the main disadvantage of this method is its nonpermanent effect, as there is a progressive loss of treatment's effectiveness with time due to surface chemical rearrangement (195,196). In addition to this, plasma treatment can affect the degradation rate of the PLA matrix, as concluded by Wan et al. (197), who observed that an increase in the treatment time or power supply led to an enhanced the degradation of PLA scaffolds. Another limitation of these

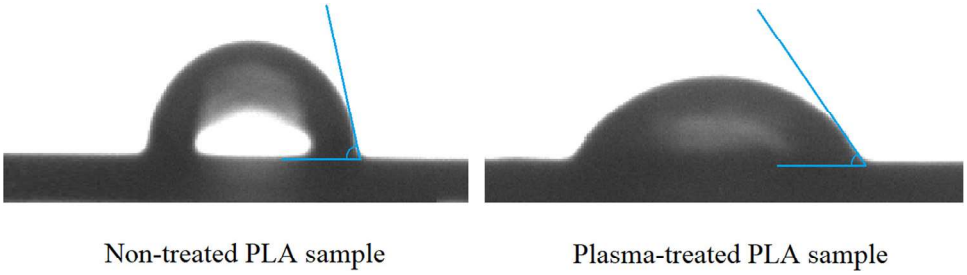

Figure 10: Water contact angle images of sessile drops over the surface of PLA and oxygen plasma-treated PLA samples obtained using a Krüss DSA100 contact angle measuring device (Krüss GmbH, Hamburg, Germany).

methods is the difficulty to generate a homogeneous modification on the samples to be treated. In this regard, for the specific case of 3D complex scaffolds, one of the challenges is to ensure that the surface modification takes place throughout the entire structure, since it is not always possible to reach the inner part of a scaffold with complex internal architecture or with small pore size (121,196,198).

4.3 Coating with bioactive substances

When the objective is to improve the biofunctionality of PLA-based scaffolds, the application of a bioactive coating to their surface is a promising approach. Several examples can be found in the literature regarding coated PLA scaffolds intended for bone regeneration. Some of the bioactive compounds investigated with this purpose include chitosan (199), alginate (200), collagen (201) or calcium phosphates (105), among others. In this section, different coating strategies to improve the biological properties of PLA-based bone scaffolds will be reviewed. The focus will be put on scaffolds manufactured by AM techniques.

In a recent work, Kao et al. (202) concluded that an improvement on stem cell adhesion, proliferation and differentiation could be obtained by coating the 3D printed scaffold surface with polydopamine (PDA). Specifically, human adipose-derived stem cells (hADSCs) were used to assess the biofunctionality of the PLA scaffolds modified by this mussel-inspired surface coating. The scaffolds were printed by using an FDM-based technique. The obtained structures were immersed into a dopamine (DA) solution with continuous stirring at room temperature. Two different concentrations were studied for this solution: 1 and 2 mg/mL of dopamine in 10 mM pH 8.5 Tris buffer. Finally, the scaffolds were soaked in the dopamine solution for 12 h. The results obtained were promising for the application of this method to enhance the properties of PLA-based bone scaffolds. A better performance of the PLA scaffolds coated with the DA solution of higher concentration (2 mg/mL) was confirmed. Some important findings in this work include the enhanced adhesion, proliferation, type I collagen secretion and cell cycle of hADSCs cultured on PLA/PDA scaffolds compared to the unmodified constructs. In addition, ALP activity and osteocalcin concentration were significantly improved after the application of the proposed coatings, being osteocalcin an osteoblast-specific protein hormone (203). According to the results, the expression of ang-1 and vWF angiogenic proteins was also significantly enhanced. The application of a PDA coating to 3D printed PLA scaffolds is also assessed in the work of Teixeira et al. (164) already mentioned in Section 3.3. These authors evaluated not only the effect of the PDA coating on the biological properties of the constructs, but also its ability to immobilize type I collagen (COL) onto the scaffold surface. With this purpose, FDM-manufactured structures were immersed into PDA and/or COL solutions after an alkali treatment. According to the results, COL immobilization increased by 92% when the PDA coating was applied. The combination of both coating steps led to an improved osteoinductivity of the 3D printed PLA scaffolds, as confirmed by the viability, adhesion and metabolic activity tests carried out using BMSCs. In contrast to the methodology used by Kao et al. (202), who directly applied the PDA coating, a previous surface treatment is used in this work. The promising results of these studies show the feasibility of both strategies to improve the scaffold properties (Figure 11).

In the already mentioned work of Martin et al. (186), 3D printed PLA scaffolds with enhanced biological properties were developed by coating the structures with bioactive compounds after applying an alkali surface treatment. Different collagen-based coatings were assessed in this work. In all cases, the treated PLA scaffolds were immersed in the coating solution for 24 h at room

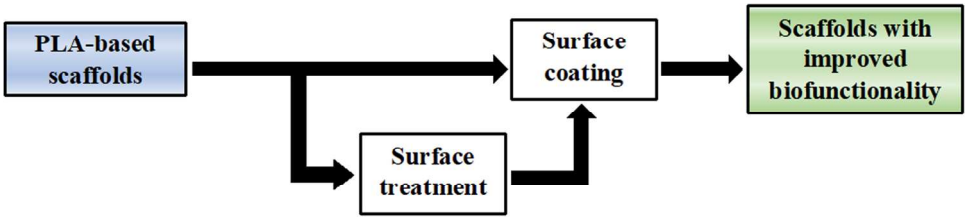

Figure 11: Application of a surface coating to scaffolds with or without previous surface treatment.

temperature and under stirring. The best results were obtained for a combination comprising collagen (COL), minocycline antibiotic (MH) and bioinspired citrate-hydroxyapatite nanoparticles (cHAp). Functionalized PLA scaffolds with this coating reduced the bacterial biofilm formation while favoring cell adhesion, proliferation and osteogenesis-related gene expression of hBMSCs. The proposed constructs could be suitable for bone regeneration, as they also showed adequate wettability and mechanical properties that match the ones reported for trabecular bone. Disparate results regarding the mechanical performance of the proposed scaffolds were obtained in the work of Fernández-Cervantes et al. (200), who presented a mathematical model to design 3D scaffolds for BTE applications. The numerical solution of this method takes into account the spatio-temporal changes that occur during the bone remodeling process (bone mass, osteoblast and osteoclast populations, etc.). The scaffolds developed were composed of PLA, sodium alginate and HAp, showing a microstructure that resembles the architecture of trabecular bone. Firstly, a mixture of HAp and the sodium alginate solution was stirred to induce the gelation process of the latter, due to its interaction with the divalent cations of the ceramic compound. Then, PLA constructs manufactured by 3D printing were immersed into the coating in a batch stirring reactor to produce the composite scaffolds. Despite their suitable morphological properties, the mechanical properties of the PLA/alginate/HAp scaffolds tested in this work do not match with the reported ranges for trabecular bone in terms of compressive strength and elastic modulus. However, the authors stated that these properties can be easily tuned by the application of a simulated body fluid (SBF) treatment. Samples immersed in SBF and incubated at 37°C for two weeks showed an improvement in compression resistance due to the induced mineralization of HAp crystals on the surface of the composite scaffolds.

The coating of PLA-based scaffolds with bioactive compounds has also been proposed for osteochondral regeneration. With this objective, Holmes et al. (204) proposed the use of biphasic 3D printed PLA-based scaffolds for osteochondral regeneration. With the aim of mimicking the architecture of natural bone and cartilage tissues, they designed 3D structures composed by two distinct parts, which varied in pore size, pore density and printing pattern. In order to increase the mechanical strength of the final construct and prevent its failure at the engineered interface, tubular-shaped structures with the length of the scaffold were incorporated in the CAD design. The authors stated that this innovative methodology allow them to improve the integration of the bone and cartilage parts, resulting in a more effective method than the conventional procedures for assembling the osteochondral unit, which are based on the separate manufacturing of the layers and their subsequent union by using glue, suture or thermal methods (205). Compression and shear test results confirmed the enhanced mechanical characteristics of the designed scaffolds. On the other hand, with the objective of improving the biocompatibility of the PLA matrix, the 3D printed scaffolds were coated with acetylated collagen. The method used for chemical functionalization of the surface involved successive immersions of the structures into different solutions, resulting in the linkage between PLA and ethylenediamine and then between the latter and glutaraldehyde. The surface coating process was completed after type I collagen binds to glutaraldehyde. The best results after 5 days in a proliferation test using hBMSCs were obtained with the collagen-coated PLA scaffolds. However, regarding chondrogenic differentiation, structures with and without coating displayed similar synthesis capacity of glycosaminoglycan, type II collagen and total protein content.

5 Conclusions and future trends perspectives in this field

PLA has been extensively applied in TE because of its good biocompatibility, biodegradability and mechanical

properties. Furthermore, PLA is very suitable to be processed by AM, which provides many advantages for bone scaffold manufacturing (customization, hierarchical and porous structures, repeatability, functional graded manufacturing, etc.). Different AM technologies have been reported for PLA-based scaffolds processing, such as material extrusion, powder bed fusion and vat photopolymerization. Nevertheless, the use of PLA in TE requires addressing some issues related to the release of acidic byproducts and their accumulation due to an inefficient removal from the surroundings of the scaffold's location. This accumulation can generate inflammatory conditions, negatively affecting tissue regeneration. This review reports some approaches to stabilize the pH, including the use of low molecular weight PLA or composites formed by PLA and bioactive glasses or calcium phosphates.

Another relevant topic shown in this review is the discussion of the different strategies to improve PLA properties. This paper highlights the use of additives to increase the mechanical properties and enhance the osteoconductivity of the matrix (HAp, β-TCP, CMC, etc.), the application of surface treatments to increase the surface hydrophilicity (alkali treatments, plasma treatments) and the use of surface coatings with bioactive substances to promote cell bioactivity (chitosan, alginate, calcium phosphate, PDA, collagen, etc.).

The future of PLA as biomaterial for bone scaffolds manufacturing is linked to the further development of some specific features for the improvement of the efficiency. Some relevant research lines include:

- Development of innovate composite materials to be used as feeding in bioprinting systems
- Improvement of the bioprinting process to enable the production of multifunctional graded scaffolds combining PLA with other biomaterials or bioinks
- Combination of AM techniques with other technologies, such as electrospinning, taking advantage of the benefits of each of them for bone scaffold manufacturing
- Loading of drugs or antibiotics for associated infections.
- Possibility of integrating sensing materials into the scaffold, aiming to monitor the properties change through time (pH level of the surroundings, mechanical stress of the structure, etc.)
- Implementation of theoretical degradation models of PLA to predict medium/long-term *in vitro* and *in vivo* behavior.

Acknowledgments: This contribution is part of the project BioAM (DPI2017-88465-R) funded by the Science, Innovation and Universities Spanish Ministry. Also, Ricardo Donate express his gratitude for the funding through the PhD grant program co-financed by the Canarian Agency for Research, Innovation and Information Society of the Canary Islands Regional Council for Employment, Industry, Commerce and Knowledge and by the European Social Fund (ESF) Canary Islands Integrated Operational Program 2014-2020, Axis 3 Priority Theme 74 (85%). Grant code: TESIS2017010036.

Conflict of interest: The authors declare no conflict of interest.

References

(1) Chung C, Burdick JA. Engineering cartilage tissue. Adv Drug Delivery Rev. 2008;60(2):243–62. doi: 10.1016/j.addr.2007.08.027.

(2) Wu S, Liu X, Yeung KWK, Liu C, Yang X. Biomimetic porous scaffolds for bone tissue engineering. Mater Sci Eng R Rep. 2014;80(1):1–36. doi: 10.1016/j.mser.2014.04.001.

(3) Zhao X, Lang Q, Yildirimer L, Lin ZY, Cui W, Annabi N, et al. Photocrosslinkable gelatin hydrogel for epidermal tissue engineering. Adv Healthc Mater. 2016;5(1):108–18. doi: 10.1002/adhm.201500005.

(4) Ghasemi-Mobarakeh L, Prabhakaran MP, Morshed M, Nasr-Esfahani MH, Ramakrishna S. Electrospun poly(ε-caprolactone)/gelatin nanofibrous scaffolds for nerve tissue engineering. Biomaterials. 2008;29(34):4532–9. doi: 10.1016/j.biomaterials.2008.08.007.

(5) Vaz CM, van Tuijl S, Bouten CVC, Baaijens FPT. Design of scaffolds for blood vessel tissue engineering using a multi-layering electrospinning technique. Acta Biomater. 2005;1(5):575–82. doi: 10.1016/j.actbio.2005.06.006.

(6) Puppi D, Chiellini F, Piras AM, Chiellini E. Polymeric material for bone and cartilage repair. Prog Polym Sci. 2010;35(4):403–40. doi: 10.1016/j.progpolymsci.2010.01.006.

(7) Lee SH, Shin H. Matrices and scaffolds for delivery of bioactive molecules in bone and cartilage tissue engineering. Adv Drug Delivery Rev. 2007;59(4–5):339–59. doi: 10.1016/j.addr.2007.03.016.

(8) Murphy CM, Haugh MG, O'Brien FJ. The effect of mean pore size on cell attachment, proliferation and migration in collagen-glycosaminoglycan scaffolds for bone tissue engineering. Biomaterials. 2010;31(3):461–6. doi: 10.1016/j.biomaterials.2009.09.063.

(9) Cabral J, Moratti SC. Hydrogels for biomedical applications. Future Med Chem. 2011;3(15):1877–88. doi: 10.4155/fmc.11.134.

(10) Rezwan K, Chen QZ, Blaker JJ, Boccaccini AR. Biodegradable and bioactive porous polymer/inorganic composite scaffolds for bone tissue engineering. Biomaterials. 2006;27(18):3413–31. doi: 10.1016/j.biomaterials.2006.01.039.

(11) Chevalier E, Chulia D, Pouget C, Viana M. Fabrication of porous substrates: a review of processes using pore forming agents in the biomaterial field. J Pharm Sci. 2008;97(3):1135–54. doi: 10.1002/jps.21059.

(12) Seyednejad H, Gawlitta D, Kuiper RV, De Bruin A, Van Nostrum CF, Vermonden T, et al. *In vivo* biocompatibility and biodegradation of 3D-printed porous scaffolds based on a hydroxyl-functionalized poly(ε-caprolactone). Biomaterials. 2012;33(17):4309–18. doi: 10.1016/j.biomaterials.2012.03.002.
(13) Zhang L, Yang G, Johnson BN, Jia X. Three-dimensional (3D) printed scaffold and material selection for bone repair. Acta Biomater. 2019;84:16–33. doi: 10.1016/j.actbio.2018.11.039.
(14) Hollister SJ. Porous scaffold design for tissue engineering. Nat Mater. 2005;4(7):518–24. doi: 10.1038/nmat1421.
(15) Loh QL, Choong C. Three-dimensional scaffolds for tissue engineering applications: role of porosity and pore size. Tissue Eng Part B Rev. 2013;19(6):485–502. doi: 10.1089/ten.teb.2012.0437.
(16) Arcaute K, Mann BK, Wicker RB. Stereolithography of three-dimensional bioactive poly(ethylene glycol) constructs with encapsulated cells. Ann Biomed Eng. 2006;34(9):1429–41. doi: 10.1007/s10439-006-9156-y.
(17) Masuko T, Iwasaki N, Yamane S, Funakoshi T, Majima T, Minami A, et al. Chitosan-RGDSGGC conjugate as a scaffold material for musculoskeletal tissue engineering. Biomaterials. 2005;26(26):5339–47. doi: 10.1016/j.biomaterials.2005.01.062.
(18) Yan J, Miao Y, Tan H, Zhou T, Ling Z, Chen Y, et al. Injectable alginate/hydroxyapatite gel scaffold combined with gelatin microspheres for drug delivery and bone tissue engineering. Mater Sci Eng C. 2016;63:274–84. doi: 10.1016/j.msec.2016.02.071.
(19) Cui H, Zhu W, Holmes B, Zhang LG. Biologically inspired smart release system based on 3D bioprinted perfused scaffold for vascularized tissue regeneration. Adv Sci. 2016;3(8):1–10. doi: 10.1002/advs.201600058.
(20) Causa F, Netti PA, Ambrosio L. A multi-functional scaffold for tissue regeneration: the need to engineer a tissue analogue. Biomaterials. 2007;28(34):5093–9. doi: 10.1016/j.biomaterials.2007.07.030.
(21) Li JP, Habibovic P, van den Doe M, Wilson CE, de Wijn JR, van Blitterswijk CA, et al. Bone ingrowth in porous titanium implants produced by 3D fiber deposition. Biomaterials. 2007;28(18):2810–20. doi: 10.1016/j.biomaterials.2007.02.020.
(22) Vallet-Regí M, Ruiz-Hernández E. Bioceramics: from bone regeneration to cancer nanomedicine. Adv Mater. 2011;23(44):5177–218. doi: 10.1002/adma.201101586.
(23) Nair LS, Laurencin CT. Biodegradable polymers as biomaterials. Prog Polym Sci. 2007;32(8–9):762–98. doi: 10.1016/j.progpolymsci.2007.05.017.
(24) Boccaccini AR, Blaker JJ. Bioactive composite materials for tissue engineering scaffolds. Expert Rev Med Devices. 2005;2(3):303–17. doi: 10.1586/17434440.2.3.303.
(25) Dorati R, DeTrizio A, Modena T, Conti B, Benazzo F, Gastaldi G, et al. Biodegradable scaffolds for bone regeneration combined with drug-delivery systems in osteomyelitis therapy. Pharmaceuticals. 2017;10(4):96. doi: 10.3390/ph10040096.
(26) Ulery BD, Nair LS, Laurencin CT. Biomedical applications of biodegradable polymers. J Polym Sci Part B Polym Phys. 2011;49(12):832–64. doi: 10.1002/polb.22259.
(27) Liu X, Ma PX. Polymeric scaffolds for bone tissue engineering. Ann Biomed Eng. 2004;32(3):477–86. http://www.ncbi.nlm.nih.gov/pubmed/15095822.
(28) Dong C, Lv Y, Dong C, Lv Y. Application of collagen scaffold in tissue engineering: recent advances and new perspectives. Polymers. 2016;8(2):42. doi: 10.3390/polym8020042.
(29) Ribeiro JCV, Vieira RS, Melo IM, Araújo VMA, Lima V. Versatility of chitosan-based biomaterials and their use as scaffolds for tissue regeneration. Sci World J. 2017;2017:1–25. doi: 10.1155/2017/8639898.
(30) Lin H-R, Yeh Y-J. Porous alginate/hydroxyapatite composite scaffolds for bone tissue engineering: preparation, characterization, and *in vitro* studies. J Biomed Mater Res. 2004;71B(1):52–65. doi: 10.1002/jbm.b.30065.
(31) Hutmacher DW, Schantz T, Zein I, Ng KW, Teoh SH, Tan KC. Mechanical properties and cell cultural response of polycaprolactone scaffolds designed and fabricated via fused deposition modeling. J Biomed Mater Res. 2001;55(2):203–16. doi: 10.1002/1097-4636(200105)55:2<203:AID-JBM1007>3.0.CO;2-7.
(32) Rajendran T, Venugopalan S. Role of polylactic acid in bone regeneration – a systematic review. J Pharm Sci Res. 2015;7(11):960–66.
(33) Santoro M, Shah SR, Walker JL, Mikos AG. Poly(lactic acid) nanofibrous scaffolds for tissue engineering. Adv Drug Delivery Rev. 2016;107:206–12. doi: 10.1016/J.ADDR.2016.04.019.
(34) Gang EH, Ki CS, Kim JW, Lee J, Cha BG, Lee KH, et al. Highly porous three-dimensional poly(lactide-*co*-glycolide) (PLGA) microfibrous scaffold prepared by electrospinning method: a comparison study with other PLGA type scaffolds on its biological evaluation. Fibers Polym. 2012;13(6):685–91. doi: 10.1007/s12221-012-0685-8.
(35) Lee KY, Mooney DJ. Alginate: properties and biomedical applications. Prog Polym Sci. 2012;37(1):106–26. doi: 10.1016/j.progpolymsci.2011.06.003.
(36) Zhu Y, Gao C, Shen J. Surface modification of polycaprolactone with poly(methacrylic acid) and gelatin covalent immobilization for promoting its cytocompatibility. Biomaterials. 2002;23(24):4889–95. doi: 10.1016/S0142-9612(02)00247-8.
(37) Rasal RM, Janorkar AV, Hirt DE. Poly(lactic acid) modifications. Prog Polym Sci. 2010;35(3):338-56. doi: 10.1016/j.progpolymsci.2009.12.003
(38) Reddy MM, Vivekanandhan S, Misra M, Bhatia SK, Mohanty AK. Biobased plastics and bionanocomposites: current status and future opportunities. Prog Polym Sci. 2013;38(10–11):1653–89. doi: 10.1016/j.progpolymsci.2013.05.006.
(39) Gritsch L, Conoscenti G, La Carrubba V, Nooeaid P, Boccaccini AR. Polylactide-based materials science strategies to improve tissue–material interface without the use of growth factors or other biological molecules. Mater Sci Eng C. 2019;94(January 2018):1083–101. doi: 10.1016/j.msec.2018.09.038.
(40) Davachi SM, Kaffashi B. Polylactic acid in medicine. Polym Plast Technol Eng. 2015;54(9):944–67. doi: 10.1080/03602559.2014.979507.
(41) Farah S, Anderson DG, Langer R. Physical and mechanical properties of PLA, and their functions in widespread

applications – a comprehensive review. Adv Drug Delivery Rev. 2016;107:367–92. doi: 10.1016/j.addr.2016.06.012.
(42) Grémare A, Guduric V, Bareille R, Heroguez V, Latour S, L'heureux N, et al. Characterization of printed PLA scaffolds for bone tissue engineering. J Biomed Mater Res Part A. 2018;106(4):887–94. doi: 10.1002/jbm.a.36289.
(43) Lim LT, Cink K, Vanyo T. Processing of poly(Lactic Acid). In: Poly(Lactic Acid): synthesis, structures, properties, processing, and applications. New Jersey: John Wiley and Sons; 2010. p. 191–215. ISBN 9780470293669.
(44) Bergsma J. Late degradation tissue response to poly (?-lactide) bone plates and screws. Biomaterials. 1995;16(1):25-31. doi: 10.1016/0142-9612(95)91092-D.
(45) Savioli Lopes M, Jardini AL, Maciel Filho R. Poly(lactic acid) production for tissue engineering applications. Procedia Eng. 2012;42(August):1402–13. doi: 10.1016/j.proeng.2012.07.534.
(46) Manavitehrani I, Fathi A, Badr H, Daly S, Negahi Shirazi A, Dehghani F. Biomedical applications of biodegradable polyesters. Polymers. 2016;8(1):20. doi: 10.3390/polym8010020.
(47) Asti A, Gioglio L. Natural and synthetic biodegradable polymers: different scaffolds for cell expansion and tissue formation. Int J Artif Organs. 2014;37(3):187–205. doi: 10.530/ijao.5000307.
(48) Vasanthan N, Ly O. Effect of microstructure on hydrolytic degradation studies of poly(L-lactic acid) by FTIR spectroscopy and differential scanning calorimetry. Polym Degrad Stab. 2009;94(9):1364–72. doi: 10.1016/j.polymdegradstab.2009.05.015.
(49) Araque-Monrós MC, Vidaurre A, Gil-Santos L, Gironés Bernabé S, Monleón-Pradas M, Más-Estellés J. Study of the degradation of a new PLA braided biomaterial in buffer phosphate saline, basic and acid media, intended for the regeneration of tendons and ligaments. Polym Degrad Stab. 2013;98(9):1563–70. doi: 10.1016/j.polymdegradstab.2013.06.031.
(50) Tsuji H, Mizuno A, Ikada Y. Properties and morphology of poly(L-lactide). III. Effects of initial crystallinity on long-termin vitro hydrolysis of high molecular weight poly(L-lactide) film in phosphate-buffered solution. J Appl Polym Sci. 2000;77(7):1452–64. doi: 10.1002/1097-4628(20000815)77:7<1452:AID-APP7>3.0.CO;2-S.
(51) Göpferich A. Mechanisms of polymer degradation and erosion. Biomaterials. 1996;17(2):103–14. doi: 10.1016/0142-9612(96)85755-3.
(52) Kang Y, Yao Y, Yin G, Huang Z, Liao X, Xu X, et al. A study on the *in vitro* degradation properties of poly(L-lactic acid)/β-tricalcuim phosphate (PLLA/β-TCP) scaffold under dynamic loading. Med Eng Phys. 2009;31(5):589–94. doi: 10.1016/j.medengphy.2008.11.014.
(53) Blaker JJ, Nazhat SN, Maquet V, Boccaccini AR. Long-term *in vitro* degradation of PDLLA/Bioglass® bone scaffolds in acellular simulated body fluid. Acta Biomater. 2011;7(2):829–40. doi: 10.1016/j.actbio.2010.09.013.
(54) Vink ETH, Rábago KR, Glassner DA, Gruber PR. Applications of life cycle assessment to NatureWorks™ polylactide (PLA) production. Polym Degrad Stab. 2003;80(3):403–19. doi: 10.1016/S0141-3910(02)00372-5.
(55) Shen P, Moriya A, Rajabzadeh S, Maruyama T, Matsuyama H. Improvement of the antifouling properties of poly(lactic acid) hollow fiber membranes with poly(lactic acid)–polyethylene glycol–poly(lactic acid) copolymers. Desalination. 2013;325:37–9. doi: 10.1016/j.desal.2013.06.012.
(56) Place ES, George JH, Williams CK, Stevens MM. Synthetic polymer scaffolds for tissue engineering. Chem Soc Rev. 2009;38(4):1139–51. doi: 10.1039/b811392k.
(57) Improta G, Balato G, Romano M, Ponsiglione AM, Raiola E, Russo MA. Improving performances of the knee replacement surgery process by applying DMAIC principles. J Eval Clin Pract. 2017;23(6):1401–7. doi: 10.1111/jep.12810.
(58) Amini AR, Laurencin CT, Nukavarapu SP. Bone tissue engineering: recent advances and challenges. Crit Rev Biomed Eng. 2012;40(5):363–408. doi: 10.1615/CritRevBiomedEng.v40.i5.10.
(59) Wubneh A, Tsekoura EK, Ayranci C, Uludağ H. Current state of fabrication technologies and materials for bone tissue engineering. Acta Biomater. 2018;80:1–30. doi: 10.1016/j.actbio.2018.09.031.
(60) Narayanan G, Vernekar VN, Kuyinu EL, Laurencin CT. Poly (lactic acid)-based biomaterials for orthopaedic regenerative engineering. Adv Drug Delivery Rev. 2016;107:247–76. doi: 10.1016/j.addr.2016.04.015.
(61) Pal S. Design of Artificial Human Joints & Organs. Boston, MA: Springer US; 2014. doi: 10.1007/978-1-4614-6255-2.
(62) Bose S, Vahabzadeh S, Bandyopadhyay A. Bone tissue engineering using 3D printing. Mater Today. 2013;16(12):496–504. doi: 10.1016/j.mattod.2013.11.017.
(63) Ashammakhi N, Hasan A, Kaarela O, Byambaa B, Sheikhi A, Gaharwar AK, et al. Advancing frontiers in bone bioprinting. Adv Healthc Mater. 2019;8(7):1–24. doi: 10.1002/adhm.201801048.
(64) Wang X, Xu S, Zhou S, Xu W, Leary M, Choong P, et al. Topological design and additive manufacturing of porous metals for bone scaffolds and orthopaedic implants: a review. Biomaterials. 2016;83:127–41. doi: 10.1016/j.biomaterials.2016.01.012.
(65) Chen S, Guo Y, Liu R, Wu S, Fang J, Huang B, et al. Tuning surface properties of bone biomaterials to manipulate osteoblastic cell adhesion and the signaling pathways for the enhancement of early osseointegration. Colloids Surf B. 2018;164:58–69. doi: 10.1016/J.COLSURFB.2018.01.022.
(66) Karageorgiou V, Kaplan D. Porosity of 3D biomaterial scaffolds and osteogenesis. Biomaterials. 2005;26(27):5474–91. doi: 10.1016/J.BIOMATERIALS.2005.02.002.
(67) Mandoli C, Mecheri B, Forte G, Pagliari F, Pagliari S, Carotenuto F, et al. Thick soft tissue reconstruction on highly perfusive biodegradable scaffolds. Macromol Biosci. 2010;10(2):127–38. doi: 10.1002/mabi.200900323.
(68) Tajbakhsh S, Hajiali F. A comprehensive study on the fabrication and properties of biocomposites of poly(lactic acid)/ceramics for bone tissue engineering. Mater Sci Eng C. 2017;70:897–912. doi: 10.1016/j.msec.2016.09.008.
(69) Liao S, Chan CK, Ramakrishna S. Stem cells and biomimetic materials strategies for tissue engineering. Mater Sci Eng C. 2008;28(8):1189–202. doi: 10.1016/j.msec.2008.08.015.

(70) Chen X, Fan H, Deng X, Wu L, Yi T, Gu L, et al. Scaffold structural microenvironmental cues to guide tissue regeneration in bone tissue applications. Nanomaterials. 2018;8(11):1–15. doi: 10.3390/nano8110960.
(71) Boyan B. Role of material surfaces in regulating bone and cartilage cell response. Biomaterials. 1996;17(2):137–46. doi: 10.1016/0142-9612(96)85758-9.
(72) Bodhak S, Bose S, Bandyopadhyay A. Role of surface charge and wettability on early stage mineralization and bone cell–materials interactions of polarized hydroxyapatite. Acta Biomater. 2009;5(6):2178–88. doi: 10.1016/J.ACTBIO.2009.02.023.
(73) Bosshardt DD, Chappuis V, Buser D. Osseointegration of titanium, titanium alloy and zirconia dental implants: current knowledge and open questions. Periodontol 2000. 2017;73(1):22–40. doi: 10.1111/prd.12179.
(74) Song P, Hu C, Pei X, Sun J, Sun H, Wu L, et al. Dual modulation of crystallinity and macro-/microstructures of 3D printed porous titanium implants to enhance stability and osseointegration. J Mater Chem B. 2019;7(17):2865–77. doi: 10.1039/c9tb00093c.
(75) Yánez A, Herrera A, Martel O, Monopoli D, Afonso H. Compressive behaviour of gyroid lattice structures for human cancellous bone implant applications. Mater Sci Eng C. 2016;68:445–8. doi: 10.1016/j.msec.2016.06.016.
(76) Matena J, Petersen S, Gieseke M, Kampmann A, Teske M, Beyerbach M, et al. SLM produced porous titanium implant improvements for enhanced vascularization and osteoblast seeding. Int J Mol Sci. 2015;16(4):7478–92. doi: 10.3390/ijms16047478.
(77) Jazayeri HE, Rodriguez-Romero M, Razavi M, Tahriri M, Ganjawalla K, Rasoulianboroujeni M, et al. The cross-disciplinary emergence of 3D printed bioceramic scaffolds in orthopedic bioengineering. Ceram Int. 2018;44(1):1–9. doi: 10.1016/j.ceramint.2017.09.095.
(78) Schiller C, Epple M. Carbonated calcium phosphates are suitable pH-stabilising fillers for biodegradable polyesters. Biomaterials. 2003;24(12):2037–43. doi: 10.1016/S0142-9612(02)00634-8.
(79) Rizwan M, Hamdi M, Basirun WJ. Bioglass® 45S5-based composites for bone tissue engineering and functional applications. J Biomed Mater Res Part A. 2017;105(11):3197–223. doi: 10.1002/jbm.a.36156.
(80) Zhang B, Sun H, Wu L, Ma L, Xing F, Kong Q, et al. 3D printing of calcium phosphate bioceramic with tailored biodegradation rate for skull bone tissue reconstruction. Bio-Design Manuf. 2019;2(3):161–71. doi: 10.1007/s42242-019-00046-7.
(81) Warnke PH, Seitz H, Warnke F, Becker ST, Sivananthan S, Sherry E, et al. Ceramic scaffolds produced by computer-assisted 3D printing and sintering: characterization and biocompatibility investigations. J Biomed Mater Res Part B Appl Biomater. 2010;93(1):212–7. doi: 10.1002/jbm.b.31577.
(82) Hench LL, Paschall HA. Direct chemical bond of bioactive glass-ceramic materials to bone and muscle. J Biomed Mater Res. 1973;7(3):25–42. doi: 10.1002/jbm.820070304.
(83) Sarker B, Hum J, Nazhat SN, Boccaccini AR. Combining collagen and bioactive glasses for bone tissue engineering: a review. Adv Healthc Mater. 2015;4(2):176–94. doi: 10.1002/adhm.201400302.
(84) Venkatesan J, Bhatnagar I, Manivasagan P, Kang K-H, Kim S-K. Alginate composites for bone tissue engineering: a review. Int J Biol Macromol. 2015;72:269–81. doi: 10.1016/j.ijbiomac.2014.07.008.
(85) Di Martino A, Sittinger M, Risbud MV. Chitosan: a versatile biopolymer for orthopaedic tissue-engineering. Biomaterials. 2005;26(30):5983-90. doi: 10.1016/j.biomaterials.2005.03.016.
(86) Turnbull G, Clarke J, Picard F, Riches P, Jia L, Han F, et al. 3D bioactive composite scaffolds for bone tissue engineering. Bioact Mater. 2018;3(3):278–314. doi: 10.1016/j.bioactmat.2017.10.001.
(87) Melke J, Midha S, Ghosh S, Ito K, Hofmann S. Silk fibroin as biomaterial for bone tissue engineering. Acta Biomater. 2016;31:1–16. doi: 10.1016/j.actbio.2015.09.005.
(88) Hajiali F, Tajbakhsh S, Shojaei A. Fabrication and properties of polycaprolactone composites containing calcium phosphate-based ceramics and bioactive glasses in bone tissue engineering: a review. Polym Rev. 2018;58(1):164–207. doi: 10.1080/15583724.2017.1332640.
(89) Gentile P, Chiono V, Carmagnola I, Hatton P. An overview of poly(lactic-*co*-glycolic) acid (PLGA)-based biomaterials for bone tissue engineering. Int J Mol Sci. 2014;15(3):3640–59. doi: 10.3390/ijms15033640.
(90) Domingos M, Gloria A, Coelho J, Bartolo P, Ciurana J. Three-dimensional printed bone scaffolds: The role of nano/micro-hydroxyapatite particles on the adhesion and differentiation of human mesenchymal stem cells. Proc Inst Mech Eng Part H J Eng Med. 2017;231(6):555–64. doi: 10.1177/0954411916680236.
(91) Rakovsky A, Gotman I, Rabkin E, Gutmanas EY. β-TCP-polylactide composite scaffolds with high strength and enhanced permeability prepared by a modified salt leaching method. J Mech Behav Biomed Mater. 2014;32(November 2016):89–98. doi: 10.1016/j.jmbbm.2013.12.022.
(92) Kang Y, Yin G, Yuan Q, Yao Y, Huang Z, Liao X, et al. Preparation of poly(l-lactic acid)/β-tricalcium phosphate scaffold for bone tissue engineering without organic solvent. Mater Lett. 2008;62(12–13):2029–32. doi: 10.1016/j.matlet.2007.11.014.
(93) Prabaharan M, Rodriguez-Perez MA, de Saja JA, Mano JF. Preparation and characterization of poly(L-lactic acid)-chitosan hybrid scaffolds with drug release capability. J Biomed Mater Res Part B Appl Biomater. 2007;81B (2):427–34. doi: 10.1002/jbm.b.30680.
(94) Nga NK, Hoai TT, Viet PH. Biomimetic scaffolds based on hydroxyapatite nanorod/poly(D,L) lactic acid with their corresponding apatite-forming capability and biocompatibility for bone-tissue engineering. Colloids Surf B. 2015;128:506–14. doi: 10.1016/j.colsurfb.2015.03.001.
(95) Charles-Harris M, Koch MA, Navarro M, Lacroix D, Engel E, Planell JA. A PLA/calcium phosphate degradable composite material for bone tissue engineering: an *in vitro* study. J Mater Sci Mater Med. 2008;19(4):1503–13. doi: 10.1007/s10856-008-3390-9.
(96) Zhang R, Ma PX. Poly(alpha-hydroxyl acids)/hydroxyapatite porous composites for bone-tissue engineering. I. Preparation and morphology. J Biomed Mater Res. 1999;44:446–55.

(97) Carfì Pavia F, Conoscenti G, Greco S, La Carrubba V, Ghersi G, Brucato V. Preparation, characterization and in vitro test of composites poly-lactic acid/hydroxyapatite scaffolds for bone tissue engineering. Int J Biol Macromol. 2018;119:945–53. doi: 10.1016/j.ijbiomac.2018.08.007.
(98) Montjovent M-O, Mathieu L, Hinz B, Applegate LL, Bourban P-E, Zambelli P-Y, et al. Biocompatibility of bioresorbable poly(L-lactic acid) composite scaffolds obtained by supercritical gas foaming with human fetal bone cells. Tissue Eng. 2005;11(11–12):1640–9. doi: 10.1089/ten.2005.11.1640.
(99) Liao SS, Cui FZ, Zhang W, Feng QL. Hierarchically biomimetic bone scaffold materials: nano-HA/collagen/PLA composite. J Biomed Mater Res Part B Appl Biomater. 2004;69(2):158–65. doi: 10.1002/jbm.b.20035.
(100) Wang D, Lin H, Jiang J, Jin Q, Li L, Dong Y, et al. Fabrication of long-acting drug release property of hierarchical porous bioglasses/polylactic acid fibre scaffolds for bone tissue engineering. IET Nanobiotechnol. 2015;9(2):58–65. doi: 10.1049/ietnbt.2013.0011.
(101) Han X, Zhou X, Qiu K, Feng W, Mo H, Wang M, et al. Strontium-incorporated mineralized PLLA nanofibrous membranes for promoting bone defect repair. Colloids Surf B. 2019;179(March):363–73. doi: 10.1016/j.colsurfb.2019.04.011.
(102) Li Y, Li D, Lu B, Gao D, Zhou J. Current status of additive manufacturing for tissue engineering scaffold. Rapid Prototyp J. 2015;21(6):747–62. doi: 10.1108/RPJ-03-2014-0029.
(103) Wu GH, Hsu SH. Review: polymeric-based 3D printing for tissue engineering. J Med Biol Eng. 2015;35(3):285–92. doi: 10.1007/s40846-015-0038-3.
(104) Li J, Chen Y, Mak AFT, Tuan RS, Li L, Li Y. A one-step method to fabricate PLLA scaffolds with deposition of bioactive hydroxyapatite and collagen using ice-based microporogens. Acta Biomater. 2010;6(6):2013–9. doi: 10.1016/j.actbio.2009.12.008.
(105) Kim SH, Oh SA, Lee WK, Shin US, Kim HW. Poly(lactic acid) porous scaffold with calcium phosphate mineralized surface and bone marrow mesenchymal stem cell growth and differentiation. Mater Sci Eng C. 2011;31(3):612–9. doi: 10.1016/j.msec.2010.11.028.
(106) Revati R, Abdul Majid MS, Ridzuan MJM, Normahira M, Mohd Nasir NF, Rahman Y M.N, et al. Mechanical, thermal and morphological characterisation of 3D porous Pennisetum purpureum/PLA biocomposites scaffold. Mater Sci Eng C. 2017;75:752–9. doi: 10.1016/j.msec.2017.02.127.
(107) Revati R, Abdul Majid MS, Ridzuan MJM, Normahira M, Mohd Nasir NF, Cheng EM. Biodegradation of PLA-Pennisetum purpureum based biocomposite scaffold. J Phys Conf Ser. 2017;908(1):012029. doi: 10.1088/1742-6596/908/1/012029.
(108) Mao D, Li Q, Li D, Chen Y, Chen X, Xu X. Fabrication of 3D porous poly(lactic acid)-based composite scaffolds with tunable biodegradation for bone tissue engineering. Mater Des. 2018;142:1–10. doi: 10.1016/j.matdes.2018.01.016.
(109) Wei G, Ma PX. Structure and properties of nano-hydroxyapatite/polymer composite scaffolds for bone tissue engineering. Biomaterials. 2004;25(19):4749–57. doi: 10.1016/j.biomaterials.2003.12.005.
(110) Lou T, Wang X, Song G, Gu Z, Yang Z. Structure and properties of PLLA/β-TCP nanocomposite scaffolds for bone tissue engineering. J Mater Sci Mater Med. 2015;26(1):1–7. doi: 10.1007/s10856-014-5366-2.
(111) Niu X, Feng Q, Wang M, Guo X, Zheng Q. *In vitro* degradation and release behavior of porous poly(lactic acid) scaffolds containing chitosan microspheres as a carrier for BMP-2-derived synthetic peptide. Polym Degrad Stab. 2009;94(2):176–82. doi: 10.1016/j.polymdegradstab.2008.11.008.
(112) Safinia L, Datan N, Höhse M, Mantalaris A, Bismarck A. Towards a methodology for the effective surface modification of porous polymer scaffolds. Biomaterials. 2005;26(36):7537–47. doi: 10.1016/j.biomaterials.2005.05.078.
(113) Lou T, Wang X, Song G, Gu Z, Yang Z. Fabrication of PLLA/β-TCP nanocomposite scaffolds with hierarchical porosity for bone tissue engineering. Int J Biol Macromol. 2014;69:464–70. doi: 10.1016/j.ijbiomac.2014.06.004.
(114) Salerno A, Fernández-Gutiérrez M, San Román Del Barrio J, Domingo C. Bio-safe fabrication of PLA scaffolds for bone tissue engineering by combining phase separation, porogen leaching and scCO2 drying. J Supercrit Fluids. 2015;97:238–46. doi: 10.1016/j.supflu.2014.10.029.
(115) Yanoso-Scholl L, Jacobson JA, Bradica G, Lerner AL, O'Keefe RJ, Schwarz EM, et al. Evaluation of dense polylactic acid/beta-tricalcium phosphate scaffolds for bone tissue engineering. J Biomed Mater Res Part A. 2010;95(3A):717–26. doi: 10.1002/jbm.a.32868.
(116) Georgiou G, Mathieu L, Pioletti DP, Bourban P-E, Månson J-AE, Knowles JC, et al. Polylactic acid–phosphate glass composite foams as scaffolds for bone tissue engineering. J Biomed Mater Res Part B Appl Biomater. 2007;80B(2):322–31. doi: 10.1002/jbm.b.30600.
(117) Rahman MM, Shahruzzaman M, Islam MS, Khan MN, Haque P. Preparation and properties of biodegradable polymer/nano-hydroxyapatite bioceramic scaffold for spongy bone regeneration. J Polym Eng. 2019;39(2):134–42. doi: 10.1515/polyeng-2018-0103.
(118) Cai X, Tong H, Shen X, Chen W, Yan J, Hu J. Preparation and characterization of homogeneous chitosan-polylactic acid/hydroxyapatite nanocomposite for bone tissue engineering and evaluation of its mechanical properties. Acta Biomater. 2009;5(7):2693–703. doi: 10.1016/j.actbio.2009.03.005.
(119) Nanda HS, Nakamoto T, Chen S, Cai R, Kawazoe N, Chen G. Collagen microgel-assisted dexamethasone release from PLLA-collagen hybrid scaffolds of controlled pore structure for osteogenic differentiation of mesenchymal stem cells. J Biomater Sci Polym Ed. 2014;25(13):1374–86. doi: 10.1080/09205063.2014.938980.
(120) Rodenas-Rochina J, Vidaurre A, Castilla Cortázar I, Lebourg M. Effects of hydroxyapatite filler on long-term hydrolytic degradation of PLLA/PCL porous scaffolds. Polym Degrad Stab. 2015;119:121–31. doi: 10.1016/j.polymdegradstab.2015.04.015.
(121) Deplaine H, Lebourg M, Ripalda P, Vidaurre A, Sanz-Ramos P, Mora G, et al. Biomimetic hydroxyapatite coating on pore walls improves osteointegration of poly(L-lactic acid)

scaffolds. J Biomed Mater Res Part B Appl Biomater. 2013;101B(1):173–86. doi: 10.1002/jbm.b.32831.
(122) Obata A, Ozasa H, Kasuga T, Jones JR. Cotton wool-like poly (lactic acid)/vaterite composite scaffolds releasing soluble silica for bone tissue engineering. J Mater Sci Mater Med. 2013;24(7):1649–58. doi: 10.1007/s10856-013-4930-5.
(123) Kooshki H, Ghollasi M, Halabian R, Kazemi NM. Osteogenic differentiation of preconditioned bone marrow mesenchymal stem cells with lipopolysaccharide on modified poly-L-lactic-acid nanofibers. J Cell Physiol. 2019;234(5):5343–53. doi: 10.1002/jcp.26567.
(124) Gibson I, Rosen D, Stucker B. Additive manufacturing technologies: 3D printing, rapid prototyping, and direct digital manufacturing. 2nd ed. New York: Springer; 2015. ISBN 9781493921133.
(125) Wang X, Jiang M, Zhou Z, Gou J, Hui D. 3D printing of polymer matrix composites: a review and prospective. Composites Part B. 2017;110:442–58. doi: 10.1016/j.compositesb.2016.11.034.
(126) González-Henríquez CM, Sarabia-Vallejos MA, Rodriguez-Hernandez J. Polymers for additive manufacturing and 4D-printing: materials, methodologies, and biomedical applications. Prog Polym Sci. 2019;94:57–116. doi: 10.1016/j.progpolymsci.2019.03.001.
(127) Chiulan I, Frone A, Brandabur C, Panaitescu D. Recent advances in 3D printing of aliphatic polyesters. Bioengineering. 2017;5(1):2. doi: 10.3390/bioengineering5010002.
(128) Jakus AE, Rutz AL, Shah RN. Advancing the field of 3D biomaterial printing. Biomed Mater. 2016;11(1):014102. doi: 10.1088/1748-6041/11/1/014102.
(129) Dávila JL, Freitas MS, Inforçatti Neto P, Silveira ZC, Silva JVL, D'Ávila MA. Fabrication of PCL/β-TCP scaffolds by 3D mini-screw extrusion printing. J Appl Polym Sci. 2016;133(15):1–9. doi: 10.1002/app.43031.
(130) Skoog SA, Goering PL, Narayan RJ. Stereolithography in tissue engineering. J Mater Sci Mater Med. 2014;25(3):845–56. doi: 10.1007/s10856-013-5107-y.
(131) Voet VSD, Strating T, Schnelting GHM, Dijkstra P, Tietema M, Xu J, et al. Biobased acrylate photocurable resin formulation for stereolithography 3D printing. ACS Omega. 2018;3(2):1403–8. doi: 10.1021/acsomega.7b01648.
(132) Melchels FPW, Feijen J, Grijpma DW. A review on stereolithography and its applications in biomedical engineering. Biomaterials. 2010;31(24):6121–30. doi: 10.1016/j.biomaterials.2010.04.050.
(133) Ronca A, Ambrosio L, Grijpma DW. Preparation of designed poly(D,L-lactide)/nanosized hydroxyapatite composite structures by stereolithography. Acta Biomater. 2013;9(4):5989–96. doi: 10.1016/j.actbio.2012.12.004.
(134) Melchels FPW, Feijen J, Grijpma DW. A poly(D,L-lactide) resin for the preparation of tissue engineering scaffolds by stereolithography. Biomaterials. 2009;30(23–24):3801–9. doi: 10.1016/J.BIOMATERIALS.2009.03.055.
(135) Helminen AO, Korhonen H, Seppälä JV. Structure modification and crosslinking of methacrylated polylactide oligomers. J Appl Polym Sci. 2002;86(14):3616–24. doi: 10.1002/app.11193.
(136) Jansen J, Ghaffar A, Van Der Horst TNS, Mihov G, Van Der Wal S, Feijen J, et al. Controlling the kinetic chain length of the crosslinks in photo-polymerized biodegradable networks. J Mater Sci Mater Med. 2013;24(4):877–88. doi: 10.1007/s10856-013-4873-x.
(137) Seck TM, Melchels FPW, Feijen J, Grijpma DW. Designed biodegradable hydrogel structures prepared by stereolithography using poly(ethylene glycol)/poly(D,L-lactide)-based resins. J Controlled Release. 2010;148(1):34–41. doi: 10.1016/j.jconrel.2010.07.111.
(138) Melchels FPW, Velders AH, Feijen J, Grijpma DW. Photo-cross-linked poly(D,L-lactide)-based networks. structural characterization by HR-MAS NMR spectroscopy and hydrolytic degradation behavior. Macromolecules. 2010;43(20):8570–9. doi: 10.1021/ma1011705.
(139) Ronca A, Ambrosio L, Grijpma DW. Design of porous three-dimensional PDLLA/nano-hap composite scaffolds using stereolithography. J Appl Biomater Funct Mater. 2012;10(3):249–58. doi: 10.5301/JABFM.2012.10211.
(140) Kruth JP, Mercelis P, Van Vaerenbergh J, Froyen L, Rombouts M. Binding mechanisms in selective laser sintering and selective laser melting. Rapid Prototyp J. 2005;11(1):26–36. doi: 10.1108/13552540510573365.
(141) Zhou WY, Lee SH, Wang M, Cheung WL, Ip WY. Selective laser sintering of porous tissue engineering scaffolds from poly(L-lactide)/carbonated hydroxyapatite nanocomposite microspheres. J Mater Sci Mater Med. 2008;19(7):2535–40. doi: 10.1007/s10856-007-3089-3.
(142) Yeong W-Y, Chua C-K, Leong K-F, Chandrasekaran M. Rapid prototyping in tissue engineering: challenges and potential. Trends Biotechnol. 2004;22(12):643–52. doi: 10.1016/J.TIBTECH.2004.10.004.
(143) Williams JM, Adewunmi A, Schek RM, Flanagan CL, Krebsbach PH, Feinberg SE, et al. Bone tissue engineering using polycaprolactone scaffolds fabricated via selective laser sintering. Biomaterials. 2005;26(23):4817–27. doi: 10.1016/J.BIOMATERIALS.2004.11.057.
(144) Gayer C, Ritter J, Bullemer M, Grom S, Jauer L, Meiners W, et al. Development of a solvent-free polylactide/calcium carbonate composite for selective laser sintering of bone tissue engineering scaffolds. Mater Sci Eng C. 2019;101(March):660–73. doi: 10.1016/j.msec.2019.03.101.
(145) Lee BK, Yun Y, Park K. PLA micro- and nano-particles. Adv Drug Delivery Rev. 2016;107:176–91. doi: 10.1016/j.addr.2016.05.020.
(146) Shuai C, Li Y, Wang G, Yang W, Peng S, Feng P. Surface modification of nanodiamond: toward the dispersion of reinforced phase in poly-L-lactic acid scaffolds. Int J Biol Macromol. 2019;126:1116–24. doi: 10.1016/j.ijbiomac.2019.01.004.
(147) Gayer C, Abert J, Bullemer M, Grom S, Jauer L, Meiners W, et al. Influence of the material properties of a poly(D,L-lactide)/β-tricalcium phosphate composite on the processability by selective laser sintering. J Mech Behav Biomed Mater. 2018;87:267–78. doi: 10.1016/J.JMBBM.2018.07.021.
(148) Guvendiren M, Molde J, Soares RMD, Kohn J. Designing biomaterials for 3D printing. ACS Biomater Sci Eng. 2016;2(10):1679–93. doi: 10.1021/acsbiomaterials.6b00121.
(149) Ouhsti M, El Haddadi B, Belhouideg S. Effect of printing parameters on the mechanical properties of parts fabricated with open-source 3D printers in PLA by fused deposition modeling. Mech Mech Eng. 2018;22(4):895–907.

(150) Serra T, Planell JA, Navarro M. High-resolution PLA-based composite scaffolds via 3-D printing technology. Acta Biomater. 2013;9(3):5521–30. doi: 10.1016/j.actbio.2012.10.041.
(151) Murariu M, Dubois P. PLA composites: from production to properties. Adv Drug Delivery Rev. 2016;107:17–46. doi: 10.1016/j.addr.2016.04.003.
(152) Gregor A, Filová E, Novák M, Kronek J, Chlup H, Buzgo M, et al. Designing of PLA scaffolds for bone tissue replacement fabricated by ordinary commercial 3D printer. J Biol Eng. 2017;11(1):31. doi: 10.1186/s13036-017-0074-3.
(153) Esposito Corcione C, Gervaso F, Scalera F, Padmanabhan SK, Madaghiele M, Montagna F, et al. Highly loaded hydroxyapatite microsphere/PLA porous scaffolds obtained by fused deposition modelling. Ceram Int. 2019;45(2):2803–10. doi: 10.1016/J.CERAMINT.2018.07.297.
(154) Esposito Corcione C, Scalera F, Gervaso F, Montagna F, Sannino A, Maffezzoli A. One-step solvent-free process for the fabrication of high loaded PLA/HA composite filament for 3D printing. J Therm Anal Calorim. 2018;134(1):575–82. doi: 10.1007/s10973-018-7155-5.
(155) Hutmacher DW, Schantz T, Zein I, Ng KW, Teoh SH, Tan KC. Mechanical properties and cell cultural response of polycaprolactone scaffold. J Biomed Mater Res An Off J Soc Biomater Japanese Soc Biomater Aust Soc Biomater Korean Soc Biomater. 2001;55:203–16. doi: 10.1002/1097-4636(200105)55:2<203:AID-JBM1007>3.0.CO;2-7.
(156) Zhao H, Li L, Ding S, Liu C, Ai J. Effect of porous structure and pore size on mechanical strength of 3D-printed comby scaffolds. Mater Lett. 2018;223:21–4. doi: 10.1016/j.matlet.2018.03.205.
(157) Germain L, Fuentes CA, van Vuure AW, des Rieux A, Dupont-Gillain C. 3D-printed biodegradable gyroid scaffolds for tissue engineering applications. Mater Des. 2018;151:113–22. doi: 10.1016/j.matdes.2018.04.037.
(158) Upadhyay K, Dwivedi R, Singh AK. Determination and comparison of the anisotropic strengths of fused deposition modeling P400 ABS. In: Advances in 3D Printing and Additive Manufacturing Technologies. Singapore: Springer; 2016. p. 9–28. ISBN 9789811008122.
(159) Song P, Zhou C, Fan H, Zhang B, Pei X, Fan Y, et al. Novel 3D porous biocomposite scaffolds fabricated by fused deposition modeling and gas foaming combined technology. Compos Part B Eng. 2018;152(April):151–9. doi: 10.1016/j.compositesb.2018.06.029.
(160) Dave HK, Rajpurohit SR, Patadiya NH, Dave SJ, Sharma KS, Thambad SS, et al. Compressive strength of PLA based scaffolds: effect of layer height, infill density and print speed. Int J Mod Manuf Technol. 2019;11(1):21–7.
(161) Murugan R, Mitilesh RN, Singamneni S. Influence of process parameters on the mechanical behaviour and processing time of 3D printing. Int J Mod Manuf Technol. 2019;1(1):21–27.
(162) Abagnale G, Steger M, Nguyen VH, Hersch N, Sechi A, Joussen S, et al. Surface topography enhances differentiation of mesenchymal stem cells towards osteogenic and adipogenic lineages. Biomaterials. 2015;61:316–26. doi: 10.1016/j.biomaterials.2015.05.030.
(163) Alksne M, Simoliunas E, Kalvaityte M, Skliutas E, Rinkunaite I, Gendviliene I, et al. The effect of larger than cell diameter polylactic acid surface patterns on osteogenic differentiation of rat dental pulp stem cells. J Biomed Mater Res Part A. 2019;107(1):174–86. doi: 10.1002/jbm.a.36547.
(164) Teixeira BN, Aprile P, Mendonça RH, Kelly DJ, Thiré RM, da SM. Evaluation of bone marrow stem cell response to PLA scaffolds manufactured by 3D printing and coated with polydopamine and type I collagen. J Biomed Mater Res Part B Appl Biomater. 2019;107(1):37–49. doi: 10.1002/jbm.b.34093.
(165) Zhang H, Mao X, Du Z, Jiang W, Han X, Zhao D, et al. Three dimensional printed macroporous polylactic acid/hydroxyapatite composite scaffolds for promoting bone formation in a critical-size rat calvarial defect model. Sci Technol Adv Mater. 2016;17(1):136–48. doi: 10.1080/14686996.2016.1145532.
(166) Pedde RD, Mirani B, Navaei A, Styan T, Wong S, Mehrali M, et al. Emerging biofabrication strategies for engineering complex tissue constructs. Adv Mater. 2017;29(19):1–27. doi: 10.1002/adma.201606061.
(167) Piard CM, Chen Y, Fisher JP. Cell-laden 3D printed scaffolds for bone tissue engineering. Clin Rev Bone Miner Metab. 2015;13(4):245–55. doi: 10.1007/s12018-015-9198-5.
(168) Mandrycky C, Wang Z, Kim K, Kim DH. 3D bioprinting for engineering complex tissues. Biotechnol Adv. 2016;34(4):422–34. doi: 10.1016/j.biotechadv.2015.12.011.
(169) Diamantides N, Dugopolski C, Blahut E, Kennedy S, Bonassar LJ. High density cell seeding affects the rheology and printability of collagen bioinks. Biofabrication. 2019;11(4):045016. doi: 10.1088/1758-5090/ab3524.
(170) Blaeser A, Duarte Campos DF, Puster U, Richtering W, Stevens MM, Fischer H. Controlling shear stress in 3D bioprinting is a key factor to balance printing resolution and stem cell integrity. Adv Healthc Mater. 2016;5(3):326–33. doi: 10.1002/adhm.201500677.
(171) Kolesky DB, Truby RL, Gladman AS, Busbee TA, Homan KA, Lewis JA. 3D bioprinting of vascularized, heterogeneous cell-laden tissue constructs. Adv Mater. 2014;26(19):3124–30. doi: 10.1002/adma.201305506.
(172) Owens CM, Marga F, Forgacs G, Heesch CM. Biofabrication and testing of a fully cellular nerve graft. Biofabrication. 2013;5(4):045007. doi: 10.1088/1758-5082/5/4/045007.
(173) Wang MO, Piard CM, Melchiorri A, Dreher ML, Fisher JP. Evaluating changes in structure and cytotoxicity during *in vitro* degradation of three-dimensional printed scaffolds. Tissue Eng Part A. 2015;21(9–10):1642–53. doi: 10.1089/ten.tea.2014.0495.
(174) Serra T, Ortiz-Hernandez M, Engel E, Planell JA, Navarro M. Relevance of PEG in PLA-based blends for tissue engineering 3D-printed scaffolds. Mater Sci Eng C. 2014;38(1):55–62. doi: 10.1016/j.msec.2014.01.003.
(175) Levato R, Visser J, Planell JA, Engel E, Malda J, Mateos-Timoneda MA. Biofabrication of tissue constructs by 3D bioprinting of cell-laden microcarriers. Biofabrication. 2014;6(3):35020. doi: 10.1088/1758-5082/6/3/035020.
(176) Niaza KV, Senatov FS, Kaloshkin SD, Maksimkin AV, Chukov DI. 3D-printed scaffolds based on PLA/HA nanocomposites for trabecular bone reconstruction. J Phys Conf Ser. 2016;741(1):5. doi: 10.1088/1742-6596/741/1/012068.
(177) Esposito Corcione C, Scalera F, Gervaso F, Montagna F, Sannino A, Maffezzoli A. One-step solvent-free process for

the fabrication of high loaded PLA/HA composite filament for 3D printing. J Therm Anal Calorim. 2018;134(1):575–82. doi: 10.1007/s10973-018-7155-5.
(178) Mathieu LM, Mueller TL, Bourban PE, Pioletti DP, Müller R, Månson JAE. Architecture and properties of anisotropic polymer composite scaffolds for bone tissue engineering. Biomaterials. 2006;27(6):905–16. doi: 10.1016/j.biomaterials.2005.07.015.
(179) Senatov FS, Niaza KV, Zadorozhnyy MY, Maksimkin AV, Kaloshkin SD, Estrin YZ. Mechanical properties and shape memory effect of 3D-printed PLA-based porous scaffolds. J Mech Behav Biomed Mater. 2016;57:139–48. doi: 10.1016/j.jmbbm.2015.11.036.
(180) Wei Q, Cai X, Guo Y, Wang G, Guo Y, Lei M, et al. Atomic-scale and experimental investigation on the micro-structures and mechanical properties of PLA blending with CMC for additive manufacturing. Mater Des. 2019;183:108158. doi: 10.1016/j.matdes.2019.108158.
(181) Ferreira BMP, Pinheiro LMP, Nascente PAP, Ferreira MJ, Duek EAR. Plasma surface treatments of poly(L-lactic acid) (PLLA) and poly(hydroxybutyrate-*co*-hydroxyvalerate) (PHBV). Mater Sci Eng C. 2009;29(3):806–13. doi: 10.1016/j.msec.2008.07.026.
(182) Yang J, Shi G, Bei J, Wang S, Cao Y, Shang Q, et al. Fabrication and surface modification of macroporous poly(L-lactic acid) and poly(L-lactic-*co*-glycolic acid) (70/30) cell scaffolds for human skin fibroblast cell culture. J Biomed Mater Res. 2002;62(3):438–46. doi: 10.1002/jbm.10318.
(183) Ogino A, Noguchia S, Nagatsu M. Effect of plasma pretreatment on heparin immobilization on polymer sheet. J Photopolym Sci Technol. 2009;22(4):461–6. doi: 10.2494/photopolymer.22.461.
(184) Huang YC, Huang CC, Huang YY, Chen KS. Surface modification and characterization of chitosan or PLGA membrane with laminin by chemical and oxygen plasma treatment for neural regeneration. J Biomed Mater Res Part A. 2007;82(4):842–51. doi: 10.1002/jbm.a.31036.
(185) Martin V, Ribeiro IA, Alves MM, Gonçalves L, Claudio RA, Grenho L, et al. Engineering a multifunctional 3D-printed PLA-collagen-minocycline-nanoHydroxyapatite scaffold with combined antimicrobial and osteogenic effects for bone regeneration. Mater Sci Eng C. 2019;101(November 2018):15–26. doi: 10.1016/j.msec.2019.03.056.
(186) Guo C, Xiang M, Dong Y. Surface modification of poly(lactic acid) with an improved alkali-acid hydrolysis method. Mater Lett. 2015;140:144–7. doi: 10.1016/j.matlet.2014.10.099.
(187) Nam YS, Yoon JJ, Lee JG, Park TG. Adhesion behaviours of hepatocytes cultured onto biodegradable polymer surface modified by alkali hydrolysis process. J Biomater Sci Polym Ed. 1999;10(11):1145–58. doi: 10.1163/156856299X00801.
(188) Liu X, Holzwarth JM, Ma PX. Functionalized synthetic biodegradable polymer scaffolds for tissue engineering. Macromol Biosci. 2012;12(7):911–9. doi: 10.1002/mabi.201100466.
(189) Jacobs T, Morent R, De Geyter N, Dubruel P, Leys C. Plasma surface modification of biomedical polymers: Influence on cell–material interaction. Plasma Chem Plasma Process. 2012;32(5):1039–73. doi: 10.1007/s11090-012-9394-8.
(190) Nakagawa M, Teraoka F, Fujimoto S, Hamada Y, Kibayashi H, Takahashi J. Improvement of cell adhesion on poly(L-lactide) by atmospheric plasma treatment. J Biomed Mater Res Part A. 2006;77(1):112–8. doi: 10.1002/jbm.a.30521.
(191) Scaffaro R, Lopresti F, Sutera A, Botta L, Fontana RM, Gallo G. Plasma modified PLA electrospun membranes for actinorhodin production intensification in Streptomyces coelicolor immobilized-cell cultivations. Colloids Surf B. 2017;157:233–41. doi: 10.1016/j.colsurfb.2017.05.060.
(192) Jordá-Vilaplana A, Fombuena V, García-García D, Samper MD, Sánchez-Nácher L. Surface modification of polylactic acid (PLA) by air atmospheric plasma treatment. Eur Polym J. 2014;58:23–33. doi: 10.1016/j.eurpolymj.2014.06.002.
(193) Yamaguchi M, Shinbo T, Kanamori T, Wang PC, Niwa M, Kawakami H, et al. Surface modification of poly(L-lactic acid) affects initial cell attachment, cell morphology, and cell growth. J Artif Organs. 2004;7(4):187–93. doi: 10.1007/s10047-004-0267-7.
(194) Wang M, Favi P, Cheng X, Golshan NH, Ziemer KS, Keidar M, et al. Cold atmospheric plasma (CAP) surface nanomodified 3D printed polylactic acid (PLA) scaffolds for bone regeneration. Acta Biomater. 2016;46:256–65. doi: 10.1016/j.actbio.2016.09.030.
(195) Koumoulos EP, Valentin M, Dragatogiannis D, Charitidis CA, Krupa I, Novak I. Nanomechanical properties of plasma treated polylactic acid. Plast Rubber Compos. 2015;44(8):322–9. doi: 10.1179/1743289815Y.0000000023.
(196) Safinia L, Datan N, Höhse M, Mantalaris A, Bismarck A. Towards a methodology for the effective surface modification of porous polymer scaffolds. Biomaterials. 2005;26(36):7537–47. doi: 10.1016/j.biomaterials.2005.05.078.
(197) Wan Y, Tu C, Yang J, Bei J, Wang S. Influences of ammonia plasma treatment on modifying depth and degradation of poly(L-lactide) scaffolds. Biomaterials. 2006;27(13):2699–704. doi: 10.1016/j.biomaterials.2005.12.007.
(198) Barry JJA, Silva MMCG, Shakesheff KM, Howdle SM, Alexander MR. Using plasma deposits to promote cell population of the porous interior of three-dimensional poly (D,L-lactic acid) tissue-engineering scaffolds. Adv Funct Mater. 2005;15(7):1134–40. doi: 10.1002/adfm.200400562.
(199) Zeng S, Cui Z, Yang Z, Si J, Wang Q, Wang X, et al. Characterization of highly interconnected porous poly(lactic acid) and chitosan-coated poly(lactic acid) scaffold fabricated by vacuum-assisted resin transfer molding and particle leaching. J Mater Sci. 2016;51(22):9958–70. doi: 10.1007/s10853-016-0203-2.
(200) Fernández-Cervantes I, Morales MA, Agustín-Serrano R, Cardenas-García M, Pérez-Luna PV, Arroyo-Reyes BL, et al. Polylactic acid/sodium alginate/hydroxyapatite composite scaffolds with trabecular tissue morphology designed by a bone remodeling model using 3D printing. J Mater Sci. 2019:9478–96. doi: 10.1007/s10853-019-03537-1.
(201) Chen Y, Mak AFT, Wang M, Li J, Wong MS. PLLA scaffolds with biomimetic apatite coating and biomimetic apatite/collagen composite coating to enhance osteoblast-like cells attachment and activity. Surf Coatings Technol. 2006;201(3–4):575–80. doi: 10.1016/j.surfcoat.2005.12.005.
(202) Kao CT, Lin CC, Chen YW, Yeh CH, Fang HY, Shie MY. Poly (dopamine) coating of 3D printed poly(lactic acid) scaffolds

for bone tissue engineering. Mater Sci Eng C. 2015;56:165–73. doi: 10.1016/j.msec.2015.06.028.
(203) Lee NK, Sowa H, Hinoi E, Ferron M, Ahn JD, Confavreux C, et al. Endocrine regulation of energy metabolism by the skeleton. Cell. 2007;130(3):456–69. doi: 10.1016/j.cell.2007.05.047.
(204) Holmes B, Zhu W, Li J, Lee JD, Zhang LG. Development of novel three-dimensional printed scaffolds for osteochondral regeneration. Tissue Eng Part A. 2015;21(1–2):403–15. doi: 10.1089/ten.tea.2014.0138.
(205) Rodrigues MT, Lee SJ, Gomes ME, Reis RL, Atala A, Yoo JJ. Bilayered constructs aimed at osteochondral strategies: the influence of medium supplements in the osteogenic and chondrogenic differentiation of amniotic fluid-derived stem cells. Acta Biomater. 2012;8(7):2795–806. doi: 10.1016/j.actbio.2012.04.013.

Comparison between calcium carbonate and β-tricalcium phosphate as additives of 3D printed scaffolds with polylactic acid matrix

Tissue Engineering and Regenerative Medicine

Comparison between calcium carbonate and β-tricalcium phosphate as additives of 3D printed scaffolds with polylactic acid matrix

Journal:	*Journal of Tissue Engineering and Regenerative Medicine*
Manuscript ID	TERM-18-0218.R2
Wiley - Manuscript type:	Research Article
Date Submitted by the Author:	18-Jan-2019
Complete List of Authors:	Donate, Ricardo; Grupo de Investigación en Fabricación Integrada y Avanzada. Universidad de Las Palmas de Gran Canaria, Departamento de Ingeniería Mecánica Monzón, Mario; Grupo de Investigación en Fabricación Integrada y Avanzada. Universidad de Las Palmas de Gran Canaria, Departamento de Ingeniería Mecánica Ortega, Zaida; Grupo de Investigación en Fabricación Integrada y Avanzada. Universidad de Las Palmas de Gran Canaria, Departamento de Ingeniería de Procesos Wang, Ling; State Key Laboratory for Manufacturing System Engineering. Xi'an Jiaotong University, School of Mechanical Engineering Ribeiro, Viviana; 3B's Research Group, I3Bs – Research Institute on Biomaterials, Biodegradables and Biomimetics, University of Minho; ICVS 3Bs PT Government Associate Lab; The Discoveries Centre for Regenerative and Precision Medicine, Headquarters at University of Minho Pestana, David; Grupo de Investigación en Fabricación Integrada y Avanzada. Universidad de Las Palmas de Gran Canaria, Departamento de Ingeniería Mecánica Oliveira, Joaquim; 3B's Research Group, I3Bs – Research Institute on Biomaterials, Biodegradables and Biomimetics, University of Minho; ICVS 3Bs PT Government Associate Lab; The Discoveries Centre for Regenerative and Precision Medicine, Headquarters at University of Minho Reis, Rui; 3B's Research Group, I3Bs – Research Institute on Biomaterials, Biodegradables and Biomimetics, University of Minho; ICVS 3Bs PT Government Associate Lab; The Discoveries Centre for Regenerative and Precision Medicine, Headquarters at University of Minho
Keywords:	polylactic acid, calcium carbonate, β-tricalcium phosphate, tissue engineering, bone regeneration, additive manufacturing, porosity, metabolic activity

Comparison between calcium carbonate and β-tricalcium phosphate as additives of 3D printed scaffolds with polylactic acid matrix

Short running title: Evaluation of polylactic acid-based 3D printed scaffolds for bone regeneration

Ricardo Donate[1,*], Mario Monzón[1], Zaida Ortega[2], Ling Wang[3], Viviana Ribeiro[4,5,6], David Pestana[1], Joaquim M. Oliveira[4,5,6] and Rui L. Reis[4,5,6].

[1] Departamento de Ingeniería Mecánica, Grupo de Investigación en Fabricación Integrada y Avanzada, Universidad de Las Palmas de Gran Canaria, Campus Universitario de Tafira s/n, 35017 Las Palmas, Spain.
[2] Departamento de Ingeniería de Procesos, Grupo de Investigación en Fabricación Integrada y Avanzada, Universidad de Las Palmas de Gran Canaria, Campus Universitario de Tafira s/n, 35017 Las Palmas, Spain.
[3] State Key Laboratory for Manufacturing System Engineering, School of Mechanical Engineering, Xi'an Jiaotong University, Science and Technology Park of Xi'an Jiaotong University, Yanta District, 710054 Xi'an City, Shaanxi Province, P.R. China.
[4] 3B's Research Group, I3Bs – Research Institute on Biomaterials, Biodegradables and Biomimetics, University of Minho, Headquarters of the European Institute of Excellence on Tissue Engineering and Regenerative Medicine, AvePark, Parque de Ciência e Tecnologia, Zona Industrial da Gandra, 4805-017 Barco, Guimarães, Portugal.
[5] ICVS 3Bs PT Government Associate Lab, Braga, Guimarães, Portugal.
[6] The Discoveries Centre for Regenerative and Precision Medicine, Headquarters at University of Minho, AvePark, 4805-017 Barco, Guimarães, Portugal.
* Correspondence: ricardo.donate@ulpgc.es; Tel.: +34-928-45-8603

Summary: In this study, polylactic acid-based (PLA) composite scaffolds with calcium carbonate ($CaCO_3$) and beta-tricalcium phosphate (β-TCP) were obtained by 3D printing. These structures were evaluated as potential 3D structures for bone tissue regeneration. Morphological, mechanical and biological tests were carried out in order to compare the effect of each additive (added in a concentration of 5% w/w), as well as the combination of both (2.5% w/w of each one), on the PLA matrix. The scaffolds manufactured had a mean pore size between 400-425 μm and a porosity value in the range of 50-60%. According to the results, both additives promoted an increase of the porosity, hydrophilicity and surface roughness of the scaffolds, leading to a significant improvement of the metabolic activity of human osteoblastic osteosarcoma SaOS-2 cells. The best results in terms of cell attachment after 7 days were obtained for the samples containing $CaCO_3$ and β-TCP particles due to the synergistic effect of both additives, which results in an increase in osteoconductivity and in a microporosity that favours cell adhesion. These scaffolds (PLA:$CaCO_3$:β-TCP 95:2.5:2.5) have suitable properties to be further evaluated for bone tissue engineering applications.

Keywords: polylactic acid, calcium carbonate, β-tricalcium phosphate, tissue engineering, bone regeneration, additive manufacturing, porosity, metabolic activity

1. Introduction

The use of additive manufacturing techniques has a major interest for the production of parts for the biomedical sector, especially scaffolds (Chia & Wu, 2015; Li, Li, Lu, Gao, & Zhou, 2015), which are three-dimensional structures used in tissue engineering to guide and promote adhesion, proliferation and migration of cells during the process of tissue regeneration (Gregor et al., 2017; Sachlos, Czernuszka, Gogolewski, & Dalby, 2003). Currently, the preferred materials for this application are those that are biodegradable and bioresorbable, so the initial foreign material and the bulk degradation by-products are eliminated through natural pathways with no residual side effects (Hutmacher, 2000).

Apart from its bioresorbability, scaffolds should be easily manufactured in different shapes and sizes (Hutmacher, 2000; Sachlos et al., 2003). This requirement could be fulfilled by the method of additive manufacturing, under the category of "material extrusion" (ISO/ASTM 52900:2015), commonly known as fused deposition modeling (FDM). In this process, a continuous filament of material is fed through a moving, heated printer extruder head. FDM has been used for the manufacture of scaffolds with synthetic

biomaterials such as polycaprolactone (PCL) (Zein, Hutmacher, Tan, & Teoh, 2002), even reaching the commercial introduction of the technique. Another of the most used biomaterials in FDM is polylactic acid (Esposito Corcione et al., 2017; Gregor et al., 2017; Patrício et al., 2014), being this, like PCL, a biocompatible and biodegradable thermoplastic polymer with low melting temperature (Esposito Corcione et al., 2017). PLA has a lower level of hydrophobicity compared to PCL, which makes it more easily reabsorbable by the organism (Sabino et al., 2013). Disadvantages in the use of PLA for scaffolds manufacturing include the low osteoconductivity of this biomaterial, the deficient cellular adhesion on its surface and, especially, the occurrence of inflammatory reactions as a consequence of the release of acidic species during degradation (Abert, Amella, Weigelt, & Fischer, 2016). Therefore, for tissue engineering applications, the use of PLA is limited to its use as a composite material in combination with natural or ceramic biomaterials that can counteract the aforementioned deficiencies.

In the present work, calcium carbonate ($CaCO_3$) and β-tricalcium phosphate ($Ca_3(PO_4)_2$, β-TCP) were evaluated as additives of PLA-based scaffold manufactured by FDM for bone tissue regeneration. β-TCP is a biodegradable high temperature phase of calcium phosphate that has been used as bone substitute due to its osteoconductivity and bone replacement capability (Canadas, Pina, Marques, Oliveira, & Reis, 2015). In comparison with hydroxyapatite ($Ca_5(PO_4)_3OH$), another calcium phosphate extensively used as bone scaffolds-filling material, β-TCP is completely reabsorbed by the organism, while hydroxyapatite has a slow resorption rate and may be integrated into the regenerated bone tissue (Canadas et al., 2015; Takahashi, Yamamoto, & Tabata, 2005). To counteract the acidic reaction products that could arise from the polymeric degradation, the addition of a buffering agent is a strategy that has been applied in previous studies (Abert et al., 2016; Schiller et al., 2004). As calcium carbonate buffers in the range of the physiological pH value of around 7.4 (Ara, Watanabe, & Imai, 2002; Schiller & Epple, 2003), it is a material of great interest to be added in PLA-based scaffolds.

Although many works can be found in the literature where the use of PLA/β-TCP composite scaffolds is investigated (Lou, Wang, Song, Gu, & Yang, 2014; Rakovsky, Gotman, Rabkin, & Gutmanas, 2014; Schiller et al., 2004), not a large number of them propose additive manufacturing techniques to obtain the 3D structures (Drummer, Cifuentes-Cuéllar, & Rietzel, 2012; Esposito Corcione et al., 2017), and no references have been found about the simultaneous addition of $CaCO_3$ and β-TCP in 3D printed PLA-based scaffolds. For that reason, in this study composite scaffolds containing one of the additives or both of them in combination with the PLA matrix were compared to pure PLA structures. Morphological, mechanical, and biological characterization of the scaffolds were carried out. In addition, the filaments produced to feed the printer were analysed by thermogravimetric and calorimetric analysis and Fourier transform infrared spectroscopy. Water contact angle measurements of the combination of materials proposed were also performed in order to assess the modification of the surface hydrophilicity when additives are used.

2. Materials and Methods

2.1. Materials

PLAL130 (melt flow index of 16 g/10 min, molecular weight of approximately 100,000 g/mol) was kindly supplied by Corbion Purac in the form of pellets. Glass transition temperature is in the range of 55 to 60 °C and the melting temperature is 175 °C according to specifications. Commercial grade calcium carbonate 0179-500G with a maximum particle size of 30 μm was purchased from VWR, while β-tricalcium phosphate (β-TCP) was kindly provided by the 3B's Research Group of Universidade do Minho (UMINHO) with a mean particle size of 45 μm.

2.2. Material Compounding and Preparation of Filaments

PLA pellets were milled at 12,000 rpm in an Ultra Centrifugal Mill ZM 200 (Retsch) to a maximum particle size of 500 μm. This powder was then mixed with the amount of powder of $CaCO_3$ and β-TCP needed to obtain the following mixtures (wt:wt): PLA:$CaCO_3$ 95:5, PLA:β-TCP 95:5 and PLA:$CaCO_3$:β-TCP 95:2.5:2.5. After homogenization, each combination of materials was fed into a lab prototype extruder to obtain the continuous filaments needed to print the scaffolds by FDM. This extruder consists of an 8 mm

screw, a cylinder with an L/D ratio of 10 and a 1.6 mm diameter nozzle tip. Due to the swelling effect, a diameter for the extruded filaments greater than the nozzle tip diameter was obtained. The extrusion was carried out at 245 °C, at a rotating speed of 7 rpm and with a final air-cooling stage. Filaments of pure PLA were obtained following the same procedure.

2.3. Scaffolds Fabrication

The filaments obtained were used to print the parts needed for the different tests described in this report with a BQ Hephestos 2 3D printer. Structures with a rectangular 0/90° pattern were printed to carry out the mechanical, morphological and biological characterization of the composite scaffolds. The designed pattern provides square shaped pores in an interconnected network, resulting in scaffolds with a theoretical porosity of 50% and pore sizes in the range of 350–450 μm. All samples were printed using a nozzle diameter of 0.4 mm, a layer height equal to 0.3 mm, a speed of extrusion of 40 mm/s and with the temperature of the liquefier set at 225 °C and room temperature at 23±1 °C.

In order to estimate the reproducibility of the 3D printer, which could be affected by internal factors such as variation of liquefier temperature, feed rate or cooling process on bed, 25 samples with the same geometry and porosity than the scaffolds of this research were tested using the working parameters described above. These scaffolds were printed using a commercial filament of PLA for 3D printing (1.75 mm, BQ), with high level of uniformity in diameter. The compression test resulted to be about 4% of variation factor (typical deviation divided by average value) in terms of Young modulus and yield strength. The reproducibility study provided a valuable reference for analysing the influence of other factors in the variation factor of the developed scaffolds (poor uniformity of filaments produced, poor uniformity of distribution of the additives, etc.).

2.4. Morphological Characterization

The surface morphology of scaffolds printed by FDM with nominal dimensions of 9.8 mm in diameter and 7 mm in height was evaluated by microscopic observation (Olympus BX51 optical microscope), scanning electron microscopy (SEM; Hitachi TM 3030 at an acceleration voltage of 15 kV) and micro-computed tomography (micro-CT; Y. Cheetah, YXLON Ltd.). Prior to SEM observation, the samples were sputtered with Pd/Au for 2 minutes at 18 mA in a Polaron SC7620 sputter.

A method broadly used in the literature (Domingos et al., 2013; Yang, Kim, & Kim, 2017) to estimate the porosity of 3D printed scaffolds was applied using the following equation:

$$\%\text{porosity} = 100 \cdot (1 - \varrho_{ap}/\varrho_{bulk}),$$

Where ϱ_{ap} is the apparent density of the structure and ϱ_{bulk} is the density of the bulk material. The density of the bulk material was determined by measuring the dimensions of short filaments of material with a cantilever (±0.01 mm) and their mass (n=8). The apparent density was measured following a similar protocol for 3D printed scaffolds of each combination of materials studied.

As the printing pattern was 0/90°, the pore size was evaluated as the distance between filaments. These measures were done using the software of the Olympus BX51 optical microscope.

2.5. Thermogravimetric and Calorimetric Analysis

Pure PLA filaments and hybrid PLA:$CaCO_3$ 95:5, PLA:β-TCP 95:5, PLA:$CaCO_3$:β-TCP 90:2.5:2.5 filaments obtained after the FDM process were subjected to thermogravimetric analysis (TGA) in a TGA/DSC 1 Mettler Toledo device. Pure PLA powder were also analysed using the same procedure. A cycle of heating up to 385°C at a heating rate of 10 °C/min with a nitrogen flow of 10 mL/min was followed in each case, using aluminium crucibles. During the TGA testing, it was possible to obtain the calorimetric data using the same thermal cycle. The melting temperature and the melting enthalpy of each type of sample were calculated using these data. The values of the melting enthalpy were used to calculate the crystallinity of the samples by applying the following equation (Esposito Corcione et al., 2017):

$$\%X_c = 100 \cdot [\Delta H_f/ (\Delta H_f^\circ \cdot W_{PLA})],$$

where X_c is the degree of crystallinity, ΔH_f is the enthalpy of fusion of the sample, $\Delta H_f°$ corresponds to the heat of fusion of 100% crystalline PLA, and W_{PLA} is the net weight fraction of the PLA in the sample tested. The value of $\Delta H_f°$ used in this study was 93.6 J/g (Garlotta, 2001).

2.6. Fourier Transform Infrared Spectroscopy (FTIR)

Filaments obtained by extrusion were characterized by FTIR. Fourier transform infrared spectra were obtained using a Perkin Elmer IR Spectrum Two in the attenuated total reflectance (ATR) mode. The range of study covers wavelengths from 4000 to 450 cm^{-1} at a resolution of 8 cm^{-1}. Five measurements were carried out for each group of samples, using twelve scans per measurement to obtain the average spectra.

2.7. Water Contact Angle Measurement (WCA)

For this test, non-porous specimens were fabricated. PLA in powder form (obtained as described in Section 2.2) was mixed with the amount of powder of $CaCO_3$ and β-TCP needed to obtain the following mixtures (wt:wt): PLA:$CaCO_3$ 95:5, PLA:β-TCP 95:5, PLA:$CaCO_3$:β-TCP 90:2.5:2.5. After homogenization, these mixtures were subjected to compression moulding in a Collin P 200 P/M press. The cycle used consisted of a first step of heating at 20 °C/min up to 190°C, a second step of constant temperature and a pressure of 10 bar applied for 90 seconds, and finally a cooling step until room temperature at 20 °C/min. Pure PLA samples were obtained following the same procedure. Five samples per group were manufactured.

The WCA was determined at room temperature using an optical contact angle measuring device (JC2000D2, Shanghai Zhongchen Digital Technology Apparatus Co., Ltd.) equipped with StreamPix software, by measuring the static contact angle of 2 μL distilled water droplets onto the surface of the samples. Reported contact angles are the average of 25 measurements per group (five measurements per sample). The test was carried out both on dry and pre-wetted samples, in order to confirm if the previous hydration of the samples has an effect on their wettability, as other authors have described when working with other polymers (Alemán-Domínguez, Ortega, et al., 2018; Conejero-García et al., 2017; Vallés-Lluch, Gallego Ferrer, & Monleón Pradas, 2010). After immersion in water for 24 h to ensure that the water content of the samples reach the equilibrium, the surface of the pre-wetted samples was gently dried with laboratory paper and the WCA was analysed immediately.

2.8. Mechanical Characterization

Compression and flexural tests were performed to evaluate the effect of the introduction of the additives in the PLA matrix. The samples were tested on an MTS (SANS CMT4304, MTS Systems Co. Ltd.) universal testing machine in displacement control mode at a crosshead speed of 1 mm/min.

Regarding the compression test, 3D printed porous scaffolds were tested. The samples were 9.8 mm in diameter and 7 mm in height. Five replicas of each combination of materials were tested: PLA, PLA:$CaCO_3$ 95:5, PLA:β-TCP 95:5, PLA:$CaCO_3$:β-TCP 90:2.5:2.5. The compressive modulus was calculated from the initial steepest straight-line portion of the load-strain curve according to ASTM D695-15. Besides, the offset compressive yield strength was evaluated as the stress at which the stress-strain curve departs from linearity by a 0.2% of deformation.

For the flexural properties, the 3 points bending test was carried out. Two types of samples were tested separately: 3D printed scaffolds with rectangular shape and dimensions of 25x12.7x3.2 mm and non-porous samples obtained by compression moulding (as described in Section 2.7) with dimensions of 80x10x1 mm. In both cases, five replicas of samples of each combination of materials were used to obtain the flexural modulus and the maximum flexural stress. The parameters were calculated according to the procedures explained in the standard ASTM D790-15.

2.9. Metabolic activity of SaOS-2 cells

A human osteoblastic osteosarcoma cell line (SaOS-2) was used to assess cell behaviour in the presence of the four groups of materials tested: PLA, PLA:$CaCO_3$ 95:5, PLA:β-TCP 95:5 and PLA:$CaCO_3$:β-TCP

90:2.5:2.5. Four replicas of 3D printed porous scaffolds of each group, with dimensions of 9.8 mm in diameter and 7 mm in height, were tested. Before cell seeding, all samples were hydrated in Dulbecco's Modified Eagle's Medium - low glucose (DMEM – low glucose; Sigma Aldrich, Missouri, EUA) supplemented with 1% antibiotic-antimycotic solution (Gibco, Life Technologies, Carlsbad, CA, USA), overnight in a CO_2 incubator. In the following day, the hydrated scaffolds were transferred to 24-well suspension cell culture plates. Cells were grown as monolayer cultures in standard basal medium consisting of DMEM – low glucose, supplemented with 10% fetal bovine serum (FBS; Life Technologies, California, USA) and 1% antibiotic-antimycotic solution. At confluence, cells were detached from the culture flasks using TrypLE Express enzyme with phenol red (Gibco, Life Technologies, Carlsbad, CA, USA), and seeded in a 50 μL cell suspension into the scaffolds, at a density of 80,000 cells/scaffold. The constructs were kept in the CO_2 incubator for 3 hours and then completed with 2 mL of culture medium. Samples were harvested after culturing for 1, 3 and 7 days and the culture medium was changed every 2-3 days.

Alamar blue assay was performed to assess the metabolic activity of cells, following the manufacturer's instructions. After each time-point, the constructs were transferred to a new 24-well suspension cell culture plate and a solution of 10% (v/v) AlamarBlue® (BioRad, Hercules, CA, USA), prepared in standard basal culture medium, was transferred to the culture plates in 1000 μL/scaffold. After 3 hours of reaction with cells at 37 °C in the CO_2 incubator, 100 μL of Alamar blue solution were taken from each well and placed in a 96-well white opaque plate (Corning-Costar Corporation, Acton, MA, USA) in triplicate. The fluorescence was measured in a microplate reader (Synergy HT, BioTek, Instruments, USA) at an excitation wavelength of 530/25 nm and at an emission wavelength of 590/35 nm. Scaffolds without cells were used as control.

After 7 days of culture, the cell-seeded scaffolds were washed with phosphate buffered saline (PBS; Sigma Aldrich, Missouri, EUA) solution and fixed with 2.5% glutaraldehyde (Sigma Aldrich, Missouri, EUA) solution in PBS for 1 hour at 4 °C. After rising with PBS, samples were dehydrated using a series of ethanol solutions (30%, 50%, 70%, 90% and 100% v/v) and treated with hexamethylidisilazane (HMDS; Electron Microscopy Sciences, USA). Samples were cut longitudinally to address cell morphology in the scaffold's interior. Samples were sputter coated with gold (Fisons Instruments, Sputter Coater SC502, UK) prior to SEM analysis (Leica Cambridge S360).

2.10. Statistical Analysis

Statistical analysis was performed using GraphPad Prism 5.0 software (GraphPad Software, La Jolla, CA, USA) and MATLAB software (MATLAB and Statistics Toolbox Release 2017a, The MathWorks, Inc., Natick, USA). The data obtained during this study were analysed by the Wilcoxon two-sided rank sum test, except for the analysis of the metabolic activity test data. In the latter case, a Kruskal-Wallis test followed by Dunn's post-test were used. The significance level was set to $*p < 0.05$, $**p < 0.01$ and $***p < 0.001$ for statistically significant, highly statistically significant and very highly statistically significant differences, respectively. All the figures show the mean values of each group and their standard deviations are represented with error bars.

3. Results

3.1. Morphological Characterization

3.1.1. Surface Morphology

As observed in the SEM images shown in Figure 1, while filaments of pure PLA scaffolds showed a smooth surface and steady filaments morphology, filaments of scaffolds composed of PLA mixed with additives exhibited a greater roughness and less constant diameter. On the other hand, according to Figures 1 (e) and (f), a good dispersion of $CaCO_3$ and β-TCP in the PLA matrix has been achieved. However, agglomerates of the additive particles are also observed in these images, being formed maybe because of the lack of interaction with the matrix or due to a limited mixing performance of the extruder used to manufacture the filaments for 3D printing. In any case, it is highly probable that the presence of these agglomerates is the cause of the final morphology presented by the filaments of the 3D printed scaffolds.

The surface morphology analysis is completed with the micro-CT images of the scaffolds (Figure 2), where the designed rectangular 0/90° pattern and the 3D structure reconstruction can be seen in detail. Micro-CT images confirmed that the additives are evenly distributed in the PLA matrix, but also the presence of agglomerates and defects in the filaments. The increase in microporosity of the composite scaffolds is especially evident in the micro-CT scans of the PLA:$CaCO_3$:β-TCP 95:2.5:2.5 scaffold.

3.1.2. Porosity and Pore Size

The bulk density of PLA L130, used in this work as the matrix of composite 3D printed scaffolds, is 1.20 ± 0.03g/cm^3 according to the results shown in Table 1 (and 1.24 according to the datasheet of the product). The bulk density of the material increased with the addition of $CaCO_3$, β-TCP and the combination of the two of them. However, the apparent density of the scaffolds remained unchanged for all the groups of samples. As a result, the porosity values were slightly higher in the composite scaffolds, with a statistically significant increment in the case of PLA:$CaCO_3$ 95:5 and PLA:β-TCP 95:5 samples (Table 1). This result was expected taking into account the conclusions drawn from the SEM and micro-CT images. The average pore size was in the range of 400–425 μm for all the groups of scaffolds evaluated (Table 1). There is no statistically significant increase of the distance between filaments (identified herein as pore size) for the composite scaffolds compared to the pure PLA scaffolds.

3.2. Thermogravimetric and Calorimetric Analysis

The thermogravimetric analysis allowed obtaining the temperature at which the degradation process of the composite materials starts (left limit temperature in Table 2) and to compare these values to pure PLA. This information was also useful to establish the maximum operation temperature to be used when processing these materials by extrusion and 3D printing. As shown in Table 2, degradation starts at 310 °C for PLA when it is in powder form or as a 3Dprinted filament. On the other hand, the temperature at which the degradation process start decreases when $CaCO_3$, β-TCP or both were added to the PLA matrix (from 310 °C to 270–280 °C). In spite of this decrease, the degradation temperature is still higher than the melting temperature of all the studied combinations of materials (173–174 °C), and there is a wide safe temperature window to process the proposed combinations of materials by thermal techniques.

The results regarding the degree of crystallinity of the matrix for 3D printed filaments indicate that the use of the additives increases the value of this property (from 31.4% for pure PLA samples up to 49.8% in the case of PLA:$CaCO_3$:β-TCP 95:2.5:2.5 samples).

3.3. Fourier Transform Infrared Spectroscopy (FTIR)

The FTIR spectra have been used to evaluate the interaction between the components in the composite materials, as well as to assess possible changes in the degree of crystallinity of the extruded filaments as complementary information to the calorimetric data (Table 2). No displacement or modification of the peaks, that could confirm an intermolecular interaction between the materials blended, is observed in the FTIR spectra showed in Figure 3. This lack of interaction could be responsible for the agglomeration of the $CaCO_3$ and β-TCP particles.

Regarding the crystallinity study of the samples derived from FTIR results, and according to literature (Kister, Cassanas, & Vert, 1998), the regions of interest in the FTIR spectrum because of their high sensitivity to crystallinity changes are: the carbonyl (C=O) stretching region at 1790–1730 cm^{-1}, the CH_3 and CH bending region at 1400–1250 cm^{-1}, the skeletal stretching (C–O–C) region at 1260–1050 cm^{-1} and the backbone stretching and CH_3 rocking region at 970–850 cm^{-1}. As crystallinity increases the peaks located in these regions become sharper and band splitting occurs in carbonyl and C–O–C stretching regions (Bhatla & Yao, 2009).

As shown in Figure 3, peaks located in the regions mentioned above increased in intensity when $CaCO_3$ and β-TCP were added compared to the group of pure PLA. The most important examples are the peak located at ~1750 cm^{-1} and associated with carbonyl (C=O) stretching, the peaks related to asymmetric C–O–C stretching at approximately 1180 cm^{-1} and 1080 cm^{-1} and the bands at 960 cm^{-1} and 875 cm^{-1} arising from C–

C backbone stretching and the CH_3 rocking mode (Bhatla & Yao, 2009; Krikorian & Pochan, 2005). The highest value of crystallinity is expected for the combination of materials where both additives are used. The observed tendency is in accordance with the results obtained from the calorimetric analysis of the printed filaments (Table 2).

3.4. Water Contact Angle Measurement (WCA)

WCA measurements of the samples in dry state showed no statically significant difference ($p>0.05$) of the values between the groups. The results of this test are included in Appendix A, while water contact angle values for samples in pre-wetted state are shown in Table 3. For the later test, it can be concluded that the addition of $CaCO_3$ and β-TCP effectively reduce the water contact angle of the PLA matrix, as very highly statistically significant difference ($p<0.001$) between the groups of samples containing additives and the group of PLA samples were obtained. There is not any significant difference ($p>0.05$) among the composite groups.

3.5. Mechanical Characterization

3.5.1. Compression Test

Regarding the compression properties, the values of the compressive modulus were 207±25 MPa for pure PLA scaffolds, 150±5 MPa for PLA:$CaCO_3$ 95:5, 151±13 MPa for PLA:β-TCP 95:5 and 126±48 MPa for PLA:$CaCO_3$:β-TCP 95:2.5:2.5 (Figure 4). These values are in the range of values reported for cancellous bone (20–500 MPa) (Leong, Chua, Sudarmadji, & Yeong, 2008). Significant differences ($p<0.05$) were obtained when comparing PLA:$CaCO_3$ 95:5 and PLA:$CaCO_3$:β-TCP 95:2.5:2.5 groups to the group of pure PLA samples, while highly statistically significant differences ($p<0.01$) were observed for PLA:β-TCP 95:5. The same conclusion is drawn from the results of the compressive yield strength, as shown in Figure 4. This parameter decreased from a mean value of 7.7 MPa in the case of pure PLA samples to 5.4 MPa for the groups including one of the additives evaluated in this study, and to 4.9 MPa when both are added. Again, the results are in the range of values for cancellous bone (Leong et al., 2008).

The variation factor for compressive modulus resulted to be 12.3% for PLA, 3.3% for PLA:$CaCO_3$ 95:5, 8.3% for PLA:β-TCP 95:5 and 37.9% for PLA:$CaCO_3$:β-TCP 95:2.5:2.5, which means that the level of reproducibility for the PLA:$CaCO_3$:β-TCP 95:2.5:2.5 group is the worst one. On the other hand, the best results were obtained for the PLA:$CaCO_3$ 95:5 group, which showed a good level of uniformity for the extruded filament, resulting a similar variation factor to the nominal value of 4% mentioned in Section 2.3. The nucleation effect caused by the presence of the additive particles resulted in a good fluidity of this particular composite providing a uniform filament. However, the introduction of both additives in the PLA matrix worsened the variation factor, probably due to a combination of two factors: the poor distribution of the additives in the polymeric matrix due to the high number and size of agglomerates, and the lowest uniformity of the diameter of the PLA:$CaCO_3$:β-TCP 95:2.5:2.5 extruded filaments caused by the presence of these agglomerates.

3.5.2. Bending Test

According to the results, the value of the flexural modulus and the maximum flexural stress remains unchanged between the groups ($p>0.05$) for the non-porous samples obtained by compression moulding, with the first property ranging from 3.1 to 3.3 GPa and being the second one between 19-23 MPa for the four groups of samples evaluated.

Flexural tests performed on the 3D printed scaffolds revealed statistically significant differences between the flexural modulus values of the three groups of samples containing additives and the group of pure PLA samples ($p<0.05$ for PLA:$CaCO_3$:β-TCP 95:2.5:2.5 group, and $p<0.01$ for PLA:$CaCO_3$ 95:5and PLA:β-TCP 95:5 groups). The flexural modulus decreased from the mean value of 0.89 GPa of the PLA scaffolds group to 0.47, 0.59 and 0.60 GPa for the PLA:$CaCO_3$ 95:5, PLA:β-TCP 95:5 and PLA:$CaCO_3$:β-TCP 95:2.5:2.5 groups, respectively. The flexural modulus of the PLA:$CaCO_3$ 95:5 group was also significantly lower ($p<0.05$) compared to the PLA:β-TCP 95:5 group. Similar results were obtained regarding the

maximum flexural stress of the samples, as the values of groups of samples containing additives showed statistically significant differences compared to the group of PLA samples (mean value of 20 MPa), being the mean value of the PLA:$CaCO_3$ group significantly lower than the values of every other group (mean values obtained were 11 MPa for PLA:$CaCO_3$ 95:5, 14 MPa for PLA:β-TCP 95:5 and 15 MPa for PLA:$CaCO_3$:β-TCP 95:2.5:2.5).

As a conclusion of the bending tests for the two type of samples (porous vs non-porous), it could be stated that the decrease in flexural properties observed for the 3D printed samples is not a consequence of the additive's introduction itself, but is more related to the manufacturing process of the part, which leads to the formation of agglomerates.

3.6. Metabolic activity of SaOS-2 cells

The highest mean value of fluorescence in the Alamar Blue test, and therefore the highest metabolic activity of cells attached to the structure after 7 days, was observed for the PLA:$CaCO_3$:β-TCP 95:2.5:2.5 group, as shown in Figure 5. Very highly statistically significant difference ($p<0.001$) between this group and the pure PLA scaffolds group was obtained. Also, there are statistically significant differences ($p<0.05$) for the group containing both additives compared to the groups of scaffolds containing only β-TCP or $CaCO_3$. According to these results, the use of the additives in the formulation of the samples enhances the metabolic activity of the SaOS-2 cells.

High magnification SEM images from cells located at the 3D printed scaffold's interior are shown in Figure 6, in which we could see that cells have a high degree of spreading after 7 days of culture, showing extended lamellipodia and some filopodia in all tested materials. On the other hand, as shown in Figure 6 (b), cells attached in this case to a PLA:$CaCO_3$ 95:5 scaffold tend to fill and grow within the micropores generated during the manufacturing process. In this way, it was possible to conclude that the cell growth in the composite scaffolds was enhanced not only because of the improved osteoconductivity of the PLA matrix (due to the addition of the β-TCP particles), but also because of the enhanced microporosity of the structures.

4. Discussion

The results obtained proved that the incorporation of $CaCO_3$ and β-TCP into the PLA matrix of 3D printed scaffolds leads to substantial modification of the characteristics of the final structure. As has been shown in SEM and micro-CT images, the roughness and microporosity of the surface of the 3D printed filaments were significantly increased when additives were used. Both modifications were attributed to the presence of agglomerates of additive particles, as a consequence of the lack of chemical interaction between them and the PLA matrix later confirmed by FTIR analysis. The formation of agglomerates was especially manifest in the case of the PLA:$CaCO_3$:β-TCP 95:2.5:2.5 group, which showed greater dispersion in the results concerning porosity (Table 1) and mechanical testing of the scaffolds (Figure 4).

An increase in the crystallinity of the extruded and 3D printed filaments was also observed due to the introduction of additives. This modification can be explained by the nucleation effect caused by the presence of the particles (Alemán-Domínguez, Giusto, et al., 2018; Drummer et al., 2012). Changes induces in the crystallinity of the PLA-based scaffolds alters the degradation rate of the structure (Esposito Corcione et al., 2017), which is a factor of great importance since the bulk degradation of PLA leads to the formation of acidic by-products (Abert et al., 2016; Schiller et al., 2004). Further investigation is needed to evaluate the effect of the addition of β-TCP (Hutmacher, 2000) and especially $CaCO_3$ into the PLA matrix in order to counteract the pH decrease.

In contrast to the dry test, in the pre-wetted state of the samples the use of the additives led to a significant reduction of the WCA, i.e., greater surface wettability. This effect has already been observed in polymers that better expose hydroxyl or carboxylic acid groups at the surface only when hydrated (Ratner, 2013). Most studies show that a hydrophilic surface is more conductive to the attachment of cells (Chen et al., 2018). In the present study, a very high statistically significant difference ($p<0.001$) between the WCA values was obtained when comparing the pure PLA scaffolds group with the composite groups of samples, with mean reduction of a 5.5% (Table 3). The decrease of the hydrophobicity of the scaffolds surface, coupled with

the increase of its roughness and microporosity, led to enhanced metabolic activity of cells adhered to the composite scaffolds (Chen et al., 2018; Perez & Mestres, 2016), as shown in Figure 5. However, the adhesive properties of cells after 7 days of culture appeared to be unaffected by the presence of the additives in the PLA-based scaffolds (Figure 6). A better understanding of this effect could be observed at early culture periods, since in the first 24 hours the surface properties dictate the first cell-material interactions (Ribeiro et al., 2017). In this way, the main differences in relation to cell behaviour were observed in terms of metabolic activity, showing the PLA:$CaCO_3$:β-TCP 95:2.5:2.5 group of scaffolds a significantly higher metabolic activity of SaOS-2 cells after 7 days of culture, as compared to the remaining PLA-based constructs.

Regarding the pore size, the distance between filaments was in the range of 400–425 μm for all the groups of scaffolds evaluated (Table 1), so according to previous literature the structures obtained fulfil the requirements for bone regeneration (150–500 μm) (Gómez-Lizárraga et al., 2017). In addition, apparent density values (0.53–0.55 g/cm^3, Table 1) were within the range reported for cancellous bone: 0.14-1.2 g/cm^3 (Deplaine et al., 2014), as well as compressive test results for all the groups of scaffolds tested (Leong et al., 2008). From the bending test results, it can be drawn that the great number of defects in the filaments was the main cause of the decrease of the mechanical properties for the composite scaffolds, but not the additive introduction itself, as no significant differences were observed between the values of the samples obtained by compression moulding. As a conclusion, the agglomerates seem having more influence in their processing than in the behaviour of the composite materials. The improvement of the mixing process prior to the extrusion of the filaments or the reduction of the additive concentration can be alternatives that could lead to the reduction or removal of these agglomerates. In this way, it would be possible to adjust the characteristics of the scaffold to achieve good metabolic activity of cells while maintaining the mechanical properties of the base material. Further research to optimize the scaffold's properties in terms of microporosity and mechanical properties may be conducted, although obtained results for the 3D printed PLA:$CaCO_3$:β-TCP 95:2.5:2.5 scaffolds regarding cell behaviour are very promising. This formulation promoted the growth and development of osteoblast-like cells in vitro, confirming the potential application of these structures for bone regeneration.

5. Acknowledgments: Ricardo Donate express his gratitude for the funding through the PhD grant program co-financed by the Canarian Agency for Research, Innovation and Information Society of the Canary Islands Regional Council for Employment, Industry, Commerce and Knowledge and by the European Social Fund (ESF) Canary Islands Integrated Operational Program 2014-2020, Axis 3 Priority Theme 74 (85%). Grant code: TESIS2017010036.
Also, the authors would like to thank H2020-MSCA-RISE program, as this work is part of developments carried out in BAMOS project, funded from the European Union's Horizon 2020 research and innovation programme under grant agreement Nº 734156.

6. Conflict of Interest Statement: The authors declare no conflict of interest. The founding sponsors had no role in the design of the study; in the collection, analyses, or interpretation of data; in the writing of the manuscript, and in the decision to publish the results.

7. References

Abert, J., Amella, A., Weigelt, S., & Fischer, H. (2016). Degradation and swelling issues of poly-(d,l-lactide)/β-tricalcium phosphate/calcium carbonate composites for bone replacement. *Journal of the Mechanical Behavior of Biomedical Materials, 54*, 82-92. doi:10.1016/j.jmbbm.2015.09.016

Alemán-Domínguez, M. E., Giusto, E., Ortega, Z., Tamaddon, M., Benítez, A. N., & Liu, C. (2018). Three-dimensional printed polycaprolactone-microcrystalline cellulose scaffolds. *Journal of Biomedical Materials Research - Part B Applied Biomaterials*. doi:10.1002/jbm.b.34142

Alemán-Domínguez, M. E., Ortega, Z., Benítez, A. N., Vilariño-Feltrer, G., Gómez-Tejedor, J. A., & Vallés-Lluch, A. (2018). Tunability of polycaprolactone hydrophilicity by carboxymethyl cellulose loading. *Journal of Applied Polymer Science, 135*(14). doi:10.1002/app.46134

Ara, M., Watanabe, M., & Imai, Y. (2002). Effect of blending calcium compounds on hydrolytic degradation of poly(DL-lactic acid-co-glycolic acid). *Biomaterials, 23*(12), 2479-2483. doi:10.1016/S0142-9612(01)00382-9

Bhatla, A., & Yao, Y. L. (2009). Effect of laser surface modification on the crystallinity of poly(l-lactic acid). *Journal of Manufacturing Science and Engineering, Transactions of the ASME, 131*(5), 0510041-05100411. doi:10.1115/1.3039519

Canadas, R. F., Pina, S., Marques, A. P., Oliveira, J. M., & Reis, R. L. (2015). Cartilage and Bone Regeneration-How Close Are We to Bedside? In *Translating Regenerative Medicine to the Clinic* (pp. 89-106).

Chen, S., Guo, Y., Liu, R., Wu, S., Fang, J., Huang, B., . . . Chen, Z. (2018). Tuning surface properties of bone biomaterials to manipulate osteoblastic cell adhesion and the signaling pathways for the enhancement of early osseointegration. *Colloids and Surfaces B: Biointerfaces, 164*, 58-69. doi:10.1016/j.colsurfb.2018.01.022

Chia, H. N., & Wu, B. M. (2015). Recent advances in 3D printing of biomaterials. *Journal of Biological Engineering, 9*(1). doi:10.1186/s13036-015-0001-4

Conejero-García, Á., Gimeno, H. R., Sáez, Y. M., Vilariño-Feltrer, G., Ortuño-Lizarán, I., & Vallés-Lluch, A. (2017). Correlating synthesis parameters with physicochemical properties of poly(glycerol sebacate). *European Polymer Journal, 87*, 406-419. doi:10.1016/j.eurpolymj.2017.01.001

Deplaine, H., Acosta-Santamaría, V. A., Vidaurre, A., Gómez Ribelles, J. L., Doblaré, M., Ochoa, I., & Gallego Ferrer, G. (2014). Evolution of the properties of a poly(L-lactic acid) scaffold with double porosity during in vitro degradation in a phosphate-buffered saline solution. *Journal of Applied Polymer Science, 131*(20). doi:10.1002/app.40956

Domingos, M., Intranuovo, F., Gloria, A., Gristina, R., Ambrosio, L., Bártolo, P. J., & Favia, P. (2013). Improved osteoblast cell affinity on plasma-modified 3-D extruded PCL scaffolds. *Acta Biomaterialia, 9*(4), 5997-6005. doi:10.1016/j.actbio.2012.12.031

Drummer, D., Cifuentes-Cuéllar, S., & Rietzel, D. (2012). Suitability of PLA/TCP for fused deposition modeling. *Rapid Prototyping Journal, 18*(6), 500-507. doi:10.1108/13552541211272045

Esposito Corcione, C., Gervaso, F., Scalera, F., Montagna, F., Sannino, A., & Maffezzoli, A. (2017). The feasibility of printing polylactic acid–nanohydroxyapatite composites using a low-cost fused deposition modeling 3D printer. *Journal of Applied Polymer Science, 134*(13). doi:10.1002/app.44656

Garlotta, D. (2001). A literature review of poly(lactic acid). *Journal of Polymers and the Environment, 9*(2), 63-84.

Gregor, A., Filová, E., Novák, M., Kronek, J., Chlup, H., Buzgo, M., . . . Hošek, J. (2017). Designing of PLA scaffolds for bone tissue replacement fabricated by ordinary commercial 3D printer. *Journal of Biological Engineering, 11*(1). doi:10.1186/s13036-017-0074-3

Gómez-Lizárraga, K. K., Flores-Morales, C., Del Prado-Audelo, M. L., Álvarez-Pérez, M. A., Piña-Barba, M. C., & Escobedo, C. (2017). Polycaprolactone- and polycaprolactone/ceramic-based 3D-bioplotted porous scaffolds for bone regeneration: A comparative study. *Materials Science and Engineering: C, 79*(Supplement C), 326-335. doi:https://doi.org/10.1016/j.msec.2017.05.003

Hutmacher, D. W. (2000). Scaffolds in tissue engineering bone and cartilage. *Biomaterials, 21*(24), 2529-2543. doi:10.1016/S0142-9612(00)00121-6

Kister, G., Cassanas, G., & Vert, M. (1998). Effects of morphology, conformation and configuration on the IR and Raman spectra of various poly(lactic acid)s. *Polymer, 39*(2), 267-273. doi:10.1016/S0032-3861(97)00229-2

Krikorian, V., & Pochan, D. J. (2005). Crystallization behavior of poly(L-lactic acid) nanocomposites: Nucleation and growth probed by infrared spectroscopy. *Macromolecules, 38*(15), 6520-6527. doi:10.1021/ma050739z

Leong, K. F., Chua, C. K., Sudarmadji, N., & Yeong, W. Y. (2008). Engineering functionally graded tissue engineering scaffolds. *Journal of the Mechanical Behavior of Biomedical Materials, 1*(2), 140-152. doi:https://doi.org/10.1016/j.jmbbm.2007.11.002

Li, Y., Li, D., Lu, B., Gao, D., & Zhou, J. (2015). Current status of additive manufacturing for tissue engineering scaffold. *Rapid Prototyping Journal, 21*(6), 747-762. doi:10.1108/RPJ-03-2014-0029

Lou, T., Wang, X., Song, G., Gu, Z., & Yang, Z. (2014). Fabrication of PLLA/β-TCP nanocomposite scaffolds with hierarchical porosity for bone tissue engineering. *International Journal of Biological Macromolecules, 69*, 464-470. doi:10.1016/j.ijbiomac.2014.06.004

Patrício, T., Domingos, M., Gloria, A., D'Amora, U., Coelho, J. F., & Bártolo, P. J. (2014). Fabrication and characterisation of PCL and PCL/PLA scaffolds for tissue engineering. *Rapid Prototyping Journal, 20*(2), 145-156. doi:10.1108/RPJ-04-2012-0037

Perez, R. A., & Mestres, G. (2016). Role of pore size and morphology in musculo-skeletal tissue regeneration. *Materials Science and Engineering C, 61*, 922-939. doi:10.1016/j.msec.2015.12.087

Rakovsky, A., Gotman, I., Rabkin, E., & Gutmanas, E. Y. (2014). β-TCP-polylactide composite scaffolds with high strength and enhanced permeability prepared by a modified salt leaching method. *Journal of the Mechanical Behavior of Biomedical Materials, 32*, 89-98. doi:10.1016/j.jmbbm.2013.12.022

Ratner, B. D. (2013). Chapter I.1.5 - Surface Properties and Surface Characterization of Biomaterials. In *Biomaterials Science (Third Edition)* (pp. 34-55): Academic Press.

Ribeiro, V. P., Almeida, L. R., Martins, A. R., Pashkuleva, I., Marques, A. P., Ribeiro, A. S., . . . Reis, R. L. (2017). Modulating cell adhesion to polybutylene succinate biotextile constructs for tissue engineering applications. *Journal of Tissue Engineering and Regenerative Medicine, 11*(10), 2853-2863. doi:10.1002/term.2189.

Sabino, M., Fermín, Z., Marielys, L., Moret, J., Rodríguez, D., Rezende, R. A., . . . Alvarez, J. (2013). *In vitro biocompatibility study of biodegradable polyester scaffolds constructed using fused deposition modeling (FDM).* Paper presented at the IFAC Proceedings Volumes (IFAC-PapersOnline).

Sachlos, E., Czernuszka, J. T., Gogolewski, S., & Dalby, M. (2003). Making tissue engineering scaffolds work. Review on the application ofsolid freeform fabrication technology to the production of tissue engineeringscaffolds. *European Cells and Materials, 5*, 29-40.

Schiller, C., & Epple, M. (2003). Carbonated calcium phosphates are suitable pH-stabilising fillers for biodegradable polyesters. *Biomaterials, 24*(12), 2037-2043. doi:10.1016/S0142-9612(02)00634-8

Schiller, C., Rasche, C., Wehmöller, M., Beckmann, F., Eufinger, H., Epple, M., & Weihe, S. (2004). Geometrically structured implants for cranial reconstruction made of biodegradable polyesters and calcium phosphate/calcium carbonate. *Biomaterials, 25*(7-8), 1239-1247. doi:10.1016/j.biomaterials.2003.08.047

Takahashi, Y., Yamamoto, M., & Tabata, Y. (2005). Osteogenic differentiation of mesenchymal stem cells in biodegradable sponges composed of gelatin and β-tricalcium phosphate. *Biomaterials, 26*(17), 3587-3596. doi:https://doi.org/10.1016/j.biomaterials.2004.09.046

Vallés-Lluch, A., Gallego Ferrer, G., & Monleón Pradas, M. (2010). Effect of the silica content on the physico-chemical and relaxation properties of hybrid polymer/silica nanocomposites of P(EMA-co-HEA). *European Polymer Journal, 46*(5), 910-917. doi:10.1016/j.eurpolymj.2010.02.004

Yang, G. H., Kim, M., & Kim, G. (2017). Additive-manufactured polycaprolactone scaffold consisting of innovatively designed microsized spiral struts for hard tissue regeneration. *Biofabrication, 9*(1). doi:10.1088/1758-5090/9/1/015005

Zein, I., Hutmacher, D. W., Tan, K. C., & Teoh, S. H. (2002). Fused deposition modeling of novel scaffold architectures for tissue engineering applications. *Biomaterials, 23*(4), 1169-1185. doi:10.1016/S0142-9612(01)00232-0

Tables

Table 1. Bulk and apparent density values of the materials evaluated and porosity and pore size values of the 3D printed scaffolds.

Material	Bulk density (g/m3)	Apparent density (g/m3)	Porosity (%)	Pore size (μm)
PLA	1.20 ± 0.03	0.54 ± 0.03	54.7 ± 2.2	421.45 ± 54.53
PLA:$CaCO_3$ 95:5	1.30 ± 0.04 [3]	0.54 ± 0.02	58.6 ± 1.5 [1]	424.61 ± 51.49
PLA:β-TCP 95:5	1.34 ± 0.11 [2]	0.55 ± 0.01	58.8 ± 0.8 [2]	396.64 ± 29.86
PLA:$CaCO_3$:β-TCP 95:2.5:2.5	1.28 ± 0.07 [1]	0.53 ± 0.05	58.3 ± 3.6	410.99 ± 48.24

[1] *p<0.05 compared to the group of pure PLA samples.
[2] **p<0.01 compared to the group of pure PLA samples.
[3] ***p<0.001 compared to the group of pure PLA samples.

Table 2. Left limit temperature, melting temperature, enthalpy of fusion and degree of crystallinity values determined from thermogravimetric and calorimetric analysis.

Type of sample	Material	Left limit temperature (°C)	Melting temperature (°C)	Enthalpy of fusion (J/g)	Degree of crystallinity (%)
powder	PLA	310	175	46.8	50.0
3D printed filament	PLA	310	173	29.4	31.4
	PLA:$CaCO_3$ 95:5	280	173	31.4	35.3
	PLA:β-TCP 95:5	270	174	41.3	46.4
	PLA:$CaCO_3$:β-TCP 95:2.5:2.5	280	174	44.3	49.8

Table 3. Water contact angle values of pre-wetted samples.

Material	WCA in pre-wetted state (°)
PLA	88.85 ± 2.24
PLA:$CaCO_3$ 95:5	84.34 ± 4.17 [1]
PLA:β-TCP 95:5	83.56 ± 3.59 [1]
PLA:$CaCO_3$:β-TCP 95:2.5:2.5	84.05 ± 3.46 [1]

[1] ***p<0.001 compared to the group of pure PLA samples.

Figure legends

Figure 1. SEM images (scale bar: 1 mm) of the 3D printed scaffolds analysed:(**a**) PLA; (**b**) PLA:$CaCO_3$ 95:5; (**c**) PLA:β-TCP 95:5; (**d**) PLA:$CaCO_3$:β-TCP 95:2.5:2.5. Also, SEM images with higher magnification (scale bar: 300 μm) are shown for (**e**)PLA:$CaCO_3$ 95:5 and (**f**) PLA:β-TCP 95:5 3D printed scaffolds.

Figure 2. Micro-CT images and 3D reconstructed model of the 3D printed scaffolds analysed. Scale bar: 1.5 mm.

Figure 3. FTIR spectra (region of wavelengths from 3200 to 500 cm^{-1}) of PLA extruded filaments and its composites.

Figure 4. Mechanical properties of the 3D printed scaffolds under compression testing (*p<0.05 and **p<0.01 compared to the group of pure PLA samples).

Figure 5. Metabolic activity of SaOS-2 cells on the scaffolds determined by the Alamar Blue assay (*p<0.05 and ***p<0.001).

Figure 6. High contrast SEM images (scale bar: 50 μm) of the 3D printed scaffolds after 7 days of cell culture with SaOS-2 cells: (a) PLA; (b) PLA:$CaCO_3$ 95:5; (c) PLA:β-TCP 95:5; (d) PLA:$CaCO_3$:β-TCP 95:2.5:2.5. The red arrow indicates filopodia and the black arrows indicate lamellipodia.

Supporting Information

Figure 7. Mechanical properties under 3 points bending testing of the non-porous samples manufactured by compression moulding.

Figure 8. Mechanical properties of the 3D printed scaffolds under 3 points bending testing (*p<0.05 and **p<0.01 compared to the group of pure PLA samples).

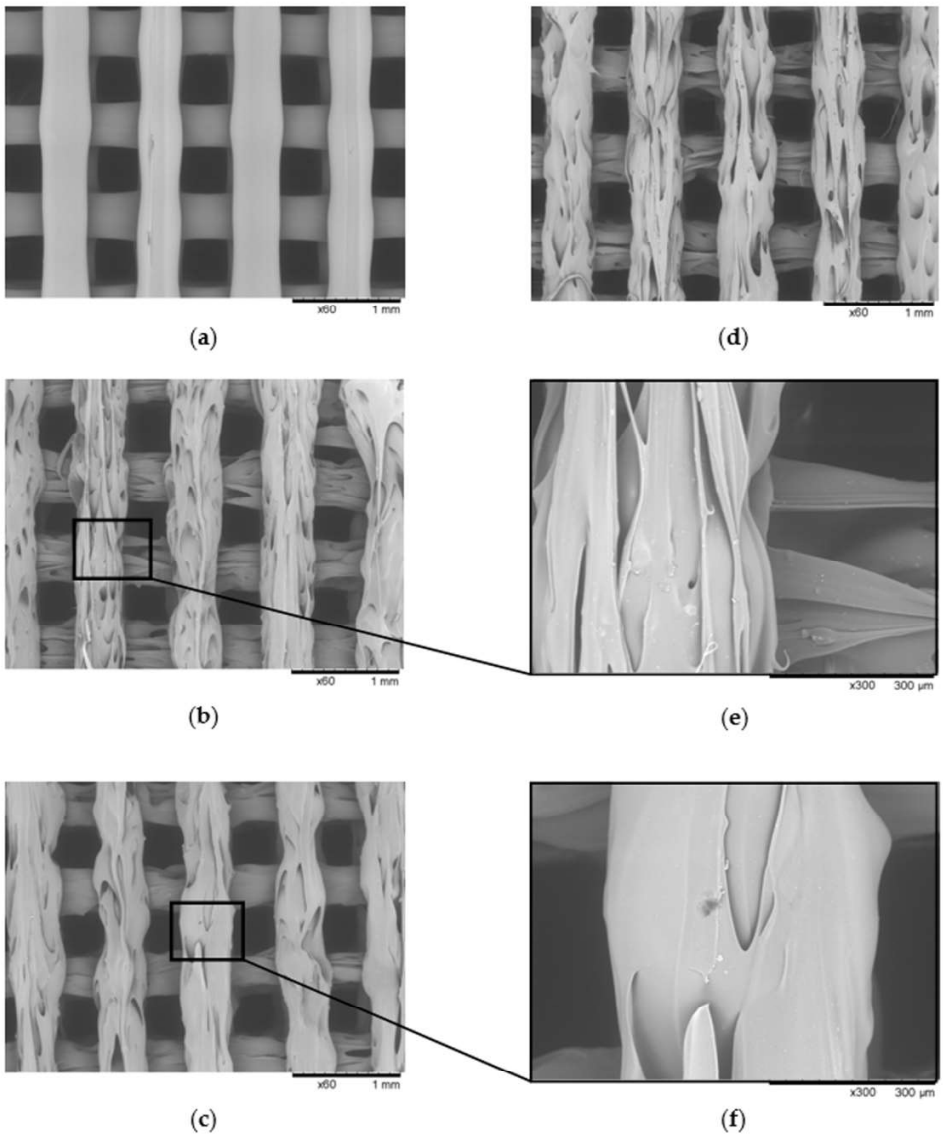

Figure 1. SEM images (scale bar: 1 mm) of the 3D printed scaffolds analysed:(a) PLA; (b) PLA:CaCO3 95:5; (c) PLA:β-TCP 95:5; (d) PLA:CaCO3:β-TCP 95:2.5:2.5. Also, SEM images with higher magnification (scale bar: 300 µm) are shown for (e) PLA:CaCO3 95:5 and (f) PLA:β-TCP 95:5 3D printed scaffolds.

152x181mm (300 x 300 DPI)

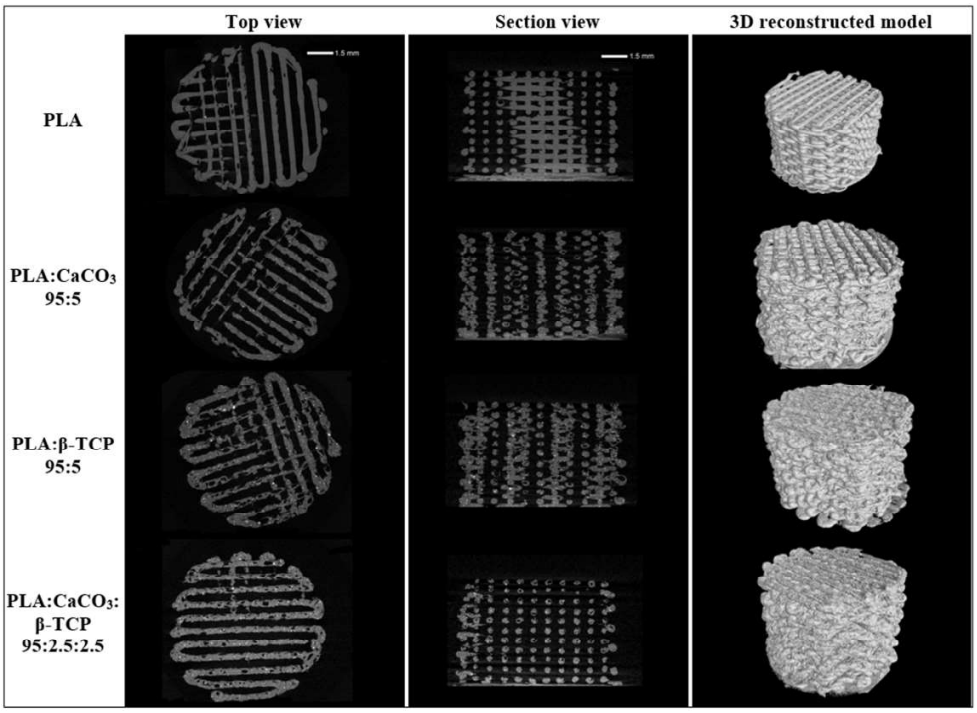

Figure 2. Micro-CT images and 3D reconstructed model of the 3D printed scaffolds analysed. Scale bar: 1.5 mm.

152x110mm (300 x 300 DPI)

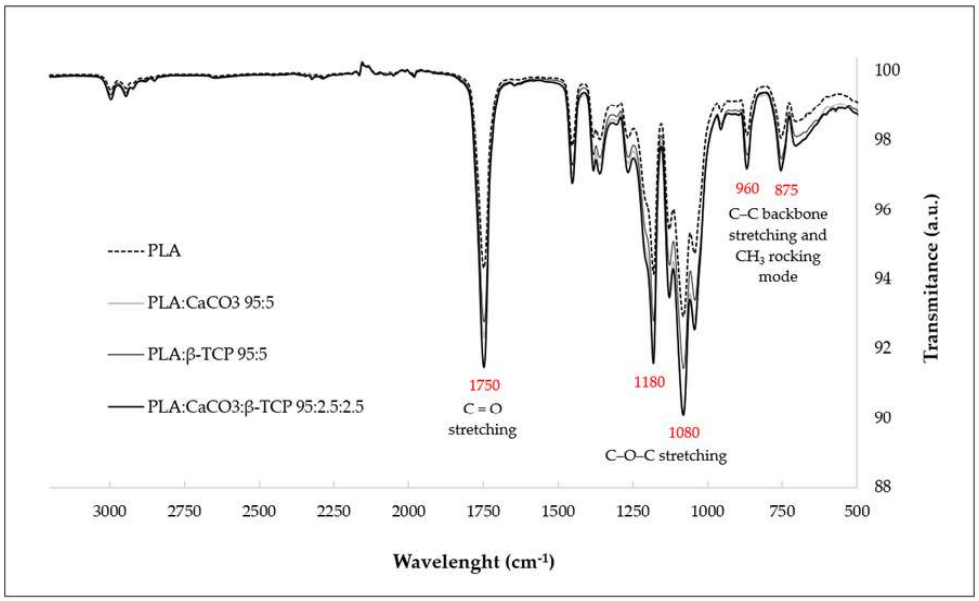

Figure 3. FTIR spectra (region of wavelengths from 3200 to 500 cm-1) of PLA extruded filaments and its composites.

76x46mm (300 x 300 DPI)

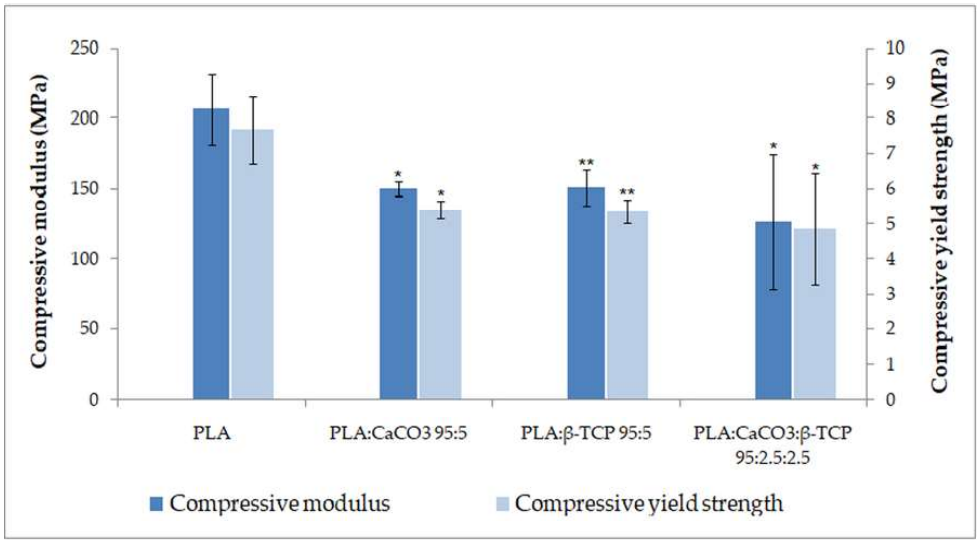

Figure 4. Mechanical properties of the 3D printed scaffolds under compression testing (*p<0.05 and **p<0.01 compared to the group of pure PLA samples).

76x41mm (300 x 300 DPI)

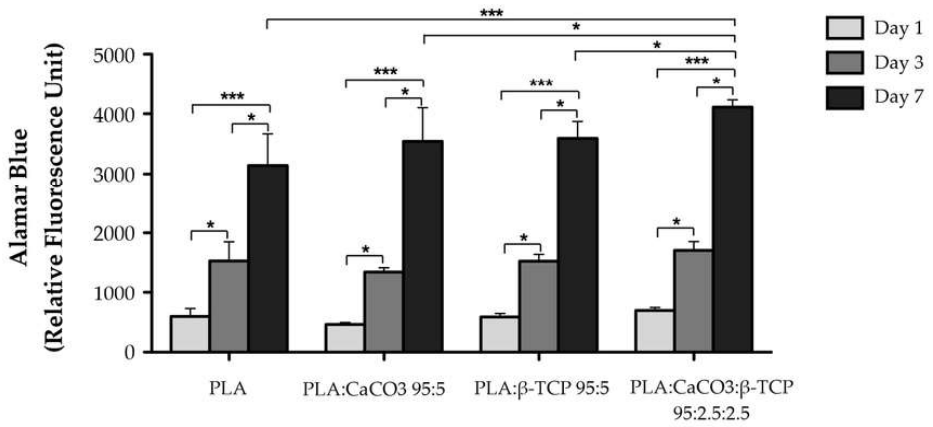

Figure 5. Metabolic activity of SaOs-2 cells on the scaffolds determined by the Alamar Blue assay (*p<0.05 and ***p<0.001).

76x36mm (300 x 300 DPI)

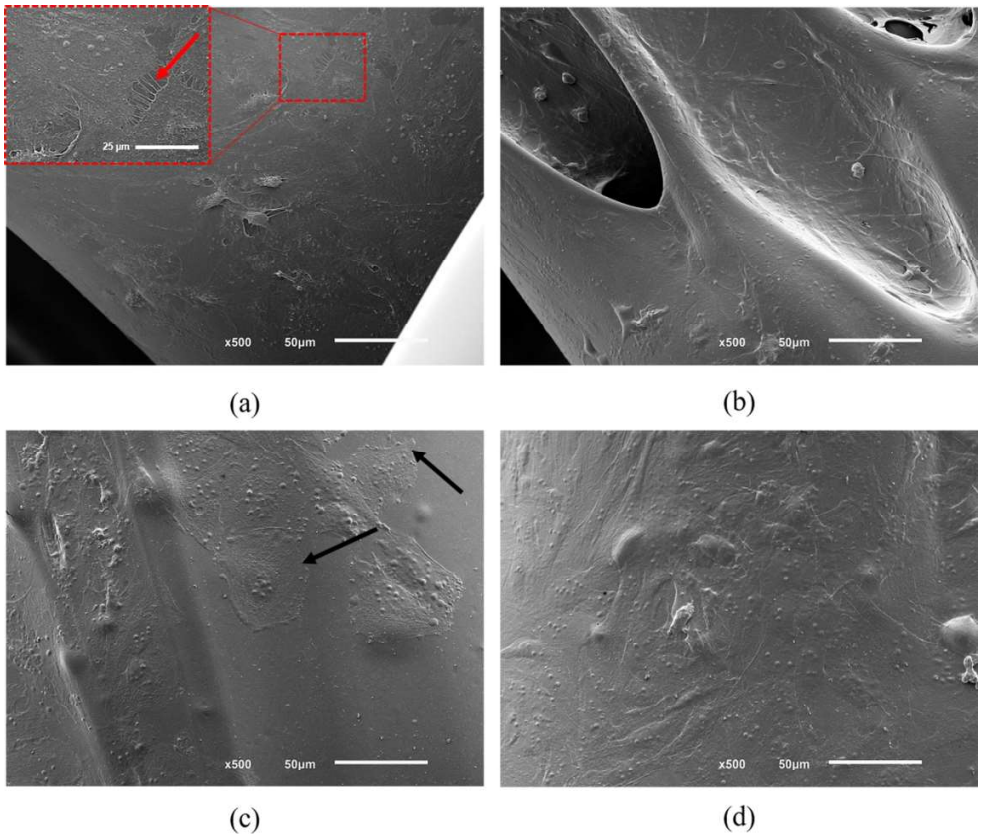

Figure 6. High contrast SEM images (scale bar: 50 µm) of the 3D printed scaffolds after 7 days of cell culture with SaOS-2 cells: (a) PLA; (b) PLA:CaCO3 95:5; (c) PLA:β-TCP 95:5; (d) PLA:CaCO3:β-TCP 95:2.5:2.5. The red arrow indicates filopodia and the black arrows indicate lamellipodia.

152x132mm (300 x 300 DPI)

Enzymatic degradation study of PLA-based composite scaffolds

Research Article

Ricardo Donate*, Mario Monzón, María Elena Alemán-Domínguez, and Zaida Ortega

Enzymatic degradation study of PLA-based composite scaffolds

https://doi.org/10.1515/rams-2020-0005
Received Sep 03, 2019; accepted Dec 11, 2019

Abstract: Disadvantages in the use of polylactic acid (PLA) as a base material for Tissue Engineering applications include the low osteoconductivity of this biomaterial, its acidic degradation and the deficient cellular adhesion on its surface. In order to counteract these drawbacks, calcium carbonate ($CaCO_3$) and β-tricalcium phosphate ($Ca_3(PO4)_2$, β-TCP) were proposed in this work as additives of PLA-based support structures. Composite scaffolds (PLA:$CaCO_3$:β-TCP 95:2.5:2.5) manufactured by fused deposition modeling (FDM) were tested under enzymatic degradation using *proteinase K* enzymes to assess the modification of their properties in comparison with neat PLA scaffolds. The samples were characterized before and after the degradation test by optical microscopy, scanning electron microscopy, compression testing and thermogravimetric and calorimetric analysis. According to the results, the combination of the PLA matrix with the proposed additives increases the degradation rate of the 3D printed scaffolds, which is an advantage for the application of the composite scaffold in the field of Tissue Engineering. The higher degradation rate of the composite scaffolds could be explained by the release of the additive particles and the statistically higher microporosity of these samples compared to the neat PLA ones.

Keywords: polylactic acid (PLA); bone tissue engineering; proteinase K

***Corresponding Author: Ricardo Donate:** Departamento de Ingeniería Mecánica, Universidad de Las Palmas de Gran Canaria, Campus Universitario de Tafira s/n, 35017, Las Palmas, Spain; Email: ricardo.donate@ulpgc.es; Tel.: +34-928-45-8603
Mario Monzón, María Elena Alemán-Domínguez: Departamento de Ingeniería Mecánica, Universidad de Las Palmas de Gran Canaria, Campus Universitario de Tafira s/n, 35017, Las Palmas, Spain
Zaida Ortega: Departamento de Ingeniería de Procesos, Universidad de Las Palmas de Gran Canaria, Campus Universitario de Tafira s/n, 35017, Las Palmas, Spain

1 Introduction

Polylactic acid (PLA) is a widely used biomaterial in Bone Tissue Engineering because of its biocompatibility, its suitable mechanical properties and ease to be processed [1]. However, there are some disadvantages which limit its efficiency as a support material for bone ingrowth, such as the low osteoconductivity of this biomaterial, its acidic degradation and the deficient cellular adhesion on its surface [2]. Furthermore, the degradation of PLA is deemed to be too slow to enhance the replacement of the material by the new bone tissue [3, 4]. In order to counteract these drawbacks, calcium carbonate ($CaCO_3$) and β-tricalcium phosphate ($Ca_3(PO_4)_2$, β-TCP) are proposed in this work as additives of PLA-based support structures intended for bone regeneration. β-TCP is a biodegradable and biocompatible ceramic material that has been extensively used in the field of Bone Tissue Engineering due to its osteoconductivity and its ability of complete bioresorption [5]. The use of the $CaCO_3$ as an additive of PLA responds to the need of counteracting the release of acidic products during the degradation of the base material, maintaining the pH around 7.4 by buffer effect [6]. The composite blend developed was used to manufacture scaffolding structures by the method of additive manufacturing, under the category of "material extrusion" (ISO/ASTM 52900:2015), commonly known as fused deposition modeling (FDM). Additive manufacturing techniques provide the possibility of controlling the porosity of the scaffolds to be used in Tissue Engineering and personalizing their design according to the patients' needs [7].

In this work, the assessment of the degradation rate modification due to the presence of $CaCO_3$ and β-TCP has been carried out. For this purpose, degradation tests of PLA and composite (PLA:$CaCO_3$:β-TCP 95:2.5:2.5) scaffolds catalyzed by proteinase K enzymes were carried out. The enzymatic degradation test was designed with the aim of accelerating the degradation of PLA and composite scaffolds, since it can take more than 6 months to obtain significant weight losses when the experiment is carried out using PBS as degradation medium [8, 9]. Several examples are found in the literature about the use of this en-

zyme to degrade PLA fibres, films or scaffolds, obtaining significant differences in terms of weight loss or mechanical properties in days or even hours [10–12]. Sheng *et al.* [13], for example, obtained weight losses of between 30-50% in only 5 days by studying the degradation of PLA scaffolds using proteinase K enzymes. Although these working conditions do not rigorously simulate the conditions for the degradation of the material in vivo, this experiment design allows us to compare the composite scaffolds manufactured with the neat PLA ones. The degradation study was complemented with the morphological, thermogravimetric and mechanical characterization of the samples, before and after degradation, in order to assess the modification of the PLA properties due to the incorporation of the additives.

2 Experimental

PLA L105 in powder form was kindly supplied by Corbion Purac. Commercial grade calcium carbonate 0179-500G with a particle size of 30 µm was purchased from VWR, while β-tricalcium phosphate (β-TCP) with a mean particle size of 45 µm was kindly provided by the 3B's Research Group of Universidade do Minho. These three materials were mixed to obtain the following mixture (wt:wt): PLA:$CaCO_3$:β-TCP 95:2.5:2.5.

PLA and composite filaments were obtained using a lab prototype extruder with an 8 mm screw, a 1.6 mm diameter nozzle tip and an L/D cylinder ratio of 10. The working parameters included a rotating speed of 7 rpm and a temperature set at 245°C for the thermal resistance (the measured temperature in the proximity of the nozzle tip was equal to 180°C). The filaments needed to print the 3D structures were obtained after a final cooling stage using compressed air. A BQ Hephestos 2 3D printer (Spain) was used to manufacture scaffolds with a rectangular 0/90° pattern, a diameter of 9.8 mm and a height of 7 mm, resulting in a theoretical porosity of 50%. A nozzle diameter of 0.4 mm was used to print the scaffolds and the printing parameters included a temperature of 215°C and a deposition speed of 40 mm/s.

For the enzymatic degradation study, PLA and composite scaffolds were tested for time periods up to 5 and 10 days. Four replicas per group and time period were used. After measuring the weight of the scaffolds using an analytical balance (±0.1 mg, A&D Scales Gemini Series, GR-200, Germany), the samples were placed individually in a 24 well-plate and immersed in 2 mL of 0.05 M pH 8.6 Tris–HCl buffer solution containing 0.2 mg/mL of proteinase K from Tritirachium album (Merck, Darmstadt, Germany) and 0.2 mg/mL of sodium azide (Merck, Darmstadt, Germany). The degradation study was carried out at 37°C and the buffer-enzyme solution was replaced daily in order to maintain a high enzymatic activity. PLA and composite scaffolds incubated without enzymes in Tris–HCl solution were also evaluated as control samples. After the time periods studied, the scaffolds were weighed again to calculate the mass loss.

Before and after the degradation test, the surface morphology of the scaffolds was evaluated by scanning electron microscopy (SEM; Hitachi TM 3030 at an acceleration voltage of 15 kV). In addition, the pore size of these structures was assessed as the distance between filaments, using an Olympus BX51 optical microscope for that purpose. The pore size was calculated as the average of 40 measures per group of samples. Furthermore, the following equation was used in order to estimate the porosity of the 3D printed scaffolds [14, 15]:

$$\%\text{porosity} = 100 \cdot (1 - \rho_{ap}/\rho_{bulk}), \quad (1)$$

Where ρ_{ap} is the apparent density of the structure and ρ_{bulk} is the density of the bulk material. The first one was calculated using the mass and dimensions of the 3D printed scaffolds of each group of samples studied. The density of the bulk material was determined by measuring the dimensions and mass of samples (n=8) extracted from the PLA and composite extruded filaments.

Samples extracted from the degraded scaffolds were subjected to thermogravimetric analysis in a TGA/DSC 1 Mettler Toledo device. PLA in powder form as well as non-degraded PLA and composite scaffolds were also analysed. The samples (n=4) were placed in aluminium crucibles and heated up to 385°C at a rate of 10°C/min. The thermal cycle was performed while working with a nitrogen flow of 10 mL/min. During the TGA testing and using the same thermal cycle, calorimetric data (heat flow curve) of each type of sample was obtained, from which the melting temperature and the melting enthalpy were estimated. The melting enthalpy values obtained were used to calculate the crystallinity of each group of samples according to the following equation [16]:

$$\%\text{Xc} = 100 \cdot [\Delta H_f/(\Delta H_f^\circ \cdot W_{PLA})], \quad (2)$$

Where Xc is the degree of crystallinity, ΔH_f is the enthalpy of fusion of the sample, ΔH_f° corresponds to the heat of fusion of 100% crystalline PLA and W_{PLA} is the net weight fraction of the PLA in the sample tested. The value used for ΔH_f° was 93.7 J/g [17].

Regarding the mechanical characterization, the scaffolds degraded were tested by compression on an LIYI

(LI-1065, Dongguan Liyi Environmental Technology Co., Ltd.,China) testing machine in displacement control mode. Crosshead speed was set at 1 mm/min. The compressive modulus was calculated according to ASTM D695-15 using the initial steepest straight-line portion of the load-strain curve. These results were compared with the ones obtained by testing non-degraded PLA and composite scaffolds. Four replicas were used per group of samples.

Statistical analysis was performed using MATLAB software (MATLAB and Statistics Toolbox Release 2017a, The MathWorks, Inc., Natick, USA). The data obtained during this study were analysed by the Wilcoxon two-sided rank sum test when comparing two groups and by the Kruskal-Wallis test when more than two groups were compared. The significance level was set to $*p < 0.05$, $**p < 0.01$ and $***p < 0.001$ for statistically significant, highly statistically significant and very highly statistically significant differences, respectively. All the figures show the mean values of each group and their standard deviations are represented with error bars.

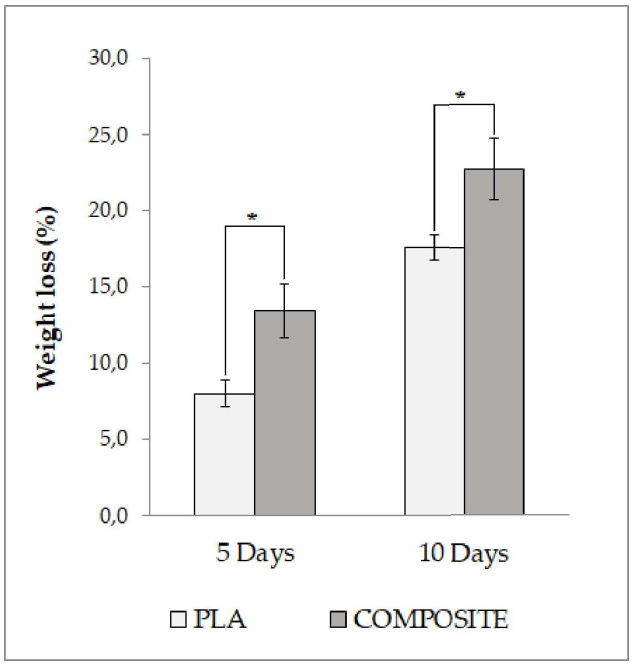

Figure 1: Weight loss percentage of 3D printed scaffolds at the time periods studied.

3 Results and Discussion

After 5 days of enzymatic degradation, the mean weight loss of the PLA scaffolds group was 8.0 %, while this value was equal to 13.4% for the group of composite samples. At the end of the experiment (day 10), the PLA and composite samples were degraded up to a 17.6% and a 22.7%, respectively. As showed in Figure 1, a statically significant difference ($p<0.05$) in terms of weight loss was obtained when comparing each type of samples at the two time periods studied. The PLA and composite samples used as control (immersed in Tris-HCl buffer solution with sodium azide but without enzymes) showed no weight loss during the degradation test. According to these results, the degradation rate of both groups between days 5 and 10 was very similar, being 9.6% and 9.3% for the PLA and composite samples, respectively. Therefore, the greater weight loss obtained for the composite scaffolds can be attributed to an increased degradation rate for these samples during the first steps of the experiment.

SEM images of each group of scaffolds showed mesostructures with well-defined square shaped pores in an interconnected network, as presented in Figure 2. Unlike PLA samples, which showed a translucent appearance, scaffolds manufactured using composite filaments exhibited a whitish colour due to the presence of $CaCO_3$ and β-TCP particles. No relevant differences in relation to the surface morphology of the filaments printed by FDM were observed when comparing PLA and composite samples before enzymatic degradation (Figures 2a and 2d). Both groups of samples showed filaments with a smooth surface but a slightly variable diameter. From the figures of the samples after 5 and 10 days of degradation (Figure 2b, 2c for PLA scaffolds and Figures 2e and 2f for the composite ones), it is evident how the diameter of the filaments is significantly reduced during the experiment, which led to an increase in the pore size and the porosity of the samples. These figures suggest different degradation profiles for the PLA and the composite samples, since for the latter group the presence of a large number of holes over the surface of the filaments can be easily observed; these voids could be attributed to the release of the additive particles during the degradation of the structure. This could be a reason for the higher rate of degradation observed in the composite scaffolds after 5 and 10 days. In the case of the PLA samples, some fractures on the surface of the filaments were found, from which the degradation of the structures progresses. We expect that the release of the additives during the degradation of the structure will have a positive effect on maintaining the pH at an appropriate level for the surrounding tissue.

Results concerning variations in porosity and pore size of the samples are presented in Table 1. Composite scaffolds showed a statistically higher porosity ($p<0.05$) in comparison with the neat PLA scaffolds before the degradation test. This result could be related to the greater varia-

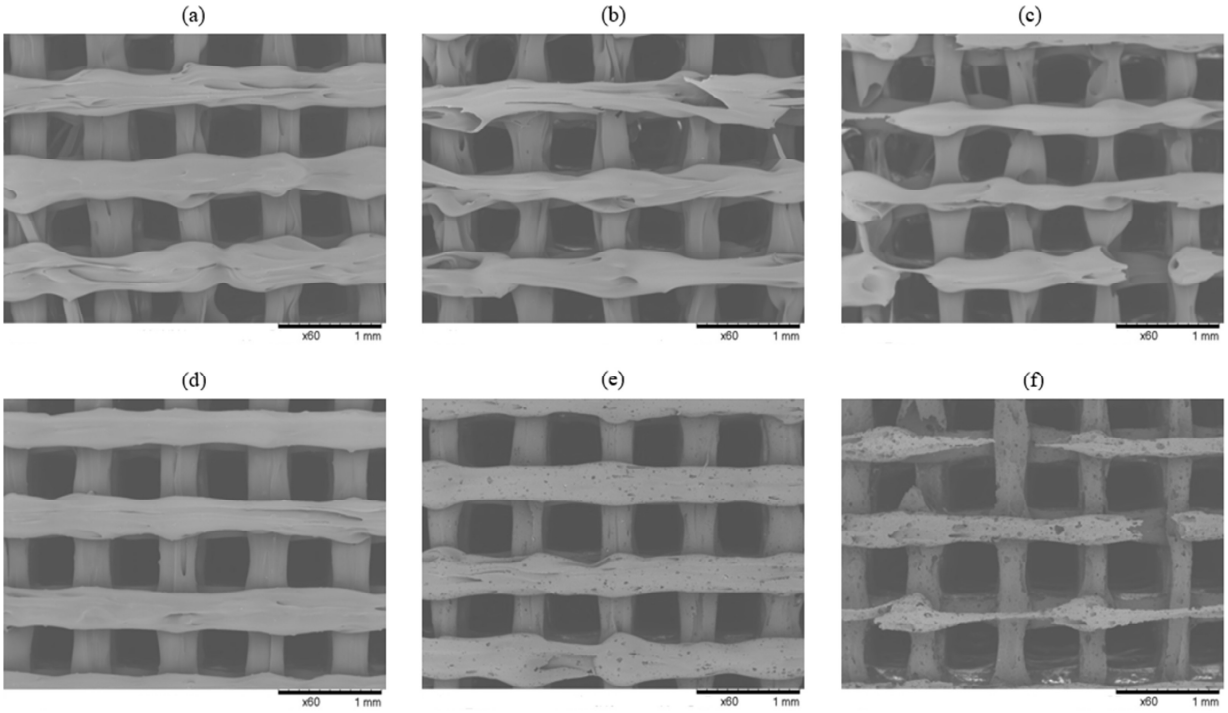

Figure 2: SEM images of the scaffolds analyzed: (a) PLA; (b) PLA 5D; (c) PLA 10D; (d) Composite; (e) Composite 5D; (f) Composite 10D. Scale bar: 1 mm.

Table 1: Porosity and pore size values of the 3D printed scaffolds before and after degradation.

Sample	Porosity (%)	Pore size (μm)
PLA	57±2	476±52
PLA 5D	57±4	531±51
PLA 10D	65±3	527±62
COMPOSITE	62±2	482±37
COMPOSITE 5D	67±4	476±58
COMPOSITE 10D	68±4	518±59

tion of the filaments diameter due to the presence of the additives. After 10 days of enzymatic degradation the mean porosity of the PLA samples was increased up to a 7.8%, while the composite scaffolds final porosity was a 6.3% higher. The difference in porosity values before and after the test for the PLA samples was statistically significant ($p<0.05$). The increase of the porosity is accompanied with the increase of the pore size of the scaffolds, as the filament's diameter is decreased by the enzymes action. The higher pore size of the composite scaffolds could explain their enhanced degradation rate during the early stages of the experiment [13]. The differences in terms of pore size before and after 10 days of degradation test were statistically significant ($p<0.05$) and very highly statistically significant ($p<0.001$) for PLA and composite samples, respectively.

The results obtained from the thermogravimetric and calorimetric analyses are shown in Table 2, in which T_{onset} represents the temperature for the start of the thermal degradation of the material and T_{peak} is the temperature of maximum degradation rate. The comparison between the results of PLA powder and 3D printed PLA samples showed a statistically significant difference ($p<0.05$) in terms of T_{onset}, but not regarding the degree of crystallinity of the samples. One important trend observed (non-statistically significant difference) is the increase of the crystallinity due to the introduction of the additives into the PLA matrix, as the $CaCO_3$ and β-TCP particles act as nucleation points [17].

On the other hand, after 10 days of enzymatic degradation PLA and composite samples showed, respectively, a statistically significant ($p<0.05$) and a highly statistically significant ($p<0.01$) decrease in terms of degree of crystallinity when compared to the non-degraded PLA and composite samples. A statistically significant ($p<0.05$) decrease was also obtained for the composite scaffolds after 10 days regarding the degradation and melting temperatures. The decrease of the samples' crystallinity was an unexpected result, as early enzymatic degradation preferentially occurs in the amorphous region of PLA [19], so

Table 2: Values determined from TGA and calorimetric analysis.

Sample	T_{onset} (˚C)	T_{peak} (˚C)	Melting temperature (˚C)	Enthalpy of fusion (J/g)	Xc (%)
PLA powder	350±1	370±1	174±2	52.3±0.9	55.9±1.0
PLA	353±1	369±1	175±3	53.6±1.8	57.2±1.9
PLA 5D	353±1	369±1	174±3	38.5±2.9	41.1±1.4
PLA 10D	350±2	369±2	174±3	37.4±1.3	40.0±1.4
COMPOSITE	353±1	370±1	177±3	58.4±2.0	59.3±2.0
COMPOSITE 5D	348±1	368±1	173±3	35.4±1.2	35.9±1.2
COMPOSITE 10D	349±1	367±2	171±2	28.6±4.0	29.0±1.0

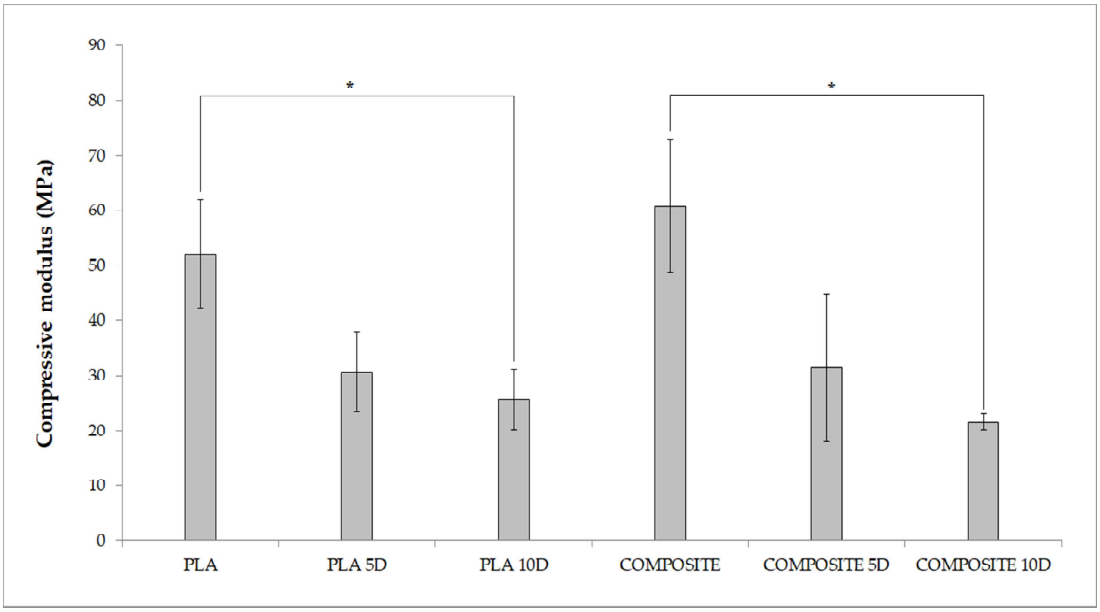

Figure 3: Mechanical properties of the 3D printed scaffolds under compression testing (*p<0.05).

the crystallinity percentage should have increased during the experiment. However, according to the literature [4], when the molecular weight of the PLA samples under enzymatic degradation decreased down to a value around 30,000 g/mol, the hydrolytic degradation of crystalline regions of the material could be also enhanced. This can be a reason for the significant reduction of the crystallinity in both groups of samples, although further research is required to clarify this extent.

Regarding the mechanical characterization, the values of the compressive modulus for non-degraded samples were 52±10 MPa for the PLA scaffolds and 61±12 MPa for composite ones (Figure 3). After 5 days of degradation, these values were decreased down to 31±7 MPa and 31±13 MPa, respectively. At the end of the experiment, the compression modulus was 26±5 MPa for PLA scaffolds and 22±1 MPa for the composite samples, both results being statistically significantly lower ($p<0.05$) than the initial values for each type of sample.

4 Conclusions

The higher rate of degradation observed in the composite scaffolds after 5 and 10 days could be explained by the release of the additive particles and the statistically higher microporosity of composite scaffolds compared to the neat PLA samples, which could enhance the degradation rate at the early steps of the test. Regarding the compression test, a statistically significant decrease of the elastic modulus after 10 days of enzymatic degradation was confirmed for both PLA and composite scaffolds, with results still in the range of values reported for cancellous bone (20–500 MPa) [20].

The combination of the PLA matrix with the proposed additives increases the degradation rate of the 3D printed scaffolds, which is an advantage for the application of the composite scaffold in the field of tissue engineering, taking into account the large amount of time necessary for the degradation of PLA structures. The ratio of use of these additives could be adjusted to the degradation rate required to match the growth rate of new bone tissue.

Acknowledgement: This contribution is part of the project BioAM (DPI2017-88465-R) funded by the Science, Innovation and Universities Spanish Ministry. Also, Ricardo Donate express his gratitude for the funding through the PhD grant program co-financed by the Canarian Agency for Research, Innovation and Information Society of the Canary Islands Regional Council for Employment, Industry, Commerce and Knowledge and by the European Social Fund (ESF) Canary Islands Integrated Operational Program 2014-2020, Axis 3 Priority Theme 74 (85%). Grant code: TESIS2017010036.

References

[1] Narayanan, G., V. N. Vernekar, E. L. Kuyinu, and C. T. Laurencin. Poly (lactic acid)-based biomaterials for orthopaedic regenerative engineering. *Advanced Drug Delivery Reviews*, Vol. 107, 2016, pp. 247–276.

[2] Abert, J., A. Amella, S. Weigelt, and H. Fischer. Degradation and swelling issues of poly-(d,l-lactide)/β-tricalcium phosphate/calcium carbonate composites for bone replacement. *Journal of the Mechanical Behavior of Biomedical Materials*, Vol. 54, 2016, pp. 82–92.

[3] Saha, S. K., and H. Tsuji. Effects of molecular weight and small amounts of d-lactide units on hydrolytic degradation of poly(l-lactic acid)s. *Polymer Degradation & Stability*, Vol. 91, No. 8, 2006, pp. 1665–1673.

[4] Mainil-Varlet, P., R. Curtis, and S. Gogolewski. Effect of in vivo and in vitro degradation on molecular and mechanical properties of various low-molecular-weight polylactides. *Journal of Biomedical Materials Research*, Vol. 36, No. 3, 1997, pp. 360–380.

[5] Laurence, J., P. M. Baptista, A. Atala, and M. Van Beusekom. *Translating Regenerative Medicine to the Clinic*. Elsevier Inc., 2015. https://doi.org/10.1016/C2013-0-15405-0.

[6] Schiller, C., and M. Epple. Carbonated calcium phosphates are suitable pH-stabilising fillers for biodegradable polyesters. *Biomaterials*, Vol. 24, No. 12, 2003, pp. 2037–2043.

[7] Zhang, Y. S., K. Yue, J. Aleman, K. M. Moghaddam, S. M. Bakht, J. Yang, W. Jia, V. Dell'Erba, P. Assawes, S. R. Shin, M. R. Dokmeci, R. Oklu, and A. Khademhosseini. 3D Bioprinting for Tissue and Organ Fabrication. *Annals of Biomedical Engineering*, Vol. 45, No. 1, 2017, pp. 148–163.

[8] de Tayrac, R., S. Chentouf, H. Garreau, C. Braud, I. Guiraud, P. Boudeville, and M. Vert. In vitro degradation and in vivo biocompatibility of poly(lactic acid) mesh for soft tissue reinforcement in vaginal surgery. *Journal of Biomedical Materials Research. Part B, Applied Biomaterials*, Vol. 85, No. 2, 2008, pp. 529–536.

[9] Yuan, X., A. F. T. Mak, and K. Yao. Comparative observation of accelerated degradation of poly(L-lactic acid) fibres in phosphate buffered saline and a dilute alkaline solution. *Polymer Degradation & Stability*, Vol. 75, No. 1, 2002, pp. 45–53.

[10] Zeng, J., X. Chen, Q. Liang, X. Xu, and X. Jing. Enzymatic degradation of poly(L-lactide) and poly(epsilon-caprolactone) electrospun fibers. *Macromolecular Bioscience*, Vol. 4, No. 12, 2004, pp. 1118–1125.

[11] Tsuji, H., and H. Muramatsu. Blends of aliphatic polyesters: V. Non-enzymatic and enzymatic hydrolysis of blends from hydrophobic poly(L-lactide) and hydrophilic poly(vinyl alcohol). *Polymer Degradation & Stability*, Vol. 71, No. 3, 2001, pp. 403–413.

[12] Liu, L., S. Li, H. Garreau, and M. Vert. Selective enzymatic degradations of poly(L-lactide) and poly(epsilon-caprolactone) blend films. *Biomacromolecules*, Vol. 1, No. 3, 2000, pp. 350–359.

[13] Sheng, S. J., X. Hu, F. Wang, Q. Y. Ma, and M. F. Gu. Mechanical and thermal property characterization of poly-l-lactide (PLLA) scaffold developed using pressure-controllable green foaming technology. *Materials Science and Engineering C*, Vol. 49, 2015, pp. 612–622.

[14] Domingos, M., F. Intranuovo, A. Gloria, R. Gristina, L. Ambrosio, P. J. Bártolo, and P. Favia. Improved osteoblast cell affinity on plasma-modified 3-D extruded PCL scaffolds. *Acta Biomaterialia*, Vol. 9, No. 4, 2013, pp. 5997–6005.

[15] Yang, G. H., M. Kim, and G. Kim. Additive-manufactured polycaprolactone scaffold consisting of innovatively designed microsized spiral struts for hard tissue regeneration. *Biofabrication*, Vol. 9, No. 1, 2016, id. 015005.

[16] Esposito Corcione, C., F. Gervaso, F. Scalera, F. Montagna, A. Sannino, and A. Maffezzoli. The feasibility of printing polylactic acid–nanohydroxyapatite composites using a low-cost fused deposition modeling 3D printer. *Journal of Applied Polymer Science*, Vol. 134, No. 13, 2017. https://doi.org/10.1002/app.44656.

[17] Garlotta, D. A literature review of poly(lactic acid). *Journal of Polymers and the Environment*, Vol. 9, No. 2, 2001, pp. 63–84.

[18] Alemán-Domínguez, M. E., E. Giusto, Z. Ortega, M. Tamaddon, A. N. Benítez, and C. Liu. Three-dimensional printed polycaprolactone-microcrystalline cellulose scaffolds. *Journal of Biomedical Materials Research. Part B, Applied Biomaterials*, Vol. 107, No. 3, 2019, pp. 521–528.

[19] Reeve, M. S., S. P. McCarthy, M. J. Downey, and R. A. Gross. Polylactide Stereochemistry: Effect on Enzymic Degradability. *Macromolecules*, Vol. 27, No. 3, 1994, pp. 825–831.

[20] Leong, K. F., C. K. Chua, N. Sudarmadji, and W. Y. Yeong. Engineering functionally graded tissue engineering scaffolds. *Journal of the Mechanical Behavior of Biomedical Materials*, Vol. 1, No. 2, 2008, pp. 140–152.

Evaluation of Aloe Vera Coated Polylactic Acid Scaffolds for Bone Tissue Engineering

applied sciences

MDPI

Article

Evaluation of Aloe Vera Coated Polylactic Acid Scaffolds for Bone Tissue Engineering

Ricardo Donate [1,*], María Elena Alemán-Domínguez [1], Mario Monzón [1], Jianshu Yu [2,3], Francisco Rodríguez-Esparragón [4] and Chaozong Liu [2]

1 Departamento de Ingeniería Mecánica, Grupo de Investigación en Fabricación Integrada y Avanzada, Universidad de Las Palmas de Gran Canaria, Campus Universitario de Tafira s/n, 35017 Las Palmas, Spain
2 Institute of Orthopaedic & Musculoskeletal Science, University College London, Royal National Orthopaedic Hospital, Stanmore HA4 4LP, London, UK
3 School of Materials Science and Engineering, Shanghai University, Shanghai 200444, China
4 Unidad de Investigación, Hospital Universitario de Gran Canaria Doctor Negrín, Barranco de la Ballena s/n, 35010 Las Palmas, Spain
* Correspondence: ricardo.donate@ulpgc.es

Received: 17 February 2020; Accepted: 7 April 2020; Published: 9 April 2020

Abstract: 3D-printed polylactic acid (PLA) scaffolds have been demonstrated as being a promising tool for the development of tissue-engineered replacements of bone. However, this material lacks a suitable surface chemistry to efficiently interact with extracellular proteins and, consequently, to integrate into the surrounding tissue when implanted in vivo. In this study, aloe vera coatings have been proposed as a strategy to improve the bioaffinity of this type of structures. Aloe vera coatings were applied at three different values of pH (3, 4 and 5), after treating the surface of the PLA scaffolds with oxygen plasma. The surface modification of the material has been assessed through X-ray photoelectron spectroscopy (XPS) analysis and water contact angle measurements. In addition, the evaluation of the enzymatic degradation of the structures showed that the pH of the aloe vera extracts used as coating influences the degradation rate of the PLA-based scaffolds. Finally, the cell metabolic activity of an in vitro culture of human fetal osteoblastic cells on the samples revealed an improvement of this parameter on aloe vera coated samples, especially for those treated at pH 3. Hence, these structures showed potential for being applied for bone tissue regeneration.

Keywords: regenerative medicine; additive manufacturing; plasma treatment; coating method; aloe vera extracts; osteoblast cells

1. Introduction

Polylactic acid (PLA)-based scaffolds have been extensively used for bone regeneration [1–6], as they have a suitable degradation rate and mechanical properties to replace the tissue in non-load-bearing applications. However, PLA is a hydrophobic material and, as a consequence, its interaction with the extracellular matrix (ECM) is low [7]. As the adsorption of adhesion-signaling proteins from the ECM is a key step to promote a good osseointegration of the scaffolds [8], the limited affinity of this biomaterial to these substances in the ECM is one of the main drawbacks of PLA-based structures.

Different strategies have been proposed to overcome this limitation and increase the number of applications of PLA-based structures in the field of tissue engineering. An important approach comprises the incorporation of additives, including bioceramics [9], graphene oxide [10] and natural-derived polymers [11]. Another strategy is the surface modification of the scaffold [12] by changing the roughness, wettability and/or surface chemistry of the structures [8]. The processes to change the properties of the surface can be classified into two groups: the functionalization of PLA or

the coating of the structure with a bioactive compound able to interact effectively with the proteins in the ECM. In the first group of techniques, it is possible to mention the plasma [13,14] or alkaline treatment [15] of the parts. These surface treatments can be used to provide anchoring points to link bioactive compounds to the surface of PLA-based scaffolds. Different substances have been proposed with this aim, including chitosan [16], alginate [17], collagen [7,12,18] or calcium phosphates [19].

In this work, the authors have tested the effect of applying an innovative coating based on extracts of aloe vera to 3D-printed PLA-based scaffolds. Aloe vera is a plant from the Liliaceal family with demonstrated healing properties [20]. In the tissue engineering field, it has been tested mainly for skin regeneration [21,22]. However, the use of this natural substance in bone tissue engineering remains limited [23] to the best of our knowledge and no references have been found regarding its use to improve the affinity of PLA and promote the attachment and proliferation of osteoblastic cells.

According to the state of the art on the chemical characterization of aloe vera extracts [24,25], acemannan is the main bioactive compound in the gel of the leaves. It is a mannose-containing polysaccharide that has demonstrated the promotion of collagen synthesis during wound healing [21,26]. This characteristic could have positive implications for enhancing the osseointegration process in aloe vera coated scaffolds. Besides, there is currently a high availability of this product at affordable prices, which makes it a viable strategy from the economic point of view compared with other options, such as the use of growth factors [27]. For these reasons, this strategy has been proposed in this work as a promising approach to improve the performance of 3D-printed PLA scaffolds in vitro. Plasma treatment was used as a first step to functionalize the surface of the materials and promote aloe vera adhesion.

2. Materials and Methods

2.1. Materials

PLA L105 (melt flow index of 65 g/10 min, molecular weight of approximately 105,000 g·mol^{-1}) was purchased from Corbion Purac (Diemen, The Netherlands) in powder form. Aloe vera juice was purchased from aloe vera Costa Canaria (Spain). The quality protocols from the company indicated that the content in aloin is below 0.0007% w/w (analysis by high performance liquid chromatography). Sodium hydroxide (NaOH) in pellets form was purchased from Honeycomb (30620, Fluka^{TM}), while hydrochloric acid (HCl) was purchased from Merck (1090571000, Supelco).

2.2. Scaffolds Manufacturing

Firstly, continuous PLA filaments were obtained using a lab prototype extruder consisting of an 8 mm screw, a cylinder with an L/D ratio of 10 and a 1.6 mm diameter nozzle tip. The extrusion was carried out at a rotating speed of 7 rpm, at a temperature of 180 °C and with a final air-cooling stage. These filaments were used to print the scaffolds by using a BQ Hephestos 2 3D printer (Spain). This additive manufacturing technique is based on the extrusion of heated material, so it can be classified as a "material extrusion" process (ISO/ASTM 52900:2015), commonly known as fused deposition modelling (FDM). Structures with a rectangular 0/90° pattern, square-shaped pores and a theoretical porosity of 50%, were manufactured. The printing settings included a nozzle diameter of 0.4 mm, a layer height of 0.3 mm, a speed of extrusion of 40 mm·s^{-1} and a printing temperature of 215 °C.

In order to better characterize the PLA surface after applying the plasma treatment or the different coatings proposed, flat-surface samples with dimensions of 80 × 10 × 1 mm were also manufactured by compression molding, using a Collin P 200 P/M press and a cycle comprising of the following steps: heating up to 190 °C at a heating rate of 20 °C·min^{-1}; maintaining the temperature at that constant value for 90 s at 10 bar of pressure; and finally cooling at a rate of 20 °C·min^{-1} while maintaining the pressure applied in the second step.

2.3. Surface Treatment and Coating Process

The plasma treatment was carried out in a low-pressure device (Zepto Diener electronic GmbH, Ebhause, Germany) using oxygen as a carrier gas (Carburos metálicos, Spain). The oxygen supply contains less than 500 ppb of H_20 and less than 400 ppb of N_2. The oxygen pressure inside the chamber was fixed at 1.8 mbar. The treatment was applied at a power of 30 W for 1 minute.

The commercial aloe vera juice was centrifuged at 3000 rpm for 15 min in a Mixtasel BL centrifuge (JP Selecta), in order to separate the water-soluble fraction (rich in acetylated polysaccharides) from the cellulose-rich solid fraction. The water-soluble fraction (the supernatant) was used to carry out the coating of the structures and it contains, apart from the bioactive polysaccharides, phenolic compounds, soluble carbohydrates, proteins and minerals [24,28]. The supernatant has a pH value of around 4 (measured with a sensION^{TM}+PH1 pHmeter ±0.01, HACH). The slightly acid behavior of the extracts can be explained by the presence of different organic acids (acetic acid, lactic acid, succinic acid, etc.) [29] Three types of samples of aloe vera extracts were obtained through pH adjustment: a pH 3 solution (adjusted with HCl 0.018 M); a pH 5 solution (adjusted with NaOH 0.5 M); and the as-obtained gel with a pH of 4 (pH was adjusted when needed).

Each scaffold to be tested was individually immersed in 1 mL of aloe vera extract solution and stirred for 3 h, allowing the interaction between the functional groups created on the surface of the plasma-treated scaffolds and the functional groups in the polysaccharides' structures to take place. Afterwards, the samples were rinsed with 70% ethanol to remove the excess of aloe vera which was not able to attach to the surface. Furthermore, as polysaccharides are not soluble in ethanol [30], their precipitation helps to fix the coating to the surface of the 3D-printed PLA scaffolds.

2.4. Water Contact Angle (WCA)

In order to analyze the effect of the coating on the hydrophilicity of the surface, the WCA was measured through the sessile drop method. For this technique, as it is recommended to use flat-surface samples [31], the samples obtained by compression molding described in Section 2.2 were used. The different group of samples tested were PLA, PLA plasma, PLA aloe vera pH 3, PLA aloe vera pH 4 and PLA aloe vera pH 5. The WCA measurements were carried out at room temperature using a Krüss DSA100 water contact angle measuring device (KRÜSS GmbH, Germany) and the open source software ImageJ was used to measure the static contact angle of 2 µL distilled water droplets placed onto the surface of the samples. Reported contact angles are the average of six measurements per group of samples.

2.5. X-ray Photoelectron Spectroscopy (XPS) Analysis

The assessment of the chemical modifications induced into the PLA surface was carried out by the XPS analysis of non-treated, plasma-treated and coated samples, using a Thermo Scientific K-Alpha XPS system (Thermo Fisher Scientific, UK) and the CasaXPS software (version 2.3.19PR1.0, Casa Software Ltd., Teignmouth, UK) for data analysis. Flat-surface samples obtained by compression molding (as detailed in Section 2.2.) were used for this test and three samples per group were analyzed. The oxygen/carbon (O/C) ratio of the surface was evaluated from the peak areas of the XPS survey using a U2 Tougaard background for peak fitting. In a first step, the hydrocarbon component of the C1s spectrum (284.80 eV) was used to calibrate the energy scale.

2.6. Mechanical Characterization

Plasma treatment is the most common technique to modify the surface chemistry of different biomaterials, since it does not alter their bulk properties [14]. However, this golden standard depends on the operating conditions that are used. Two mechanisms have been reported about the chemical reactions during the plasma treatment of polylactic acid: an oxidative one and a destructive one [32]. The interaction of oxygen and free radicals could lead to the formation of hydroxyl and peroxide groups,

while the mechanism of destruction of plasma-treated PLA generates free radicals, accompanied with the formation of volatile gases. If the treatment is too aggressive, the chemical reaction may take place preferentially through the destruction mechanism rather than the oxidation one and, as a consequence, the mechanical properties of the structure could be affected. Therefore, it is recommended to confirm the lack of modification on the mechanical properties of the structure after plasma treatment. For this reason, non-treated and plasma-treated samples were subjected to mechanical characterization in the compression mode. In addition, aloe vera coated scaffolds after plasma treatment were tested to assess the effect of the different coatings (pH 3, 4 and 5) on the mechanical properties of the structures. Four replicas per group were used. Scaffolds with a diameter of 9.8 mm and a height of 5 mm were tested in a LIYI (LI-1065, Dongguan Liyi Environmental Technology Co., Ltd., China) testing machine in displacement control mode. Crosshead speed was set at 1 mm·min^{-1}. The compressive modulus and the offset compressive yield strength (2% deviation from linearity) were calculated according to ASTM D695-15.

2.7. Degradation Analysis

In order to confirm if the presence of the aloe vera coating increases the degradation rate of the base material, an enzymatic degradation test was carried out. The enzymatic degradation test was preferred over a more common hydrolytic degradation study in PBS, since the first one offers the possibility of accelerating the test while obtaining comparative results. The enzymatic degradation test was carried out using *proteinase K* enzymes from *Tritirachium album* (30 units per mg of protein, Merck) diluted in Tris-HCl buffer pH 8.6 (BioReagent, Merck), at a concentration of 0.2 mg·mL^{-1}. Sodium azide (ReagentPlus® , ≥99.5%, Merck) was added at the same concentration, in order to diminish the probability of bacterial contamination. Several examples can be found in the literature about the use of this type of enzymes to accelerate the degradation study of PLA samples from several months to a few days or even hours [33–36]. Under enzymatic degradation and according to the literature, PLA structures are able to retain their properties almost unchanged for up to 8 months [37].

Scaffolds with a diameter of 9.8 mm and a height of 7 mm were used for the enzymatic degradation test. Four replicas were analyzed per group: PLA, PLA plasma, PLA aloe vera pH 3, PLA aloe vera pH 4 and PLA aloe vera pH 5. The samples were placed in a non-treated 24-well plate and 2 mL of degradation media were added to each well. In addition, non-treated PLA samples immersed in Tris–HCl solution without enzymes were used as control samples. The buffer-enzyme solution was replaced daily to maintain a high enzymatic activity, as the reduction of the pH value due to the release of lactic acid would cause the denaturation of the enzyme [37]. The weight loss of the structures after 5 days of degradation at 37 °C was assessed by using an analytical balance (±0.1 mg, A&D Scales Gemini Series, GR-200, Germany), to measure the weight of the scaffolds before and after the test. In addition, the pH value of the media was measured (±0.01) in order to follow up the evolution of this parameter during the enzymatic degradation process. The morphology of the scaffolds' surface before and after degradation was evaluated by scanning electron microscopy (SEM; Hitachi TM 3030 at an acceleration voltage of 15 kV).

2.8. Cell Seeding and Culture

A human fetal osteoblastic cell line (hFOB 1.19, from ATCC® CRL-11372TM) was used to analyze the influence of the surface modifications proposed on the bioactivity of the scaffold's surface. The cell culture medium used was a mixture 1:1 of DMEM and Ham's F-12 without fenol red (Dulbecco's Modified Eagle Medium/Nutrient Mixture F-12, high glucose, L-glutamine, Gibco), supplemented with 10% of FBS (Gibco) and 0.3 mg·mL^{-1} of G-148 antibiotic solution (Geneticin, Biowest). The cells were cultured in 75 cm^2 flasks (T75, Sarstedt) until reaching an 80–90% confluence. At this level, they were trypsinized with trypsin-EDTA 0.5% (no phenol red, HyClone).

The scaffolds to be seeded were 9.8 mm in diameter and 5 mm in height. Four replicas were used per group of samples: PLA plasma, PLA aloe vera pH 3, PLA aloe vera pH 4 and PLA aloe vera pH 5.

The scaffolds were sterilized by soaking them in ethanol 75% v/v followed by later exposure to UV light under the fume hood for 30 min. Afterwards, they were washed three times with PBS (59321C Dulbecco's Phosphate Buffered Saline, Merck) and with the culture medium in order to remove any trace of ethanol. Then, for cell seeding, the scaffolds were placed individually in sterilized centrifuge tubes (CFT011150, 15 mL sterile tubes, Jet Biofil) and immersed in 2 mL of culture media containing 110,000 hFOB cells. The constructs were kept in an incubator at 37 °C and 5% CO_2 for 3 h before adding 2 mL of fresh culture medium to the tubes, in order to provide enough nutrients for cell culture during the first 24 h.

2.9. Cell Metabolic Activity Evaluation

Cell metabolic activity was evaluated through the CCK-8 protocol (Cell Counting Kit-8, Dojindo Molecular Technologies). At day 1 of cell culture, the samples were transferred from the tubes to a non-treated 24-well plate (Thermo Scientific™ Nunc™), where they were kept until the end of the experiment. The scaffolds were washed with 1 mL of PBS and afterwards 1 mL of a solution of the CCK-8 reagent in supplemented media was added (10% v/v). The same procedure was followed with 4 empty wells, so the data from these replicas could be used as negative controls. The plate was incubated at 37 °C and 5% CO_2 for 4 h. After incubation, two 100 µL-aliquots were transferred from each well of the culture plate to a 96-well reader plate (Thermo Scientific™ Nunc™ MicroWell™). The absorbance of the samples was read at an excitation wavelength of 450 nm with a BioTek ELx800 reader (Bio Tek Instruments Inc., Winooski, VT, USA). After sampling, the solution containing the CCK-8 was removed from the culture, the samples were rinsed with PBS three times and 2 mL of fresh supplement media was added, before placing the plate into the incubator again. This procedure was repeated at days 3, 7 and 10 of cell culture, while the culture medium was changed every 2–3 days.

2.10. Statistical Analysis

Statistical analysis was performed using MATLAB software (MATLAB and Statistics Toolbox Release 2017a, The MathWorks, Inc., Natick, USA). The data obtained during this study were analyzed by the Wilcoxon two-sided rank sum test when comparing two groups and by the Kruskal–Wallis test when more than two groups were compared. The significance level was set to * $p < 0.05$, ** $p < 0.01$ and *** $p < 0.001$, for statistically significant, highly statistically significant and very highly statistically significant differences, respectively. All the figures show the mean values of each group, and their standard deviations are represented with error bars.

3. Results

3.1. Water Contact Angle (WCA) Measurement

A water contact angle of 79 ± 4° was obtained for the PLA samples, while the treated and coated samples showed a value around 50° (Figure 1). As expected, the plasma treatment of PLA surfaces decreases their WCA significantly ($p < 0.01$) compared to the non-treated samples. The aloe vera coating of the samples at pH 4 and 5 does not reduce this effect, as these groups provide similar results to the ones obtained for the samples that were only plasma-treated. However, a very highly statistically significant difference ($p < 0.001$) was obtained for the PLA samples coated with aloe vera at pH 3, when compared to the non-treated samples.

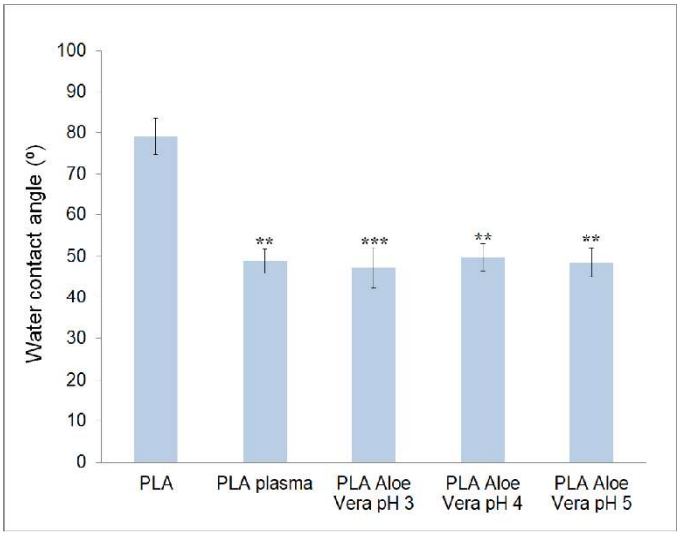

Figure 1. Water contact angle values for the non-treated, plasma-treated and coated samples obtained by compression molding (** $p < 0.01$ and *** $p < 0.001$), compared to the group of non-treated polylactic acid (PLA) samples.

3.2. X-ray Photoelectron Spectroscopy (XPS) Analysis

The oxygen and carbon composition (%), as well as the O/C ratio of each group of samples, are shown in Table 1. Non-significant differences were obtained between the non-treated and plasma-treated samples. On the other hand, the aloe vera coating of the plasma-treated samples promoted the reduction of the O/C ratio. Highly statistically significant ($p < 0.01$) and statistically significant ($p < 0.05$) differences were obtained between the plasma-treated samples and the ones coated with aloe vera at pH 3 and 4, respectively. In contrast, a non-significant difference ($p > 0.05$) was obtained between the PLA group and the group coated with aloe vera at pH 5. Therefore, in the case of the coated samples, the reduction of the O/C ratio could be an indicator of the attachment efficiency of the aloe vera extracts to the plasma-treated surface.

Table 1. XPS results, including the oxygen and carbon content of the surface and the O/C ratio of the non-treated, plasma-treated and coated samples analyzed.

Group of Scaffolds	O %	C %	O/C
PLA	33.89 ± 1.87	66.11 ± 1.87	0.51 ± 0.04
PLA plasma	35.44 ± 1.05	61.89 ± 2.53	0.57 ± 0.03
PLA aloe vera pH 3	17.13 ± 1.99	82.14 ± 1.40	0.21 ± 0.03
PLA aloe vera pH 4	28.83 ± 0.79	70.60 ± 1.78	0.41 ± 0.02
PLA aloe vera pH 5	34.09 ± 1.30	65.91 ± 1.30	0.52 ± 0.03

3.3. Mechanical Characterization

Prior to the compression test, the scaffolds' morphology was assessed in terms of porosity and pore size by the methods described in our previous work [38]. Non-significant differences were obtained between the non-treated, plasma-treated and aloe vera coated samples in regard to these parameters. The average pore size and porosity of all groups of samples were 480 ± 66 μm and 61 ± 5%, respectively. As shown in Figure 2, no significant differences were obtained in terms of compressive modulus or compressive yield strength between the different groups of scaffolds tested. Regarding the compressive modulus, the values obtained were 31.60 ± 7.97 MPa for non-treated scaffolds and 28.52 ± 3.53 MPa for the plasma-treated ones. The compressive modulus of aloe vera coated samples

at pH 3, 4 and 5 were 29.79 ± 10.36 MPa, 25.07 ± 8.04 MPa and 36.11 ± 11.16 MPa, respectively. These values are in the range of values reported for cancellous bone (20–500 MPa) [39].

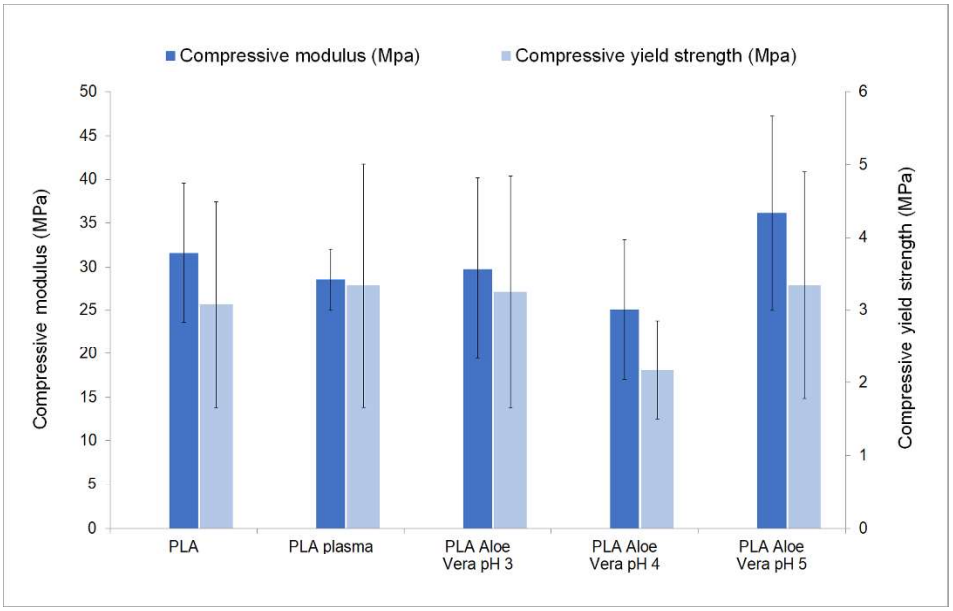

Figure 2. Mechanical properties of non-treated, plasma-treated and aloe vera-coated PLA 3D-printed scaffolds under compression testing.

3.4. Degradation Study

The mean weight loss of each group of samples after five days of enzymatic degradation is shown in Table 2. Non-significant differences ($p > 0.05$) were obtained among the groups tested, resulting in a total mean value of around 5.5%. The weight of the PLA scaffolds used as control (immersed in Tris-HCl buffer solution with sodium azide but without enzymes) showed no variation during the degradation test.

Table 2. Average weight loss (%) of the scaffolds after five-day enzymatic degradation.

Group of Scaffolds	Weight Loss %
PLA	5.62 ± 0.37
PLA plasma	5.37 ± 0.85
PLA aloe vera pH 3	4.81 ± 0.79
PLA aloe vera pH 4	6.01 ± 0.90
PLA aloe vera pH 5	5.85 ± 0.75

Regarding the pH of the degradation media during the experiment, its value decreased remarkably from day 2 for all the group of scaffolds tested (Figure 3). This reduction was less drastic for the plasma-treated samples and for the samples coated with aloe vera at pH 3, which maintained a pH value greater than 6 at day 3. However, at days 4 and 5, similar results were obtained for all the groups of samples tested. While the coating at pH 3 seems to influence the maintenance of the pH at a higher level, the samples coated with aloe vera at pH 4 or 5 showed a degradation profile that nearly matched the one of the non-treated PLA scaffolds.

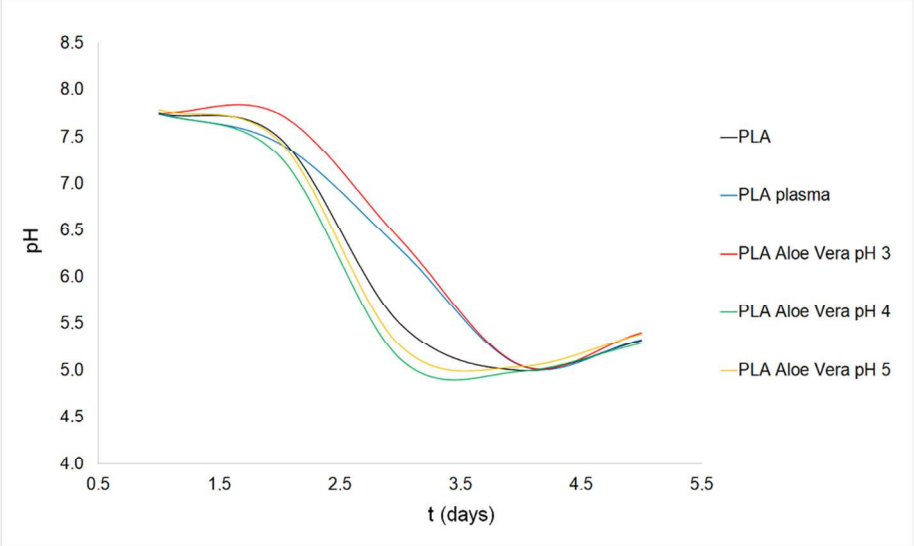

Figure 3. Variation of the pH level of the degradation medium during the enzymatic degradation study of the 3D-printed scaffolds.

In Figure 4, SEM images obtained for each type of scaffold tested are shown, including non-degraded PLA samples for comparison (Figure 4a,g). A slight reduction of the diameter of the filaments is observed after 5 days of enzymatic degradation. There is also an evident increment of the microporosity of the scaffolds' surface after the degradation test. This was an expected result, as while immersed in the buffer solution the hydrolytic degradation of PLA takes place via a bulk erosion mechanism; in the presence of the *proteinase K* enzymes the degradation of the structure is enhanced via a surface-erosion mechanism [40]. The evaluation of the high magnification SEM images (Figure 4g–l) suggests that the enzymatic degradation of the PLA samples followed a different mechanism than the plasma-treated or coated samples, as for the latter, the presence of newly formed voids over the surface can be observed (especially in Figure 4l), which correspond to the scaffolds coated with aloe vera at pH 5). In contrast, the non-treated PLA scaffolds surface showed some small fractures, from which the degradation of the structure progresses.

3.5. Cell Metabolic Activity Evaluation

The values of absorbance obtained from the CCK-8 assay are shown in Figure 5. All the groups of coated samples showed higher values of absorbance from day 3 until the end of the experiment (day 10). It is remarkable that for the plasma-treated samples and the coated samples at pH 4 and 5 there was a decrease between day 1 and day 3. One possible explanation for this result may be that some of the seeded cells were able to attach and survive until day 1, but the attachment was not steady enough to live until day 3 or to proliferate. Only the group coated at pH 3 was able to support the growth of cells from day 1 to day 3. Furthermore, this group offered the best results for the overall experiment, as it provides a very highly statically significant difference ($p < 0.001$) compared to the plasma-treated group of samples.

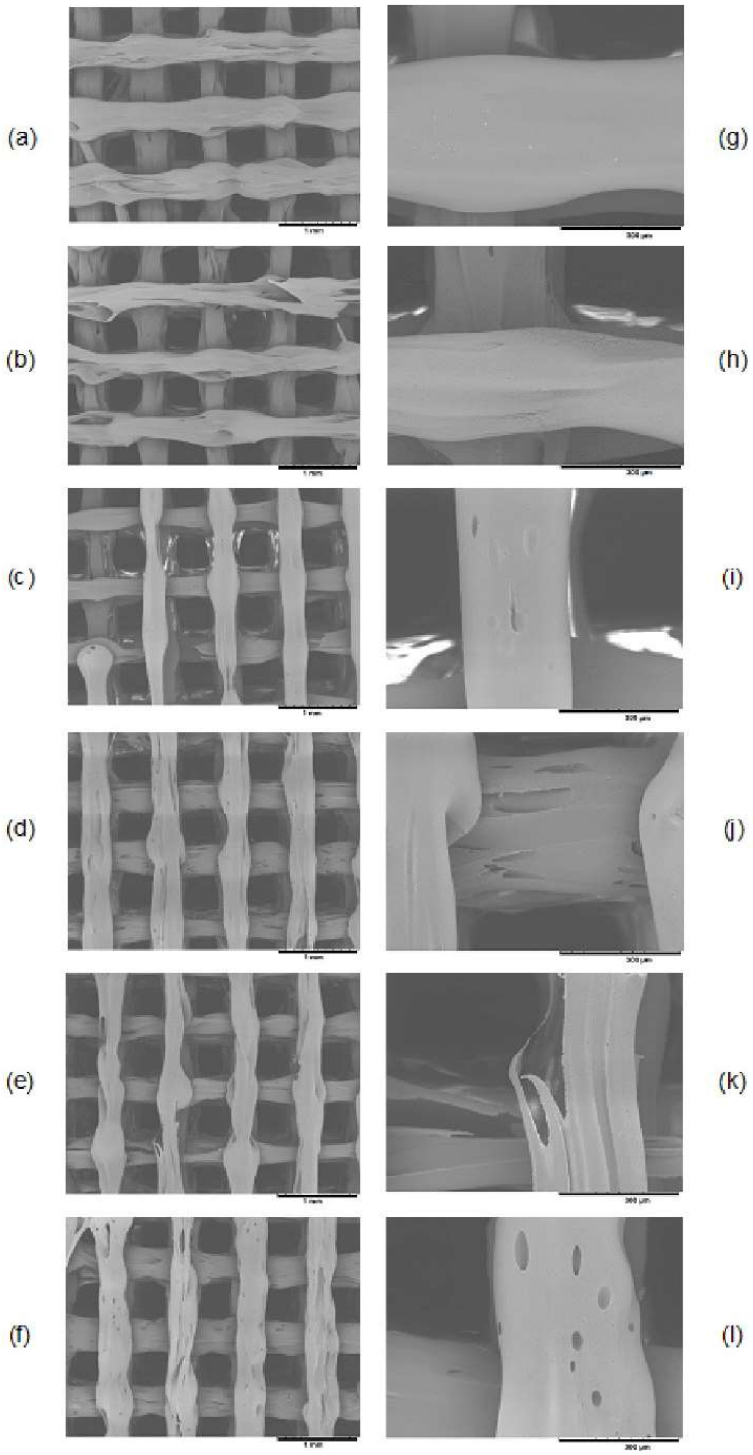

Figure 4. SEM images (scale bar: 1 mm) of the 3D-printed PLA scaffolds analyzed: (**a**) non-degraded PLA; (**b**) PLA; (**c**) PLA plasma; (**d**) PLA aloe vera pH 3; (**e**) PLA aloe vera pH 4 and (**f**) PLA aloe vera pH 5. Additionally, SEM images with higher magnification (scale bar: 300 μm) are shown for (**g**) non-degraded PLA; (**h**) PLA; (**i**) PLA plasma; (**j**) PLA aloe vera pH 3; (**k**) PLA aloe vera pH 4 and (**l**) PLA aloe vera pH 5.

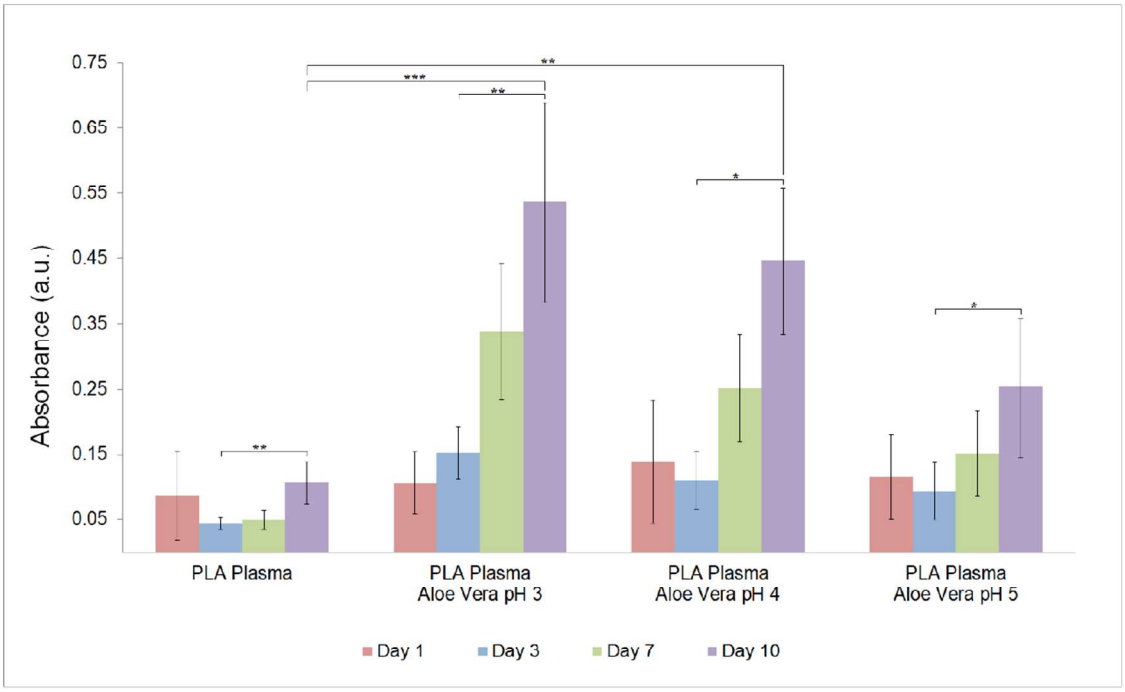

Figure 5. Metabolic activity of human fetal osteoblastic cell line (hFOB) cells on the plasma-treated and coated scaffolds determined by the CCK-8 assay (* $p < 0.05$, ** $p < 0.01$ and *** $p < 0.001$).

4. Discussion

The aloe vera coating method proposed introduces several changes in the physicochemical properties of the PLA surface and influences its biological activity. The increase of the hydrophilicity of plasma-treated PLA scaffolds enhance the affinity of the surface to support the aloe vera coating in an effective way. The functional groups created during plasma treatment of PLA are mainly hydroxyl and carbonyl ones [13,41]. These groups are not reactive with the functional groups in the structure of the polysaccharides in aloe vera extracts (mainly hydroxyl and acetyl) [42]. Nevertheless, they provide an increase in the polarity of the surface which is more favorable for attaching the extract by intermolecular forces.

The similarity of the WCA results between coated and non-coated groups indicates that the hydrophilicity increases similarly (compared to untreated PLA samples) whether the surface modification consisted only in the application of the plasma treatment or if it is followed by the aloe vera coating. Therefore, any change in the biological properties of the scaffolds needs to be explained by the change in the chemical composition of the surfaces, not by their surface energy.

Regarding the surface chemistry, despite being a non-significant difference ($p > 0.05$), the modification in the O/C ratio of the PLA surface before and after the plasma treatment suggests the prevalence of the oxidation mechanism over the destructive one [32]. It is important to take into account that both mechanisms may take place simultaneously and the predominance of one of them depends on the treatment time, as demonstrated by Izdebska-Podsiadly et al. [43] The prevalence of the oxidation route during the plasma treatment in the present study is also supported by the results from the mechanical characterization, as a non-significant difference ($p > 0.05$) was detected when the plasma treated samples and the non-treated ones were compared (Figure 2). These results also evidenced that the aloe vera coating does not play a role on the mechanical properties of the final structure. The low thickness of the coating and the absence of etching compounds in the aloe vera extract justify this lack of modification on the mechanical properties of the scaffolds after the coating.

With respect to the coated samples, it is worth mentioning that there is a significant decrease of the O/C ratio ($p < 0.05$) for the samples coated at pH 3 and pH 4, but not for those coated at pH 5.

This trend could be related to the amount and type of bioactive compounds that are able to be fixed on the PLA surface. The O/C ratio expected from the coating depends on the mannose:glucose:galactose ratio of the polysaccharides in the extracts [25]. The composition of aloe vera extracts is complex and it depends on different parameters, such as the geographical location of the plants or the season when the leaves are harvested, as the carbohydrates have a storage biological function in the living plants [25], or the extraction and processing procedures used; so it is difficult to predict a clear expected trend of this parameter.

Regarding the enzymatic degradation of the scaffolds, the results confirm an influence of the coating on the degradation rate of the material. As the adsorption of the enzymes to the surface is the first step of any enzymatic degradation process, the modifications introduced on the surface chemistry can potentially modify the enzymatic degradation mechanism of PLA. In fact, the adsorption process has been demonstrated to be a key element to understand the enzymatic degradation of PLA and, in general, of any poly(hydroxyalkanoates), according to Yamashita et al. [44]. These authors stated that the adsorption of *proteinase K* on PLA surfaces is an irreversible process that could be related to a hydrophobic interaction between the PLA and the enzymes. This conclusion can explain why the degradation of the scaffolds is delayed (during the first steps of the test) when they are plasma-treated or coated. As demonstrated by the WCA results (Figure 1), any of the strategies applied lead to a decrease of the hydrophobicity. Consequently, according to the conclusions of Yamashita et al., this trend would hinder the adsorption of the enzymes on the PLA surface and delay the degradation process. The coating applied at pH 3 seems to limit this adsorption step especially, as this group of samples shows the lowest levels of degradation measured as mass loss (Table 2). The protein adsorption on solid surfaces is a complex process affected by different parameters [45], so the reason why the coating at this pH value limits the adsorption process needs to be further analyzed, although it is out of the scope of the present work.

The trend evidenced by the mass loss results is also supported by the pH measurements of the degradation media (Figure 3), as the decrease of this parameter is explained by the presence of carboxylic acids released during the degradation process [46]. If the degradation is delayed (as it is especially for plasma-treated samples and pH 3 coated samples), the pH value of the media will be higher during the process, as confirmed in this experiment. The results obtained from the enzymatic degradation test open the possibility of controlling the degradation rate of the proposed constructs intended for bone regeneration, aiming to match this rate to the specific tissue growth rate.

Finally, the results of the cell viability evaluation prove that the aloe vera coating offers an improvement on the ability of the bone cells to proliferate and remain viable on the scaffolds compared to the results from the structures that were plasma-treated but not coated. As plasma treatment is the most common method to modify the surface of PLA scaffolds [14,47,48], the results from this work confirm the potential of the coating strategy to increase the biological performance of PLA-based scaffolds for bone regeneration.

In addition, the pH of the aloe vera extracts has been demonstrated to be a parameter that strongly affects the bioaffinity of the surface coating, as the best results were obtained for the aloe vera coating applied at pH 3. The adjustment of the pH may change the chemistry of the bioactive polysaccharides in the aloe vera extracts. According to different studies, the presence of the acetyl group in the acemannan structure (one of the most important components in the aloe vera extracts) seems to be a key parameter to explain its bioactivity [42]. Chokboribal et al. [49] have already proven that the deacetylation in alkaline conditions of acemannan decreases its bioactivity. Although in this work, the pH level is not aggressive enough to produce the deacetylation of the bioactive molecules, it is possible that the introduction of an alkali (NaOH used for pH adjustment of the extract solutions) changed the conformation of these active functional groups. This modification could hinder the effectiveness of the aloe vera attachment to the surface, leading to a lower bioactivity of the coating at pH 5 compared to the coating applied at pH 3.

5. Conclusions

This study shows the feasibility of improving the biological response of PLA-based scaffolds by applying a coating of aloe vera extracts. The pH value used during the coating process has demonstrated to be a parameter that strongly influences the characteristics of the final surface, as the pH 3 level offers better results in terms of cell viability during the cell culture of human osteoblasts. Regarding the effect of the coating on the enzymatic degradation of the structures, the coating applied at pH 3 seems to hinder the enzyme adsorption and, consequently, delays the degradation of the scaffold. Therefore, the pH level of the aloe vera coating can be used as an important parameter, in order to tune the degradation process of the structures intended for bone regeneration.

Author Contributions: Conceptualization, R.D. and M.E.A.-D.; Methodology, R.D. and M.E.A.-D.; Formal analysis, R.D.; Investigation, R.D. and J.Y.; Resources, M.M., F.R.-E. and C.L.; Writing—Original Draft, R.D. and M.E.A.-D; Writing—Review and Editing, M.M., J.Y., F.R.-E. and C.L.; Visualization, R.D.; Supervision, M.M.; Project administration, M.M.; Funding acquisition, M.M. All authors have read and agreed to the published version of the manuscript.

Funding: This contribution is part of the BioAM project (DPI2017-88465-R) funded by the Science, Innovation and Universities Spanish Ministry. Additionally, the authors would like to thank the H2020-MSCA-RISE program for providing funding for mobility through the BAMOS project, funded from the European Union's Horizon 2020 research and innovation program, under grant agreement N° 734156. Ricardo Donate express his gratitude for the funding through the PhD grant program co-financed by the Canarian Agency for Research, Innovation and Information Society of the Canary Islands Regional Council for Employment, Industry, Commerce and Knowledge and by the European Social Fund (ESF) Canary Islands Integrated Operational Program 2014-2020, Axis 3 Priority Theme 74 (85%). Grant code: TESIS2017010036.

Conflicts of Interest: The authors declare no conflict of interest. The funders had no role in the design of the study; in the collection, analyses, or interpretation of data; in the writing of the manuscript, or in the decision to publish the results.

References

1. Grémare, A.; Guduric, V.; Bareille, R.; Heroguez, V.; Latour, S.; L'heureux, N.; Fricain, J.C.; Catros, S.; Le Nihouannen, D. Characterization of printed PLA scaffolds for bone tissue engineering. *J. Biomed. Mater. Res. Part A* **2018**, *106*, 887–894. [CrossRef] [PubMed]
2. Kao, C.T.; Lin, C.C.; Chen, Y.W.; Yeh, C.H.; Fang, H.Y.; Shie, M.Y. Poly(dopamine) coating of 3D printed poly(lactic acid) scaffolds for bone tissue engineering. *Mater. Sci. Eng. C* **2015**, *56*, 165–173. [CrossRef] [PubMed]
3. Savioli Lopes, M.; Jardini, A.L.; Maciel Filho, R. Poly (lactic acid) production for tissue engineering applications. *Procedia Eng.* **2012**, *42*, 1402–1413. [CrossRef]
4. Teixeira, B.N.; Aprile, P.; Mendonça, R.H.; Kelly, D.J.; Thiré, R.M.D.S.M. Evaluation of bone marrow stem cell response to PLA scaffolds manufactured by 3D printing and coated with polydopamine and type I collagen. *J. Biomed. Mater. Res. Part B Appl. Biomater.* **2019**, *107*, 37–49. [CrossRef] [PubMed]
5. Martin, V.; Ribeiro, I.A.; Alves, M.M.; Gonçalves, L.; Claudio, R.A.; Grenho, L.; Fernandes, M.H.; Gomes, P.; Santos, C.F.; Bettencourt, A.F. Engineering a multifunctional 3D-printed PLA-collagen-minocycline-nanoHydroxyapatite scaffold with combined antimicrobial and osteogenic effects for bone regeneration. *Mater. Sci. Eng. C* **2019**, *101*, 15–26. [CrossRef]
6. Esposito Corcione, C.; Scalera, F.; Gervaso, F.; Montagna, F.; Sannino, A.; Maffezzoli, A. One-step solvent-free process for the fabrication of high loaded PLA/HA composite filament for 3D printing. *J. Therm. Anal. Calorim.* **2018**, *134*, 575–582. [CrossRef]
7. Ma, Z.; Gao, C.; Ji, J.; Shen, J. Protein immobilization on the surface of poly-L-lactic acid films for improvement of cellular interactions. *Eur. Polym. J.* **2002**, *38*, 2279–2284. [CrossRef]
8. Chen, S.; Guo, Y.; Liu, R.; Wu, S.; Fang, J.; Huang, B.; Li, Z.; Chen, Z.; Chen, Z. Tuning surface properties of bone biomaterials to manipulate osteoblastic cell adhesion and the signaling pathways for the enhancement of early osseointegration. *Colloids Surf. B Biointerfaces* **2018**, *164*, 58–69. [CrossRef]
9. Niaza, K.V.; Senatov, F.S.; Kaloshkin, S.D.; Maksimkin, A.V.; Chukov, D.I. 3D-printed scaffolds based on PLA/HA nanocomposites for trabecular bone reconstruction. *J. Phys. Conf. Ser.* **2016**, *741*, 012068. [CrossRef]

10. Belaid, H.; Nagarajan, S.; Teyssier, C.; Barou, C.; Barés, J.; Balme, S.; Garay, H.; Huon, V.; Cornu, D.; Cavaillès, V.; et al. Development of new biocompatible 3D printed graphene oxide-based scaffolds. *Mater. Sci. Eng. C* **2020**, *110*, 110595. [CrossRef]
11. Wei, Q.; Cai, X.; Guo, Y.; Wang, G.; Guo, Y.; Lei, M.; Song, Y.; Yingfeng, Z.; Wang, Y. Atomic-scale and experimental investigation on the micro-structures and mechanical properties of PLA blending with CMC for additive manufacturing. *Mater. Des.* **2019**, *183*, 108158. [CrossRef]
12. Chen, Y.; Mak, A.F.T.; Wang, M.; Li, J.; Wong, M.S. PLLA scaffolds with biomimetic apatite coating and biomimetic apatite/collagen composite coating to enhance osteoblast-like cells attachment and activity. *Surf. Coat. Technol.* **2006**, *201*, 575–580. [CrossRef]
13. Nakagawa, M.; Teraoka, F.; Fujimoto, S.; Hamada, Y.; Kibayashi, H.; Takahashi, J. Improvement of cell adhesion on poly(L-lactide) by atmospheric plasma treatment. *J. Biomed. Mater. Res. Part A* **2006**, *77*, 112–118. [CrossRef]
14. Jacobs, T.; Morent, R.; De Geyter, N.; Dubruel, P.; Leys, C. Plasma Surface Modification of Biomedical Polymers: Influence on Cell-Material Interaction. *Plasma Chem. Plasma Process.* **2012**, *32*, 1039–1073. [CrossRef]
15. Guo, C.; Xiang, M.; Dong, Y. Surface modification of poly (lactic acid) with an improved alkali-acid hydrolysis method. *Mater. Lett.* **2015**, *140*, 144–147. [CrossRef]
16. Zeng, S.; Cui, Z.; Yang, Z.; Si, J.; Wang, Q.; Wang, X.; Peng, K.; Chen, W. Characterization of highly interconnected porous poly(lactic acid) and chitosan-coated poly(lactic acid) scaffold fabricated by vacuum-assisted resin transfer molding and particle leaching. *J. Mater. Sci.* **2016**, *51*, 9958–9970. [CrossRef]
17. Fernández-Cervantes, I.; Morales, M.A.; Agustín-Serrano, R.; Cardenas-García, M.; Pérez-Luna, P.V.; Arroyo-Reyes, B.L.; Maldonado-García, A. Polylactic acid/sodium alginate/hydroxyapatite composite scaffolds with trabecular tissue morphology designed by a bone remodeling model using 3D printing. *J. Mater. Sci.* **2019**, *54*, 9478–9496. [CrossRef]
18. Li, J.; Chen, Y.; Mak, A.F.T.; Tuan, R.S.; Li, L.; Li, Y. A one-step method to fabricate PLLA scaffolds with deposition of bioactive hydroxyapatite and collagen using ice-based microporogens. *Acta Biomater.* **2010**, *6*, 2013–2019. [CrossRef]
19. Kim, S.H.; Oh, S.A.; Lee, W.K.; Shin, U.S.; Kim, H.W. Poly(lactic acid) porous scaffold with calcium phosphate mineralized surface and bone marrow mesenchymal stem cell growth and differentiation. *Mater. Sci. Eng. C* **2011**, *31*, 612–619. [CrossRef]
20. Liu, P.; Chen, D.; Shi, J. Chemical Constituents, Biological Activity and Agricultural Cultivation of Aloe vera. *Asian J. Chem.* **2013**, *25*, 6477–6485. [CrossRef]
21. Suganya, S.; Venugopal, J.; Ramakrishna, S.; Lakshmi, B.S.; Dev, V.R.G. Naturally derived biofunctional nanofibrous scaffold for skin tissue regeneration. *Int. J. Biol. Macromol.* **2014**, *68*, 135–143. [CrossRef]
22. Garcia-Orue, I.; Gainza, G.; Gutierrez, F.B.; Aguirre, J.J.; Evora, C.; Pedraz, J.L.; Hernandez, R.M.; Delgado, A.; Igartua, M. Novel nanofibrous dressings containing rhEGF and Aloe vera for wound healing applications. *Int. J. Pharm.* **2017**, *523*, 556–566. [CrossRef]
23. Shanmugavel, S.; Reddy, V.J.; Ramakrishna, S.; Lakshmi, B.S.; Dev, V.G. Precipitation of hydroxyapatite on electrospun polycaprolactone/aloe vera/silk fibroin nanofibrous scaffolds for bone tissue engineering. *J. Biomater. Appl.* **2014**, *29*, 46–58. [CrossRef]
24. Femenia, A.; Sánchez, E.S.; Simal, S.; Rosselló, C. Compositional features of polysaccharides from Aloe vera (Aloe barbadensis Miller) plant tissues. *Carbohydr. Polym.* **1999**, *39*, 109–117. [CrossRef]
25. Hamman, J.H. Composition and applications of Aloe vera leaf gel. *Molecules* **2008**, *13*, 1599–1616. [CrossRef]
26. Tabandeh, M.R.; Oryan, A.; Mohammadalipour, A. Polysaccharides of Aloe vera induce MMP-3 and TIMP-2 gene expression during the skin wound repair of rat. *Int. J. Biol. Macromol.* **2014**, *65*, 424–430. [CrossRef]
27. Blackwood, K.A.; Bock, N.; Dargaville, T.R.; Ann Woodruff, M. Scaffolds for growth factor delivery as applied to bone tissue engineering. *Int. J. Polym. Sci.* **2012**. [CrossRef]
28. Maan, A.A.; Nazir, A.; Khan, M.K.I.; Ahmad, T.; Zia, R.; Murid, M.; Abrar, M. The therapeutic properties and applications of Aloe vera: A review. *J. Herb. Med.* **2018**, *12*, 1–10. [CrossRef]
29. Bozzi, A.; Perrin, C.; Austin, S.; Arce Vera, F. Quality and authenticity of commercial aloe vera gel powders. *Food Chem.* **2007**, *103*, 22–30. [CrossRef]

30. Xu, J.; Yue, R.Q.; Liu, J.; Ho, H.M.; Yi, T.; Chen, H.B.; Han, Q. Bin Structural diversity requires individual optimization of ethanol concentration in polysaccharide precipitation. *Int. J. Biol. Macromol.* **2014**, *67*, 205–209. [CrossRef]
31. Yuan, Y.; Lee, T.R. Contact angle and wetting properties. In *Springer Series Surface Sciences*; Springer: Berlin/Heidelberg, Germany, 2013; Volume 51, pp. 3–34.
32. Laput, O.; Vasenina, I.; Salvadori, M.C.; Savkin, K.; Zuza, D.; Kurzina, I. Low-temperature plasma treatment of polylactic acid and PLA/HA composite material. *J. Mater. Sci.* **2019**, *54*, 11726–11738. [CrossRef]
33. Zeng, J.; Chen, X.; Liang, Q.; Xu, X.; Jing, X. Enzymatic Degradation of Poly(L-lactide) and Poly(ε-caprolactone) Electrospun Fibers. *Macromol. Biosci.* **2004**, *4*, 1118–1125. [CrossRef]
34. Tsuji, H.; Muramatsu, H. Blends of aliphatic polyesters: V. Non-enzymatic and enzymatic hydrolysis of blends from hydrophobic poly(L-lactide) and hydrophilic poly(vinyl alcohol). *Polym. Degrad. Stab.* **2001**, *71*, 403–413. [CrossRef]
35. Liu, L.; Li, S.; Garreau, H.; Vert, M. Selective enzymatic degradations of poly(L-lactide) and poly(∈-caprolactone) blend films. *Biomacromolecules* **2000**, *1*, 350–359. [CrossRef]
36. De Tayrac, R.; Chentouf, S.; Garreau, H.; Braud, C.; Guiraud, I.; Boudeville, P.; Vert, M. In vitro degradation and in vivo biocompatibility of poly(lactic acid) mesh for soft tissue reinforcement in vaginal surgery. *J. Biomed. Mater. Res. Part B Appl. Biomater.* **2008**, *85*, 529–536. [CrossRef]
37. Hegyesi, N.; Zhang, Y.; Kohári, A.; Polyák, P.; Sui, X.; Pukánszky, B. Enzymatic degradation of PLA/cellulose nanocrystal composites. *Ind. Crops Prod.* **2019**, *141*. [CrossRef]
38. Donate, R.; Monzón, M.; Ortega, Z.; Wang, L.; Ribeiro, V.; Pestana, D.; Joaquim, M.; Reis, R.L. Comparison between calcium carbonate and β -tricalcium phosphate as additives of 3D printed scaffolds with polylactic acid matrix. *J. Tissue Eng. Regen. Med.* **2019**, *14*, 272–283. [CrossRef]
39. Leong, K.F.; Chua, C.K.; Sudarmadji, N.; Yeong, W.Y. Engineering functionally graded tissue engineering scaffolds. *J. Mech. Behav. Biomed. Mater.* **2008**, *1*, 140–152. [CrossRef]
40. Tsuji, H.; Ishida, T. Poly(l-lactide). X. Enhanced surface hydrophilicity and chain-scission mechanisms of poly(l-lactide) film in enzymatic, alkaline, and phosphate-buffered solutions. *J. Appl. Polym. Sci.* **2002**, *87*, 1628–1633. [CrossRef]
41. Scaffaro, R.; Lopresti, F.; Sutera, A.; Botta, L.; Fontana, R.M.; Gallo, G. Plasma modified PLA electrospun membranes for actinorhodin production intensification in Streptomyces coelicolor immobilized-cell cultivations. *Colloids Surf. B Biointerfaces* **2017**, *157*, 233–241. [CrossRef]
42. Liu, C.; Cui, Y.; Pi, F.; Cheng, Y.; Guo, Y.; Qian, H. Extraction, purification, structural characteristics, biological activities and pharmacological applications of acemannan, a polysaccharide from aloe vera: A review. *Molecules* **2019**, *24*, 1554. [CrossRef]
43. Izdebska-Podsiadły, J.; Dörsam, E. Effects of argon low temperature plasma on PLA film surface and aging behaviors. *Vacuum* **2017**, *145*, 278–284. [CrossRef]
44. Yamashita, K.; Kikkawa, Y.; Kurokawa, K.; Doi, Y. Enzymatic degradation of poly(L-lactide) film by proteinase K: Quartz crystal microbalance and atomic force microscopy study. *Biomacromolecules* **2005**, *6*, 850–857. [CrossRef]
45. Fang, F.; Szleifer, I. Kinetics and thermodynamics of protein adsorption: A generalized molecular theoretical approach. *Biophys. J.* **2001**, *80*, 2568–2589. [CrossRef]
46. Elsawy, M.A.; Kim, K.H.; Park, J.W.; Deep, A. Hydrolytic degradation of polylactic acid (PLA) and its composites. *Renew. Sustain. Energy Rev.* **2017**, *79*, 1346–1352. [CrossRef]
47. Yamaguchi, M.; Shinbo, T.; Kanamori, T.; Wang, P.C.; Niwa, M.; Kawakami, H.; Nagaoka, S.; Hirakawa, K.; Kamiya, M. Surface modification of poly(L-lactic acid) affects initial cell attachment, cell morphology, and cell growth. *J. Artif. Organs* **2004**, *7*, 187–193. [CrossRef]

48. Wang, M.; Favi, P.; Cheng, X.; Golshan, N.H.; Ziemer, K.S.; Keidar, M.; Webster, T.J. Cold atmospheric plasma (CAP) surface nanomodified 3D printed polylactic acid (PLA) scaffolds for bone regeneration. *Acta Biomater.* **2016**, *46*, 256–265. [CrossRef]
49. Chokboribal, J.; Tachaboonyakiat, W.; Sangvanich, P.; Ruangpornvisuti, V.; Jettanacheawchankit, S.; Thunyakitpisal, P. Deacetylation affects the physical properties and bioactivity of acemannan, an extracted polysaccharide from Aloe vera. *Carbohydr. Polym.* **2015**, *133*, 556–566. [CrossRef]

3. PUBLICATIONS PENDING ACCEPTANCE

On the effectiveness of oxygen plasma and alkali surface treatments to modify the properties of polylactic acid scaffolds

polymers

MDPI

Article

On the effectiveness of oxygen plasma and alkali surface treatments to modify the properties of polylactic acid scaffolds

Ricardo Donate [1,*], María Elena Alemán-Domínguez [1] and Mario Monzón [1]

[1] Departamento de Ingeniería Mecánica, Grupo de Investigación en Fabricación Integrada y Avanzada, Universidad de Las Palmas de Gran Canaria, Campus Universitario de Tafira s/n, 35017 Las Palmas, Spain; mariaelena.aleman@ulpgc.es (M.E.A.-D.); mario.monzon@ulpgc.es (M.M.)

* Correspondence: ricardo.donate@ulpgc.es (R.D.)

Abstract: Surface modification of 3D printed PLA structures is a major issue in terms of increasing the biofunctionality and expanding the Tissue Engineering applications of these parts. In this paper, different exposure times were used for low-pressure oxygen plasma applied on PLA 3D printed scaffolds. Alkali surface treatments were also evaluated, aiming to compare the modifications introduced on the surface properties by each strategy. Surface-treated samples were characterized through the quantification of carboxyl groups, energy-dispersive X-ray spectroscopy, water contact angle measurements and differential scanning calorimetry analysis. The change in the surface properties was studied over a 2-week period. In addition, an enzymatic degradation analysis was carried out in order to evaluate the effect of the surface treatments on the degradation profile of the 3D structures. The physicochemical characterization results suggest different mechanism pathways for each type of treatment. Alkali-treated scaffolds showed a higher concentration of carboxyl groups on their surface, which enhanced the enzymatic degradation rate, but were also proven to be more aggressive towards 3D printed structures. In contrast, the application of the plasma treatments led to an increased hydrophilicity of the PLA surface without affecting the bulk properties. However, the changes on the properties were less steady over time.

Keywords: polymer; low-pressure plasma; plasma treatment; surface modification; biomedical applications; additive manufacturing; toluidine blue method; enzymatic degradation

Citation: Lastname, F.; Lastname, F.; Lastname, F. Title. *Polymers* **2021**, *13*, x. https://doi.org/10.3390/xxxxx

Academic Editor: Firstname Lastname

Received: date
Accepted: date
Published: date

1. Introduction

The use of 3D scaffolds constitutes one of the most promising approaches in the biomedical field to regenerate damaged tissue. As scaffolds act as artificial structures that support and direct new tissue formation, various requirements must be fulfilled, including: biocompatibility, suitable mechanical properties, interconnected porosity, promotion of cell's attachment and growth, supported vascularization and ease of sterilization [1]. Unlike other commonly used biomaterials in the Tissue Engineering field (TE), such as titanium [2] and bioceramic materials [3], polymeric scaffolds also possess a distinctive feature: their biodegradability. As the byproducts of the degradation process of the polymer are excreted through usual metabolic pathways, a complete integration of the scaffold can be achieved, avoiding the need of an explant surgical procedure [4]. On the negative side, the degradation profile of polymeric scaffolds needs to be carefully adjusted so they ensure sufficient mechanical support during new tissue formation, and no immune or inflammatory response happens in the implantation site due to the release of acidic byproducts [5].

Polylactic acid (PLA) is a biodegradable thermoplastic aliphatic polyester that has been extensively used for scaffold manufacturing. Apart from its biocompatibility, adjustable biodegradability and suitable mechanical properties, PLA has a good processability by Additive Manufacturing (AM) techniques (ISO/ASTM 52900:2015); allowing

obtaining patient-specific constructs with great control over the pore size, pore shape and porosity of the structure. On the other hand, the main drawbacks for the biomedical application of PLA scaffolds include: a) release of acidic degradation byproducts; b) poor toughness; c) lack of reactive side chain groups, which limits the treatments available for improving its surface properties and d) low hydrophilicity, which hinders cell attachment and scaffold-tissue interaction.

In order to overcome the limitations of PLA, different surface treatments can be applied to the scaffold to modify its topography or surface chemistry. Among them, one simple and effective strategy is the alkali treatment, based on the immersion of the PLA scaffolds in sodium hydroxide (NaOH) solutions. The hydrolysis of the ester bonds of PLA take places due to the nucleophilic attack of hydroxide ions to the carbonyl carbon [6,7], leading to the incorporation of hydroxyl (-OH) groups and the increase of surface roughness; thus increasing the hydrophilicity of the base material [8,9]. Generally, after alkali hydrolysis, the samples are washed with inorganic acids to remove the excess of NaOH. However, if organic acids are used instead, the carboxyl groups (-COOH) of these compounds can hydrolyze the PLA´s ester bonds [8], while also removing the excess of NaOH. Carboxyl groups incorporated to the PLA surface lead to an enhancement of roughness and wettability [8,10], serve as anchoring points for biological substances [11,12] and promote the cell adhesion and proliferation processes [13,14]. The modifications generated by alkali treatment methods depend strongly on the concentration of the solution used and the treatment time, and could affect the surface morphology and mechanical properties of the scaffolds [15].

In contrast, plasma treatments allow the modification of the polymeric surface without affecting the bulk properties. The effects generated on the surface depend on the working conditions (power/voltage and time of exposure) and the carrier gas used. Oxygen plasma treatments can incorporate hydroxyl and carboxyl groups to the surface of PLA scaffolds [16,17], achieving a reduction of the water contact angle while affecting the roughness of the samples at a nanometric scale [17,18]. Overall, the plasma treatment of PLA samples can lead to an enhanced cell adhesion, morphology and proliferation [17,19,20]. The change on the chemical structure of the surface material may also have an impact on the bulk crystallinity of 3D printed structures, as the width of the struts is low enough to be affected by the changes in the surface. While in some cases the modifications introduced by these surface treatments are enough to fulfill the requirements for the tissue-engineered PLA scaffolds [19], these treatments are usually combined with a later coating step, based on the immobilization of bioactive substances within the polymeric matrix [12,21]. A subsequent coating procedure or the direct application of the surface-treated scaffolds should not be delayed too long, as the modifications generated by these treatments are not permanent, showing a progressive decay of the modifications introduced on the polymer´s surface [22–24].

In this work, a comparison between alkali and plasma treatments of PLA scaffolds obtained by AM was carried out. Different treatment times were selected to assess the modifications introduced by the oxygen plasma treatment, while for alkali treatments the sodium hydroxide solution concentration was varied. In addition, the use of organic and inorganic acids for a final washing step after alkali treatment was evaluated. Few examples can be cited from the literature comprising an experimental assessment of different treatment methods with varying conditions applied to PLA surfaces, including films [25] and composite samples [26], but no references were found regarding 3D structures. In addition to this, there is a lack of information in the literature about the comparison of how the surface modifications on PLA surfaces evolve over time. These data would be essential if the induced modifications are intended to be used for coating the structures or if storage before utilization is needed (as it is for commercially availability).

The characterization of the surface-treated PLA scaffolds included the assessment on the incorporation of carboxyl groups, the evaluation of the hydrophilicity by measuring the water contact angle and the analysis of the chemical composition of the surface by

energy-dispersive X-ray spectroscopy. Also, the effect of the treatments on the degree of crystallinity and calorimetric properties of the PLA samples was studied by differential scanning calorimetry analysis. Two weeks after applying the treatments, the samples were tested again to evaluate the aforementioned loss of modifications over time. Finally, an enzymatic degradation test using *Proteinase K* enzymes was carried out to assess the degradation rate of the structures, the pH and conductivity profile of the media during the 5-day test and the morphological and mechanical properties of the surface-treated scaffolds after degradation.

2. Materials and Methods

2.1. Materials

PLA L105 was purchased from Corbion Purac (Diemen, The Netherlands). This material, supplied in powder form, has a melt flow index of 65 g/10 min and molecular weight of approximately 105,000 g/mol. The reagents used in this study include sodium hydroxide (NaOH; 30620, Honeywell Fluka™), hydrochloric acid (HCl; 131020, Panreac), citric acid (20282, VWR Chemicals) and acetic acid (ACAC-GIA-2K5, Labkem).

2.2. Manufacturing of scaffolds

PLA scaffolds were manufactured using a material extrusion process (ISO/ASTM 52900:2015), commonly known as fused deposition modelling (FDM). Specifically, a BQ Hephestos 2 3D printer (Spain) was used to manufacture scaffolds with 9.8 mm diameter, 7 mm height, rectangular 0/90 pattern, square-shaped pores and a 50% theoretical porosity. Other printing settings included a nozzle diameter of 0.4 mm, a layer height of 0.3 mm, a speed of extrusion of 40 mm/s and a printing temperature of 215 °C.

The continuous PLA filaments fed to the 3D printed (mean diameter of around 1.75 mm) were obtained using a lab prototype extruder consisting of an 8 mm screw, a cylinder with an L/D ratio of 10 and a 1.6 mm diameter nozzle tip. The extrusion of PLA L105 powder was carried out at a rotating speed of 7 rpm, a temperature of 180 °C and with a final air- and water-cooling stage.

Apart from the PLA scaffolds, flat-surface samples were manufactured by compression molding in order to better characterize the PLA surface after applying the different treatments. A Collin P 200 P/M press and the following cycle were used: heating up to 190 °C at a heating rate of 20 °C/min; maintaining the temperature at that constant value for 90 s at 10 bar of pressure; and finally cooling at a rate of 20 °C/min while maintaining the pressure applied in the second step.

As the first step of every experiment included in this work, the samples were measured and weighted to ensure that there were no significant differences regarding these parameters between the different groups tested.

2.3. Surface treatment

2.3.1. Oxygen plasma treatments

The plasma treatment of the samples was carried out in a low-pressure device (Zepto Diener electronic GmbH, Ebhause, Germany). Oxygen was used as carrier gas (Carburos Metálicos, Spain), containing less than 500 ppb of H_20 and less than 400 ppb of N_2. The oxygen pressure inside the chamber was fixed at 1.8 mbar, and the surface treatment was applied at a power of 30 W for 1 or 10 minutes. Both sides of the samples were treated. Depending on the treatment time, plasma-treated group of samples are referred in this text as PLASMA 1 min or PLASMA 10 min.

2.3.2. Alkali treatments

PLA samples were placed in a 24-well plate (144530, Thermo Scientific™ Nunc™) and immersed during 1 h at room temperature in 2 mL of 0.2 N or 1 N NaOH solutions. Then, the samples were rinsed with distillate water, washed with a 0.1 N HCl solution

and rinsed again with distillate water. PLA samples treated with these methods are referred in the text as 0.2 N NaOH and 1 N NaOH.

In a third alkali surface treatment evaluated, the samples were immersed in 2 mL of 0.2 N NaOH solution, rinsed with distillate water, washed with a 0.05 g/L citric acid solution and finally rinsed again with distillate water. Samples treated with this method are referred in the text as 0.2 N NaOH + citric acid.

2.4. Physicochemical characterization

2.4.1. Evaluation of carboxyl groups on the treated surface

The relative surface concentration of carboxyl groups was evaluated by using the Toluidine Blue O (TBO) method [27]. This cationic dye binds to carboxyl groups in a 1: 1 molar ratio in a basic medium and can later be desorbed with an acid solution [27,28]. Four replicas of each of the treated scaffolds groups were tested right after applying the different surface treatments. PLA scaffolds were used as control. The samples were placed individually in centrifuge tubes (CFT011150, 15 mL sterile tubes, Jet Biofil) and immersed in 2 mL of a 0.5 mM Toluidine Blue O (T3250, Sigma Aldrich) solution in 0.1 mM NaOH (pH 10). After 20 h, the samples were transferred to a 24-well plate and rinsed thrice with 1 mL of 0.1 mM NaOH solution. Then, the bounded toluidine was desorbed by adding at each well 2 mL of 50% (v/v) acetic acid solution for 10 min. Finally, the samples were discarded and the absorbance of the solutions was measured using a Bio-Tek ELx800 reader (Bio Tek Instruments Inc., Winooski, VT, USA) at an excitation wavelength of 595 nm. The 50% (v/v) acetic acid solution was used as blank of the measurements.

This procedure was also applied to PLA scaffolds that were surface-treated and then stored in a desiccator for 2 weeks, in order to evaluate whether the modifications introduced are maintained during that period.

2.4.2. Energy-dispersive X-ray (EDX) spectroscopy analysis

The assessment of the chemical composition of the non-treated, plasma-treated and alkali-treated PLA samples was carried out by a scanning electron microscope (SEM; Hitachi TM 3030 at an acceleration voltage of 15 kV) coupled with an EDX detector. Flat-surface samples obtained by compression molding (as detailed in Section 2.2.) were used for this test. The main result of the EDX analysis is the oxygen/carbon ratio (O/C), which is an important indicator of the effectiveness of the proposed treatments to incorporate oxygen groups to the PLA surface. Four measurements were obtained per group on the day of treatment. The analysis was repeated 2 weeks later using the same samples and procedure.

2.4.3. Water contact angle (WCA) measurements

The sessile drop method was used to analyze the WCA of the surface-treated samples and therefore the effect of the treatments on the hydrophilicity of the base material. As it is recommended to use flat-surface samples for this test, the samples obtained by compression molding described in Section 2.2 were used. The WCA measurements (n=4) were carried out at room temperature using an Ossila water contact angle measuring device (Ossila Ltd, UK) and the open source software ImageJ was used to measure the static contact angle of 2 μL distilled water. The WCA was measured every 24 h during 2 weeks after applying the different surface treatments.

2.4.4. Differential scanning calorimetry analysis (DSC)

Samples extracted from non-treated and treated scaffolds were subjected to DSC analysis in a differential scanning calorimeter DSC 4000 (Perkin Elmer). The scaffolds were surface-treated on the same day or 2 weeks before the analysis. The samples (n=4) were placed in aluminum crucibles and subjected to a heating/cooling/heating cycle from 30 to 230 °C, with a nitrogen flow of 20 mL/min and heating and cooling rates of 10 °C/min. The calorimetric data obtained include the glass transition temperature, the onset

temperature (at which melting process start), the peak melting temperature and the melting enthalpy. Then, the melting enthalpy values were used to calculate the crystallinity of each group of samples according to the following equation:

$$\%X_C = 100 \cdot \frac{\Delta H_f}{\Delta H_f^\circ} \quad (1)$$

Where Xc is the degree of crystallinity, ΔH_f is the melting enthalpy of the sample and ΔH_f° the melting enthalpy of 100% crystalline PLA. The value for ΔH_f° was 93.7 J/g [29].

2.5. Enzymatic degradation study

An enzymatic degradation test was carried out to evaluate the effect of the oxygen plasma and alkali surface treatments on the degradation rate of the PLA scaffolds. *Proteinase K* enzymes from Tritirachium album (30 units per mg of protein, Merck) were used to accelerate the degradation study of the PLA samples [30]. The enzymes were diluted in Tris-HCl buffer (pH 8.6, BioReagent, Merck) at a concentration of 0.2 mg/mL. Sodium azide (ReagentPlus®, ≥99.5%, Merck) was added at the same concentration, with the aim of avoiding possible bacterial contamination.

Four replicas per group were placed in a non-treated 24-well plate and 2 mL of degradation media were added per well. PLA scaffolds were used as control. The well plate was maintained in an incubator at 37 °C for 5 days. In order to avoid the denaturation of the enzymes (due to the lactic acid released during the scaffolds degradation) and therefore maintain a high enzymatic activity, the buffer-enzyme solution was replaced daily. The pH (sensIONTM+PH1, ±0.01, HACH) and conductivity (COND7+, ±0.01, Labbox) of the media were measured every day to follow up the evolution of these parameters during the enzymatic degradation process.

The weight loss of the structures after 5 days was assessed by using an analytical balance (±0.1 mg, A&D Scales Gemini Series, GR-200, Germany), while the porosity change of the structures was determined with the following equation [31]:

$$\%\text{porosity} = 100 \cdot \left(1 - \frac{\varrho_{ap}}{\varrho_{bulk}}\right) \quad (2)$$

where ϱ_{ap} is the apparent density of the structure and ϱ_{bulk} is the density of the bulk material. The latter parameter was estimated by measuring the mass and the dimensions of short filaments of material (n = 8), giving a result of 1.22±0.03 g/cm^3. The apparent density was calculated following a similar protocol for the 3D printed scaffolds.

Finally, the degraded scaffolds were mechanically characterized under compression test in a LIYI (LI-1065, Dongguan Liyi Environmental Technology Co., Ltd., China) testing machine in displacement control mode. Crosshead speed was set at 1 mm/min. The compressive modulus, offset compressive yield strength (2% deviation from linearity), compression strength and strain at maximum strength were calculated according to ASTM D695-15. Non-degraded PLA scaffolds were used as reference control (RC).

2.10. Statistical Analysis

Statistical analysis was performed using MATLAB software (MATLAB and Statistics Toolbox Release 2021a, The MathWorks, Inc., Natick, USA). The data obtained during this study were analyzed by the Kruskal–Wallis test, except for those cases were only two groups were compared. In the latter case, the Wilcoxon two-sided rank sum test was used. The significance level was set to * $p < 0.05$, ** $p < 0.01$ and *** $p < 0.001$, for statistically significant, highly statistically significant and very highly statistically significant differences, respectively. All figures and tables show the mean values obtained for each group tested. Standard deviations are represented with error bars in the case of figures.

3. Results

3.1. Physicochemical characterization

3.1.1. Weight loss due to the application of the surface treatments

In order to assess the effect of the evaluated surface treatments on the PLA scaffold structure, the weight of each group of samples (n=4) was measured before and after treatment. The scaffolds tested had an initial weight of 0.258±0.01 g, with not-statistically significant differences between groups. After the application of the surface treatments, as showed in Table 1, a statistically significant weight loss was obtained for the 1 N NaOH and 0.2 N NaOH + citric acid groups. The weight loss in the case of alkali treatments was related to NaOH concentration, as the weight decreased more for the most concentrated solution. These data evidenced that these treatments are the most aggressive among the ones tested, so it is expected that they have affected the bulk properties of the material (as described below for crystallinity). For plasma-treated samples, the effect of the treatment depends on the time of exposure: scaffolds treated for 10 min showed a statistically significant weight loss ($p<.05$) compared with the ones treated for 1 min, although in both cases the values remain below 1%.

Table 1. Weight loss (%) due to the application of the different surface treatments evaluated.

Group of samples	%weight loss
PLASMA 1 min	0.01±0.02
PLASMA 10 min	0.21±0.02
0.2 N NaOH	1.93±0.11
1 N NaOH	5.85±0.25 [1]
0.2 N NaOH + citric acid	2.08±0.12 [2]

[1] $p < .05$ compared with PLASMA 10 min and $p < .01$ compared with PLASMA 1 min.
[2] $p < .05$ compared with PLASMA 1 min.

3.1.2. Evaluation of carboxyl groups on the treated surface

The incorporation of carboxyl groups onto the PLA surface was achieved with the three alkali treatments proposed, as demonstrated by the results obtained at day 0 (day of treatment) with the TBO method (Figure 1).

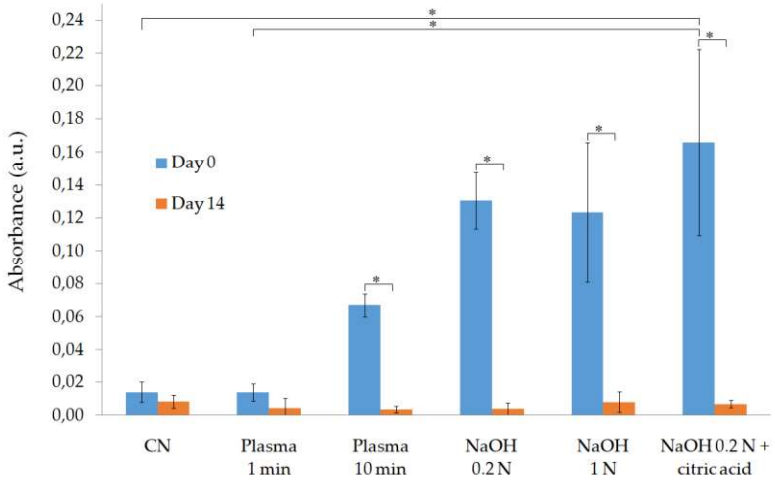

Figure 1. Physicochemical characterization of surface-treated samples by the TBO test.

As expected, the highest mean value of absorbance was obtained for the group of samples treated with 0.2 N NaOH + citric acid (0.17±0.06 a.u.), which showed a significantly higher value of this parameter compared with the samples treated with plasma for 1 min and the non-treated PLA scaffolds used as control. On the other hand, the results suggest that there is no concentration of carboxyl groups on the surface when applying the PLASMA 1 min treatment method, as this is the only group that showed a non-significant difference with the control group at day 0 (absorbance value equal to

0.01±0.01 a.u. in both cases). At day 14, this statement becomes true for all the groups tested.

3.1.3. EDX analysis

The O/C ratio of each group of samples is represented in Figure 2. In comparison to the PLA control group (O/C ratio equal to 0.693±0.004), statistically significant and highly statistically significant differences were obtained for the 0.2 N NaOH (0.718±0.001) and 1 N NaOH groups (0.737±0.015), respectively. The incorporation of oxygen groups to the PLA surface is especially relevant for 1 N NaOH group, since it showed the highest value at day 0 and is the only group that maintained a significantly higher O/C ratio (0.702±0.008) after 14 days.

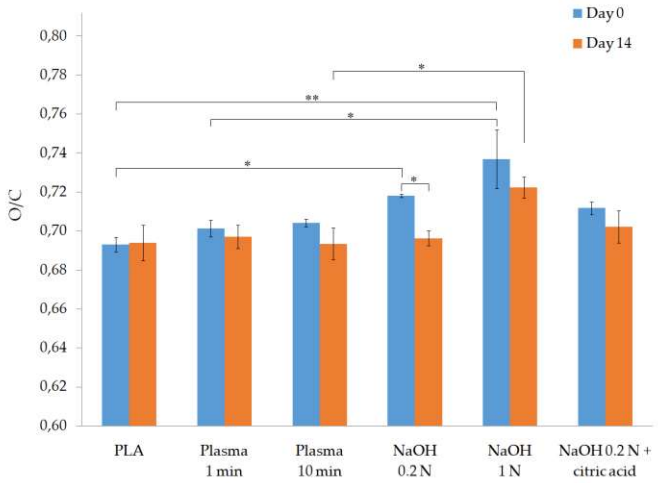

Figure 2. Physicochemical characterization of surface-treated samples by EDX analysis.

3.1.4. Water contact angle (WCA) measurements

The evolution of the WCA of the samples during two weeks is showed in Figure 3. The mean WCA value of the PLA samples right after treatment (day 0) decreased from the value of 77.2±0.9° (non-treated PLA) to 48.5±3.0° and 45.1±5.2° for the PLASMA 1 min and PLASMA 10 min groups, respectively. The 1 N NaOH group showed a similar result (50.7±3.0°), while the lowest WCA values were obtained for the 0.2 N NaOH (67.4±1.8°) and 0.2 N NaOH + citric acid (66.8±2.7°) treatments. The surface-treated samples tend to recover their initial state, but following a different profile: the effects induced by the oxygen plasma were lost at a higher rate, with the samples treated for 1 min showing a WCA similar to that of the base material in only 4 days (6 days for 10-min plasma); alkali-treated samples, however, reached the WCA value of the base material 13 days after treatment.

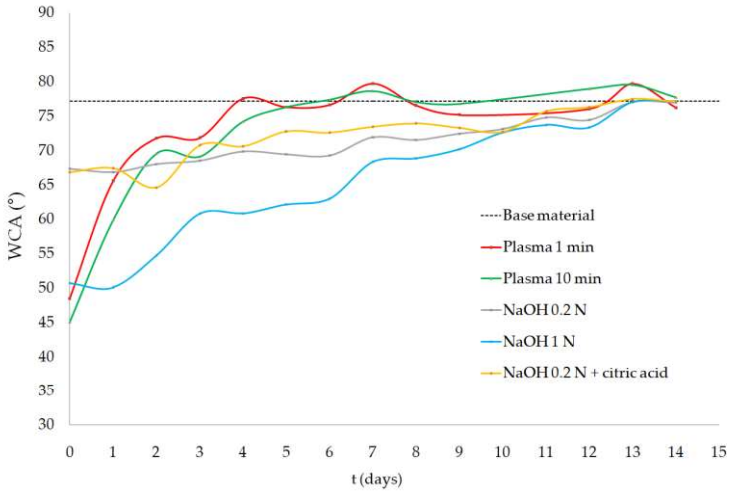

Figure 3. Water contact angle measurements of surface-treated samples.

3.1.5. Differential scanning calorimetry analysis (DSC)

As shown in Table 2, the proposed surface treatments have an effect on the calorimetric properties of the bulk material. Thus, at day 0, a statistically significant reduction was obtained for the samples treated with 1 N NaOH in terms of glass transition temperature in comparison to the plasma-treated samples. The onset and melting temperatures also tend to be reduced for surface-treated samples. Finally, a significant increase of the melting enthalpy and the crystallinity values were obtained for the 0.2 N NaOH group. This increase in crystallinity, despite being not-statistically significant, was also observed for the PLASMA 10 min and the rest of the alkali treatments.

Table 2. DSC results of all groups of samples at the day of treatment (a) and 2 weeks later (b).

(a)

Group of samples	Tg (°C)	T_{onset} (°C)	T_{peak} (°C)	ΔH (J/g)	%Xc
PLA	63.5±1.2	167.0±3.2	176.0±0.1	47.0±1.5	50.1±1.6
PLASMA 1 min	64.2±0.6	169.0±0.1	175.6±0.2	46.8±1.5	50.0±1.6
PLASMA 10 min	64.4±0.5	169.3±0.2	175.6±0.1 [2]	49.5±1.1	52.9±1.2
0.2 N NaOH	61.5±0.6	169.7±1.2	175.9±0.1	50.5±1.4 [3]	53.9±2.4 [4]
1 N NaOH	60.3±0.6 [1]	169.5±1.2	175.7±0.1	50.3±1.4	53.6±2.7
0.2 NaOH + citric acid	63.4±0.6	164.8±1.2	175.7±0.1	48.8±1.4	52.1±2.1

[1] $p < .01$ compared with PLASMA 10 min and $p < .05$ compared with PLASMA 1 min.
[2] $p < .05$ compared with PLA.
[3] $p < .05$ compared with PLASMA 1 min.
[4] $p < .05$ compared with PLA and PLASMA 1 min.

(b)

Group of samples	Tg (°C)	T_{onset} (°C)	T_{peak} (°C)	ΔH (J/g)	%Xc
PLA	63.5±1.2	167.0±3.2	176.0±0.1	47.0±1.5	50.1±1.6
PLASMA 1 min	63.9±0.2	169.2±0.2	176.3±0.1 *	47.1±3.0	49.6±2.1
PLASMA 10 min	63.8±0.4	169.3±0.3	176.0±0.1 *	47.8±2.9	51.0±3.1
0.2 N NaOH	63.4±0.4 *	167.8±2.3	176.1±0.1 *	50.9±0.9	54.3±0.9
1 N NaOH	63.2±0.9 *	168.0±2.4	176.0±0.1 *	46.4±2.0 *	49.6±2.1
0.2 NaOH + citric acid	63.5±0.2	166.0±2.3	175.8±0.1 [1]	49.2±2.8	52.5±3.0

* $p<.05$ compared with the result at day 0.
[1] $p < .01$ compared with PLASMA 1 min.

On the other hand, the differences mentioned at day 0 were not found in the samples treated and analyzed two weeks later. As shown in Table 2.b., statistically significant differences were obtained for the value of most of the groups and parameters analyzed compared with day 0, leading to the loss of the modifications introduced by the proposed treatments.

3.2. Enzymatic degradation study

The weight loss of each group of scaffolds after the 5-day enzymatic degradation test is shown in Figure 4. Alkali-treated scaffolds showed a higher level of degradation, with a mean weight loss of around 9% and a statistically significant difference obtained for the 1 N NaOH group compared with the non-treated PLA samples.

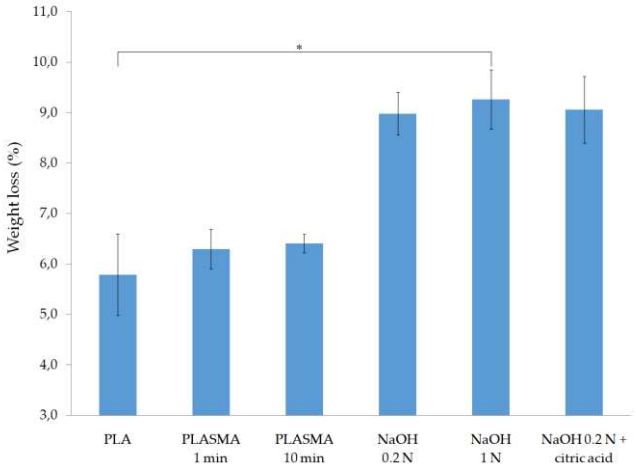

Figure 4. Enzymatic degradation test results of surface-treated samples: % weight loss after 5 days.

Regarding the pH variation of the degradation media (Figure 5), PLASMA 1min samples maintained the initial pH (7.94) until almost day 2, and then rapidly decreased to a value of 4.36±0.01 at day 3. In the case of PLASMA 10 min samples, the pH decreased from day 1, giving as a result a less pronounce slope of the curve of pH variation. Alkali-treated groups showed a pH around 4.5 in all 5 days of test. From day 3 similar results were obtained for all the groups of samples tested.

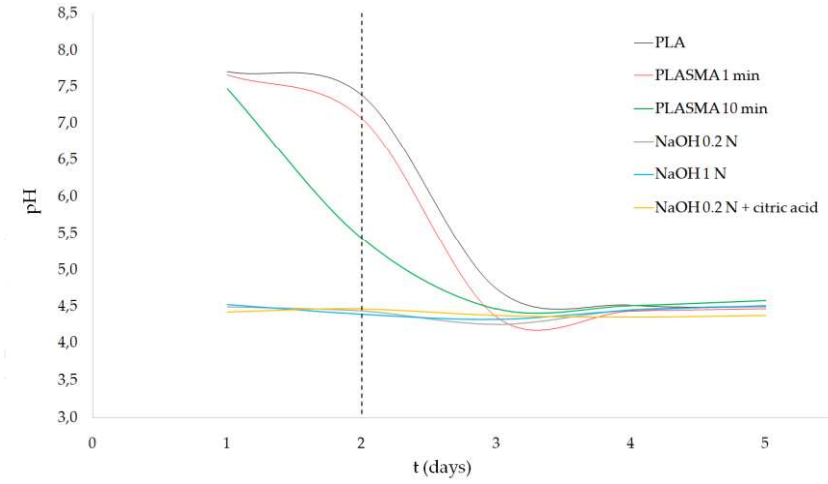

Figure 5. Enzymatic degradation test results of surface-treated samples: pH variation.

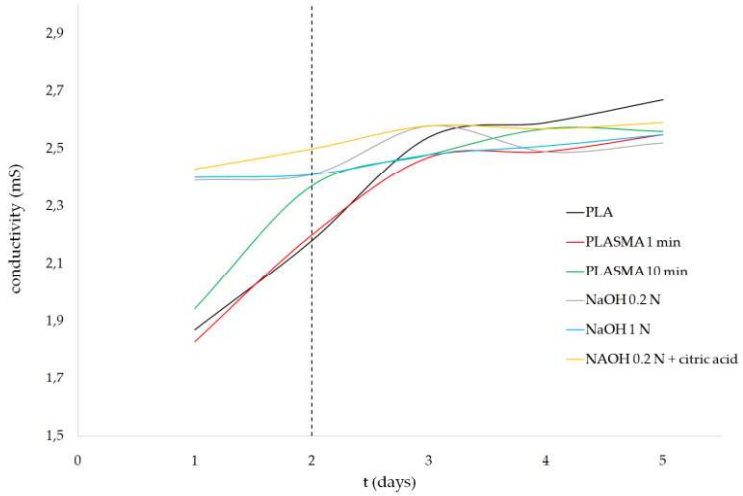

Figure 6. Enzymatic degradation test results of surface-treated samples: conductivity variation.

An increase in the porosity of the scaffolds has also been obtained as a consequence of the enzymatic degradation of the structure (Table 3). This increment is statistically significant for the 0.2 N NaOH and 1 N NaOH groups.

Table 3. Porosity values (before and after the degradation test) and compression test results.

Group of samples	Initial porosity (%)	Final porosity (%)	Elastic modulus (MPa)	Compressive yield strength (MPa)	Compression strength (MPa)	Strain at maximum strength
RC (compression test)			83.6±7.9	7.2±1.0	-	-
PLA	55.5±2.9	58.0±3.0	81.0±10.7	7.0±1.5	9.7±2.0	0.24±0.07
PLASMA 1 min	56.0±2.5	59.0±2.1	72.7±4.9	6.5±1.7	9.9±2.9	0.27±0.04
PLASMA 10 min	56.1±1.6	58.8±1.5	73.7±13.3	6.6±1.4	9.2±1.9	0.24±0.03
NaOH 0.2 N	55.9±1.8	60.1±1.7 *	69.2±13.5	6.9±1.5	8.9±0.9	0.23±0.04
NaOH 1 N	58.8±0.9	61.7±1.6 *	67.7±8.4	6.0±0.8	8.4±1.1	0.25±0.01
NaOH 0.2 N + citric acid	56.4±2.4	60.8±2.3	63.2±7.5	5.2±0.8	8.2±1.8	0.26±0.02

* $p<.05$ compared with the initial porosity of this group.

In spite of being not-statistically significant, the compression test results (Table 3) of the degraded scaffolds showed a reduction of the elastic modulus, compressive yield strength and compressive strength of the surface-treated scaffolds. The decrease in mechanical properties is more notorious in the alkali-treated samples, especially for the NaOH 0.2 N + citric acid group, which showed the lowest values in all cases. Notably, the break point of the non-degraded PLA scaffolds, used as reference control (RC), was not reached during the test.

4. Discussion

The use of material extrusion techniques offers the possibility of obtaining PLA scaffolds with controlled pore size and porosity, so the characteristics of the 3D construct can be tailored to the specific patient and target tissue. The precision in the design and manufacturing of the scaffolds is severely compromise when applying an alkali surface treatment, as the weight loss of the samples will surely be accompanied by changes in the struts dimensions, microporosity and mechanical properties of the structure [15]. The percentage of weight loss for scaffolds treated with NaOH depends on the concentration of the solution, being in this study of around a 2% for 0.2 N NaOH solutions and more

than a 5% for 1 N NaOH treatment (Table 1). On the other hand, scaffolds treated with plasma showed a non-significant difference of weight before and after treatment for 1 min. When the time of exposure to the oxygen plasma was increased to 10 min, the value of weight loss significantly increased ($p<.05$) to 0.21±0.02 % compare with the group of PLASMA 1 min. Thus, the weight loss depends in this case on the time of treatment, which can be adjusted to maximize the incorporation of oxygen groups while reducing the effects on the structure.

Regarding the physicochemical characterization of the treated samples, the results of the EDX analysis at day 0 revealed that all treatments effectively introduce new oxygen groups on the PLA surface, as the mean O/C ratio increased in comparison to the control group in all cases (Figure 2). Alkali treatments showed the highest values of O/C ratio, with significant differences for the 0.2 N NaOH and 1 N NaOH groups compared with the non-treated PLA group. A non-significant increase of the O/C ratio was obtained when comparing PLA and PLASMA 1 min groups of samples. Similar results have been obtained in previous studies that carried out a comparison between oxygen plasma and alkali treatments [25]. Reactive species contained in the oxygen plasma (which include neutral oxygen molecules and atoms, radicals, free electrons and positively and negatively charged ions [16,32]) are less prone to react with the carbonyl groups of the polymer chain than hydroxide ions, giving the strong nucleophilic nature of the latter [33]. Thus, a greater amount of oxygen groups incorporated to the polymeric surface is expected for alkali treatments.

Results of the TBO test (Figure 1) showed that the 0.2 N NaOH + citric acid group had the highest concentration of carboxyl groups on their surface. This was an expected result, since carboxyl groups are predominantly incorporated when applying an alkali treatment method [25] and the subsequent washing step with an organic acid add more of these hydrophilic groups onto the PLA surface by ester bond´s hydrolysis [8,12]. Carboxyl groups were also generated, but to a lesser extent, by applying the alkali treatments coupled with a washing step using an inorganic acid (HCl), or in the scaffolds treated with the PLASMA 10 min method.

Despite being the only group that showed a non-significant difference compared with the control group in the TBO test, the PLASMA 1 min samples showed a reduction of the WCA from 77.2±0.9° to 48.5±3.0° (Figure 3). This highly statistically significant difference ($p<.01$) was also observed for the group of PLASMA 10 min, for which the lowest mean WCA value was obtained (45.1±5.2°). These results, coupled with the ones obtained by EDX analysis (Figure 2), suggest that the oxygen groups incorporated to the plasma-treated PLA surface were mainly hydroxyl groups [16,17]. In the case of the alkali treatments, a statistically significant ($p<.05$) reduction of the WCA was only obtained for the 1 N NaOH group. The difference in WCA observed between this group and the ones treated with 0.2 N NaOH could be related to the distinct surface roughness generated depending on the solution concentration [9]. Overall, the incorporation of hydroxyl groups and the changes in the surface roughness seems to have a more important effect on the hydrophilicity improvement of the PLA surface than the incorporation of carboxyl groups.

The modifications introduced on the PLA surface were lost after 2 weeks, as confirmed by the results showed in Figures 1-3. Since the WCA was evaluated during 14 days, it was possible to determine the time at which the properties recovered their initial values. The decay on the modifications introduced can be explained by the reorientation and diffusion of the polar groups introduced [24], the rearrangement of hydrophilic and hydrophobic macromolecules fragments within the polymer [22] and the adsorption of ambient humidity [23]; although samples were kept on a desiccator to limit the latter cause. The rearrangement of the polymers chains, which caused the migration of hydrophobic macromolecules fragments to the surface, was evidenced by the recovery of the initial crystallinity value after 2 weeks (Table 2). In addition, the results suggest that the diffusion or reorientation of the hydroxyl groups introduced is faster than that of the

carboxyl groups; samples treated with plasma recovered their initial WCA value in 4-6 days, while for the alkali-treated samples (with a higher formation of carboxyl groups) it took almost two weeks.

The same loss of the modifications introduced by the treatments was observed for the calorimetric properties of the scaffolds (Table 2). At day 0, however, a reduction of glass transition, onset and peak temperatures was obtained for the treated groups compared with the non-treated PLA scaffolds. An increase of the crystallinity of the bulk material was also observed, which could be explained by the increased mobility of the polymer´s chains due to the absorption of water molecules (for alkali treatments) and the incorporation of new oxygen groups to the polymer surface. Both factors have an effect on the movement of the chains in the amorphous region, allowing a rearrangement in part of them to a crystalline structure, according to the principle of thermodynamic equilibrium [23,24]. Another option is the scission of chains in the amorphous regions as a consequence of the surface treatments applied [34]. As previously mentioned, the crystallinity of the base material was recovered within 2 weeks possibly because hydrophobic macromolecules fragments migrated to the PLA surface [22]. These results give relevant information for the design of procedures regarding scaffold treatment, application of subsequent modifications (such as coating procedures) and storage conditions, having important implications in industrial practice.

Results concerning the enzymatic degradation study showed a significantly higher degradation of the alkali-treated scaffolds after 5 days (Figure 4), which can be explained by two factors: a) increased surface roughness, expected from the significant weight loss of the scaffolds after treatment (Table 1); b) higher concentration of carboxyl groups on the scaffold´s surface, which promotes the enzyme-material interaction [35]. Despite the relatively low hydrophilicity of the samples treated with 0.2 N NaOH, according to the WCA measurements (Figure 3), the degradation rate of these groups was as high as that of the 1 N NaOH group. From these results, it can be concluded that the contribution of the incorporation of carboxyl groups, which are present in the three alkali-treated groups, have a more important effect on the degradation of the 3D structures than the wettability of the surface.

In Appendix 1, the results of a 1-day enzymatic degradation test carried out using PLA and 0.2 N NaOH +citric acid groups are presented. While for the alkali-treated group the weight of the scaffolds was reduced only around a 1%, the pH decreased significantly to a value of 4.57±0.01. Similar values of pH were measured every day of the 5-day test (Figure 5) for all three alkali-treated groups, as well as for the plasma-treated groups after day 3. These results suggest that the degradation of the alkali-treated PLA scaffolds progressed to a point where the concentration of dissolved lactic acid was high enough to cause denaturation of the enzymes, stopping the degradation process [36]. This limiting concentration of lactic acid is related to the minimum pH measured during the test.

In contrast to alkali-treated samples, the groups treated with oxygen plasma maintained a higher level of pH during the first two days of the experiment, which can be related to the limited presence of carboxyl groups on their surface. The TBO test (Figure 1) showed that the application of the plasma treatment for 10 min allowed the incorporation of carboxyl groups, while non-significant difference was obtained for the PLASMA 1 min group compared with the control. Carboxyl groups incorporated to the PLASMA 10 min group enhanced the interaction of the enzymes with the polymer [35] from the beginning of the test, which led to a less drastic decrease of the pH between days 2 and 3 compared with the profile observed for the PLASMA 1 min group. In the case of PLA and PLASMA 1 min groups, the enzymatic degradation progressed by a surface-erosion mechanism [37] that enhances the surface roughness with a minimal weight reduction during the first days of the test (similarly to the results showed for non-treated PLA scaffolds in Appendix 1). From this point, the degradation of the structure is accelerated as new regions of the polymer are exposed to the enzymes, due to the increased surface roughness

and chains cleavage reactions [37]. According to these assumptions, the differenced observed in terms of weight loss for the different groups of samples tested (Figure 4) can be related to the first 2 days of the experiment. The increase of conductivity (for plasma-treated samples) followed by the maintenance of a value around 2.55 mS for all groups tested after day 3 (Figure 6) supported the latter conclusions.

The abrupt release of the acidic degradation byproducts could generate a strong inflammatory response, hindering cell growth and affecting the surrounding tissues [38]. Therefore, the degradation profile of PLA scaffolds must be precisely adjusted by optimizing the surface treatment conditions and/or combining the polymeric matrix with additives that can act as buffers [39,40]. The objective in the addition of ceramic or natural biomaterials to the PLA structure can also be related with the need of ensuring enough mechanical support during the new tissue formation. As showed in Table 3, a reduction of mechanical properties takes place as the degradation of the PLA scaffolds progresses. Finally, the treated surface of the PLA scaffolds must promote cell adhesion and growth to allow tissue regeneration. This requirement can be fulfilled by the methods proposed in this study, mainly with the incorporation of carboxylic groups in the case of alkali treatments [14] and the decrease of the inherent hydrophobicity of the base material to values suitable for cell attachment [41] by applying a plasma treatment.

5. Conclusions

The present study involves a comparative experimental study between alkali and plasma treatments applied to PLA scaffolds manufactured by AM. The results obtained suggest an important contribution of the carboxyl groups incorporated to the base material surface on the degradation profile of the 3D structures, but not in the hydrophilicity improvement, which was concluded to be more related to the incorporation of hydroxyl groups. The evaluation of these properties over time showed a recovery of the initial state of the surface within two weeks. These findings are of the utmost importance when defining the treatment procedure of the PLA scaffold for biomedical applications, especially if the proposed methods are transferred to the clinic. According to the results, the scaffolds tested possess suitable properties to be further evaluated for biomedical applications.

Author Contributions: Conceptualization, R.D. and M.E.A.-D.; methodology, R.D. and M.E.A.-D.; formal analysis, R.D.; investigation, R.D.; resources, M.M.; writing—original draft preparation, R.D.; writing—review and editing, M.E.A.-D. and M.M.; visualization, R.D.; supervision, M.M.; project administration, M.M.; funding acquisition, M.M. All authors have read and agreed to the published version of the manuscript.

Funding: This contribution is part of the BioAM project (DPI2017-88465-R) funded by the Science, Innovation and Universities Spanish Ministry. Also, the authors would like to acknowledge the support of the Spanish Ministry of Science and Innovation for funding the UNLP10-3E-726 infrastructure project, co-financed with ERDF funds. Finally, Ricardo Donate express his gratitude for the funding received through the PhD grant program co-financed by the Canarian Agency for Research, Innovation and Information Society of the Canary Islands Regional Council for Employment, Industry, Commerce and Knowledge and by the European Social Fund (ESF) Canary Islands Integrated Operational Program 2014-2020, Axis 3 Priority Theme 74 (85%). Grant code: TESIS2017010036.

Data Availability Statement: The data presented in this study are available on request from the corresponding author.

Conflicts of Interest: The authors declare no conflict of interest. The funders had no role in the design of the study; in the collection, analyses, or interpretation of data; in the writing of the manuscript, or in the decision to publish the results.

Appendix A

An enzymatic degradation test was carried out using PLA scaffolds treated with 0.2 N NaOH and washed with citric acid for 1 day, following the procedure described in Section 2.5. PLA scaffolds were used as control. The results of this test are shown in Table A1, including weight loss of the samples, pH and conductivity of the media and porosity change after degradation.

Table A1. Results of the 1-day enzymatic degradation test.

Group of samples	Weight loss (%)	pH	Conductivity (mS)	Initial porosity (%)	Final porosity (%)
PLA	0.01±0.01	7.56±0.01	2.00±0.01	44.1±3.8	43.1±2.2
NaOH 0.2 N + citric acid	1.37±0.11 [1]	4.57±0.01 [1]	2.41±0.01 [1]	41.0±1.3	44.2±2.8

[1] $p<.05$ compared with PLA.

References

1. Puppi, D.; Chiellini, F.; Piras, A.M.; Chiellini, E. Polymeric materials for bone and cartilage repair. *Prog Polym Sci* **2010**, *35*, 403–440.
2. Wang, X.; Xu, S.; Zhou, S.; Xu, W.; Leary, M.; Choong, P.; Qian, M.; Brandt, M.; Xie, Y.M. Topological design and additive manufacturing of porous metals for bone scaffolds and orthopaedic implants: A review. *Biomaterials* 2016, *83*, 127–141.
3. Vallet-Regí, M.; Ruiz-Hernández, E. Bioceramics: From bone regeneration to cancer nanomedicine. *Adv Mater* 2011, *23*, 5177–5218.
4. Ulery, B.D.; Nair, L.S.; Laurencin, C.T. Biomedical applications of biodegradable polymers. *J Polym Sci Part B Polym Phys* 2011, *49*, 832–864.
5. Liu, X.; Ma, P.X. Polymeric scaffolds for bone tissue engineering. *Ann Biomed Eng* **2004**, *32*, 477–86.
6. Croll, T.I.; O'Connor, A.J.; Stevens, G.W.; Cooper-White, J.J. Controllable surface modification of poly(lactic-co-glycolic acid) (PLGA) by hydrolysis or aminolysis I: Physical, chemical, and theoretical aspects. *Biomacromolecules* **2004**, *5*, 463–473.
7. De Jong, S.J.; Arias, E.R.; Rijkers, D.T.S.; Van Nostrum, C.F.; Kettenes-Van Den Bosch, J.J.; Hennink, W.E. New insights into the hydrolytic degradation of poly(lactic acid): Participation of the alcohol terminus. *Polymer (Guildf)* **2001**, *42*, 2795–2802.
8. Guo, C.; Xiang, M.; Dong, Y. Surface modification of poly (lactic acid) with an improved alkali-acid hydrolysis method. *Mater Lett* **2015**, *140*, 144–147.
9. Nam, Y.S.; Yoon, J.J.; Lee, J.G.; Park, T.G. Adhesion behaviours of hepatocytes cultured onto biodegradable polymer surface modified by alkali hydrolysis process. *J Biomater Sci Polym Ed* **1999**, *10*, 1145–1158.
10. Shao, J.; Chen, S.; Du, C. Citric acid modification of PLLA nano-fibrous scaffolds to enhance cellular adhesion, proliferation and osteogenic differentiation. *J Mater Chem B* **2015**, *3*, 5291.
11. Lao, L.; Tan, H.; Wang, Y.; Gao, C. Chitosan modified poly(l-lactide) microspheres as cell microcarriers for cartilage tissue engineering. *Colloids Surfaces B Biointerfaces* **2008**, *66*, 218–225.
12. Martin, V.; Ribeiro, I.A.; Alves, M.M.; Gonçalves, L.; Claudio, R.A.; Grenho, L.; Fernandes, M.H.; Gomes, P.; Santos, C.F.; Bettencourt, A.F. Engineering a multifunctional 3D-printed PLA-collagen-minocycline-nanoHydroxyapatite scaffold with combined antimicrobial and osteogenic effects for bone regeneration. *Mater Sci Eng C* **2019**, *101*, 15–26.

13. Li, B.; Ma, Y.; Wang, S.; Moran, P.M. Influence of carboxyl group density on neuron cell attachment and differentiation behavior: Gradient-guided neurite outgrowth. *Biomaterials* **2005**, *26*, 4956–4963.
14. Arima, Y.; Iwata, H. Preferential adsorption of cell adhesive proteins from complex media on self-assembled monolayers and its effect on subsequent cell adhesion. *Acta Biomater* **2015**, *26*, 72–81.
15. Chen, W.; Nichols, L.; Brinkley, F.; Bohna, K.; Tian, W.; Priddy, M.W.; Priddy, L.B. Alkali treatment facilitates functional nano-hydroxyapatite coating of 3D printed polylactic acid scaffolds. *Mater Sci Eng C* **2021**, *120*, 111686.
16. Scaffaro, R.; Lopresti, F.; Sutera, A.; Botta, L.; Fontana, R.M.; Gallo, G. Plasma modified PLA electrospun membranes for actinorhodin production intensification in Streptomyces coelicolor immobilized-cell cultivations. *Colloids Surfaces B Biointerfaces* **2017**, *157*, 233–241.
17. Nakagawa, M.; Teraoka, F.; Fujimoto, S.; Hamada, Y.; Kibayashi, H.; Takahashi, J. Improvement of cell adhesion on poly(L-lactide) by atmospheric plasma treatment. *J Biomed Mater Res - Part A* **2006**, *77*, 112–118.
18. Jordá-Vilaplana, A.; Fombuena, V.; García-García, D.; Samper, M.D.; Sánchez-Nácher, L. Surface modification of polylactic acid (PLA) by air atmospheric plasma treatment. *Eur Polym J* 2014, *58*, 23–33.
19. Wang, M.; Favi, P.; Cheng, X.; Golshan, N.H.; Ziemer, K.S.; Keidar, M.; Webster, T.J. Cold atmospheric plasma (CAP) surface nanomodified 3D printed polylactic acid (PLA) scaffolds for bone regeneration. *Acta Biomater* **2016**, *46*, 256–265.
20. Yamaguchi, M.; Shinbo, T.; Kanamori, T.; Wang, P.C.; Niwa, M.; Kawakami, H.; Nagaoka, S.; Hirakawa, K.; Kamiya, M. Surface modification of poly(L-lactic acid) affects initial cell attachment, cell morphology, and cell growth. *J Artif Organs* **2004**, *7*, 187–193.
21. Teixeira, B.N.; Aprile, P.; Mendonça, R.H.; Kelly, D.J.; Thiré, R.M. da S.M. Evaluation of bone marrow stem cell response to PLA scaffolds manufactured by 3D printing and coated with polydopamine and type I collagen. *J Biomed Mater Res - Part B Appl Biomater* **2019**, *107*, 37–49.
22. Moraczewski, K.; Stepczyńska, M.; Malinowski, R.; Rytlewski, P.; Jagodziński, B.; Zenkiewicz, M. Stability studies of plasma modification effects of polylactide and polycaprolactone surface layers. *Appl Surf Sci* **2016**, *377*, 228–237.
23. Li, J.; Oh, K.; Yu, H. Surface rearrangements of oxygen plasma treated polystyrene: Surface dynamics and humidity effect. In Proceedings of the Chinese Journal of Polymer Science (English Edition); 2005; Vol. 23, pp. 187–196.
24. Canal, C.; Molina, R.; Bertran, E.; Erra, P. Wettability, ageing and recovery process of plasma-treated polyamide 6. *J Adhes Sci Technol* **2004**, *18*, 1077–1089.
25. Durán, I.R.; Vanslambrouck, S.; Chevallier, P.; Hoesli, C.A.; Laroche, G. Atmospheric pressure cold plasma versus wet-chemical surface treatments for carboxyl functionalization of polylactic acid: A first step toward covalent immobilization of bioactive molecules. *Colloids Surfaces B Biointerfaces* **2020**, *189*.
26. Gibeop, N.; Lee, D.W.; Prasad, C.V.; Toru, F.; Kim, B.S.; Song, J. Il Effect of plasma treatment on mechanical properties of jute fiber/poly (lactic acid) biodegradable composites. *Adv Compos Mater* **2013**, *22*, 389–399.
27. Uchida, E.; Uyama, Y.; Ikada, Y. Sorption of Low-Molecular-Weight Anions into Thin Polycation

Layers Grafted onto a Film. *Langmuir* **1993**, *9*, 1121–1124.
28. Liu, Y.; He, T.; Gao, C. Surface modification of poly(ethylene terephthalate) via hydrolysis and layer-by-layer assembly of chitosan and chondroitin sulfate to construct cytocompatible layer for human endothelial cells. *Colloids Surfaces B Biointerfaces* **2005**, *46*, 117–126.
29. Garlotta, D. A literature review of poly(lactic acid). *J Polym Environ* **2001**, *9*, 63–84.
30. Tsuji, H.; Muramatsu, H. Blends of aliphatic polyesters: V. Non-enzymatic and enzymatic hydrolysis of blends from hydrophobic poly(L-lactide) and hydrophilic poly(vinyl alcohol). *Polym Degrad Stab* **2001**, *71*, 403–413.
31. Yang, G.H.; Kim, M.; Kim, G. Additive-manufactured polycaprolactone scaffold consisting of innovatively designed microsized spiral struts for hard tissue regeneration. *Biofabrication* **2017**, *9*.
32. Vesel, A.; Mozetic, M. New developments in surface functionalization of polymers using controlled plasma treatments. *J Phys D Appl Phys* **2017**, *50*.
33. Ouellette, R.J.; Rawn, J.D. Nucleophilic Substitution and Elimination Reactions. In *Organic Chemistry Study Guide*; Elsevier, 2015; pp. 169–182.
34. Yip, J.; Chan, K.; Sin, K.M.; Lau, K.S. Comprehensive study of polymer fiber surface modifications Part 2: low-temperature oxygen-plasma treatment. *Polym Int Polym Int* **2004**, *53*, 634–639.
35. Ye, P.; Wan, R.B.; Wang, X.P. Quantitative enzyme immobilization: Control of the carboxyl group density on support surface. *J Mol Catal B Enzym* **2009**, *61*, 296–302.
36. Hegyesi, N.; Zhang, Y.; Kohári, A.; Polyák, P.; Sui, X.; Pukánszky, B. Enzymatic degradation of PLA/cellulose nanocrystal composites. *Ind Crops Prod* **2019**, *141*.
37. Tsuji, H.; Ishida, T. Poly(l-lactide). X. Enhanced surface hydrophilicity and chain-scission mechanisms of poly(l-lactide) film in enzymatic, alkaline, and phosphate-buffered solutions. *J Appl Polym Sci* **2002**, *87*, 1628–1633.
38. Araque-Monrós, M.C.; Vidaurre, A.; Gil-Santos, L.; Gironés Bernabé, S.; Monleón-Pradas, M.; Más-Estellés, J. Study of the degradation of a new PLA braided biomaterial in buffer phosphate saline, basic and acid media, intended for the regeneration of tendons and ligaments. *Polym Degrad Stab* **2013**, *98*, 1563–1570.
39. Schiller, C.; Epple, M. Carbonated calcium phosphates are suitable pH-stabilising fillers for biodegradable polyesters. *Biomaterials* **2003**, *24*, 2037–2043.
40. Niaza, K. V.; Senatov, F.S.; Kaloshkin, S.D.; Maksimkin, A. V.; Chukov, D.I. 3D-printed scaffolds based on PLA/HA nanocomposites for trabecular bone reconstruction. *J Phys Conf Ser* **2016**, *741*, 012068.
41. Chen, S.; Guo, Y.; Liu, R.; Wu, S.; Fang, J.; Huang, B.; Li, Z.; Chen, Z.; Chen, Z. Tuning surface properties of bone biomaterials to manipulate osteoblastic cell adhesion and the signaling pathways for the enhancement of early osseointegration. *Colloids Surfaces B Biointerfaces* **2018**, *164*, 58–69.

4. CONCLUSIONS

In this section, the main conclusions drawn from the scientific publications covered in this document are summarized. Additionally, since the work developed during the thesis goes beyond the currently published results, other unpublished finding are detailed. Finally, future research lines derived from the work carried out in this doctoral thesis are presented.

4.1. MAIN CONCLUSIONS

- The scaffolds manufactured by AM had a pore size between 400–500 μm and a porosity value of around 50-60%, matching the requirements for bone tissue-engineered scaffolds.

- A significant increase in the roughness, microporosity and crystallinity of the 3D printed samples was obtained when the $CaCO_3$ and β-TCP particles were added to the PLA matrix.

- Composite samples showed a reduction of the hydrophobicity of the base material, which coupled with the improved surface roughness and microporosity of the 3D structure promoted cell adhesion and proliferation of osteoblasts cultured in vitro.

- The simultaneous introduction of both ceramic additives into the PLA matrix led to the best results in terms of the metabolic activity after 7 days of human osteoblastic osteosarcoma cells. These scaffolds showed potential to be further evaluated for their application in the Bone Tissue Engineering field.

- The enzymatic degradation study of the PLA and composite scaffolds (PLA:$CaCO_3$:β-TCP 95:2.5:2.5) showed that the use of the proposed additives increased the degradation rate of the constructs during the first steps of the experiment. These results were attributed to the release of the additive particles and the statistically higher pore size and porosity of the composite scaffolds compared with the neat PLA ones.

- Improving the degradation rate of 3D printed PLA scaffolds could be an advantage for its application in the field of Tissue Engineering, considering the long time required for the complete degradation of PLA structures in vivo.

- The application of alkali treatments to PLA scaffolds led to a higher incorporation of carboxyl groups to the polymeric surface, thus promoting the enzymatic degradation rate. These methods, however, were confirmed to significantly affect the morphology of the 3D constructs.

- For oxygen plasma treatments, the generation of hydroxyl groups on the polymeric surface prevailed, leading to a greater improvement of the hydrophilicity of the samples without affecting the bulk properties.

- The characterization of the surface-treated scaffolds over a 2-weeek period showed that the modifications introduced on the PLA surface were non-permanent. Having this information is essential when designing a post-treatment coating procedure to anchor bioactive compounds or when the surface-treated constructs have to be stored until their biomedical application.

- The pH of the Aloe vera extracts used as bioactive coating was shown to influence the degradation rate of the PLA scaffolds. Notably, results from the enzymatic degradation test carried out showed that the Aloe vera coating applied at pH 3 delayed the degradation of the constructs. Therefore, the pH of the Aloe vera extract can be used as an important parameter to adjust the degradation profile of the 3D structures.

- PLA scaffolds treated with oxygen plasma and then coated with Aloe vera at pH 3 also showed the best results in terms of cell metabolic activity of human osteoblasts cultured during 10 days in vitro. Very highly statistically significant differences ($p < .001$) were obtained between this group and the plasma-treated samples, confirming the increased biofunctionality of the Aloe vera coated scaffolds and their potential to be applied for bone tissue regeneration.

4.2. OTHER UNPUBLISHED FINDINGS

- After applying the different Aloe vera coating proposed (pH 3, 4 or 5) to composite samples, a very highly statistically significant reduction ($p < .001$) of the PLA surface hydrophobicity was obtained.

- Despite the physicochemical changes on the polymeric surface, determined by X-ray Photoelectron Spectroscopy (XPS) and water contact angle measurements, non-significant differences were obtained in terms of pore size, porosity or mechanical properties after the application of the surface coating to the composite scaffolds. Therefore, it was concluded that there was no effect on the bulk properties due to the procedure used to incorporate bioactive compounds to the constructs.

- The pH of the Aloe vera extracts used to coat the 3D structures showed a more marked influence on the degradation rate of the composite scaffolds than in the case of neat PLA samples. Thus, while the degradation profile of composite scaffolds coated with Aloe vera at pH 5 was similar to the one of untreated samples, at pH 3 the degradation rate was reduced during the first days of a degradation test using *Proteinase K* enzymes. At pH 4, however, the enzymatic degradation process was significantly hindered and the pH of the media was maintained at a high value during the 5-day test.

- Composite scaffolds coated with Aloe vera extracts showed a significant improvement of their biofunctionality in terms of cell metabolic activity. The attachment and proliferation of human osteoblastic cells cultured on the scaffolds for 13 days were enhanced by the application of the surface coating methods evaluated. The best results were obtained for the scaffolds coated at pH 3 and 4, which showed a highly statistically significant difference ($p < .01$) compared with the group of plasma-treated scaffolds. The proposed scaffolds possess suitable properties to be further evaluated for Bone Tissue Engineering applications.

4.3. FUTURE RESEARCH LINES

- Despite the promising results obtained, limitations imposed by the manufacturing technique were found in the production of composite scaffolds. The formation of agglomerates of the ceramic particles restricted their use to a maximum mass ratio of a 5%. The **improvement of the mixing and extrusion processes** of the composite filaments needed to feed the 3D printer would allow improving the dispersion of the ceramic particles into the PLA matrix. In that way, an increased concentration of the additives could be used, thus having a greater effect on the base material properties.

- Further chemical characterization of the surface-treated scaffolds is needed to assess the type of bonds formed and the **bioactive compounds incorporated** to the PLA surface after the application of the different Aloe Vera coatings proposed. These results would clarify which of the components of the Aloe vera extract has an effect on promoting the cell metabolic activity of osteoblast-like cells.

- In addition to the in vitro enzymatic degradation studies presented in this work, a **hydrolytic degradation test** of the proposed 3D structures should be performed, since hydrolytic conditions are more representative of the in vivo implantation conditions. Results from this test would provide relevant information about the capability of the ceramic additives to counteract the pH decrease of the surrounding media due to the degradation of the polymeric matrix.

- A second step in the biological evaluation of the proposed 3D structures will include **ex-vivo tests** in a perfusion flow bioreactor. The proliferation, viability and differentiation of mesenchymal stem cells will be analyzed to understand the relationship in the mechanotransduction process and its effect on the final biological response of the biofunctionalized scaffolds obtained by AM.

- Work will be done on the development of biphasic scaffolds for the regeneration of tissue located in articular regions. The assembly of the developed bone scaffolds with a hydrogel-based construct intended for cartilage regeneration would allow obtaining an **osteochondral unit**.

ULPGC
Universidad de
Las Palmas de
Gran Canaria